PHOTOMETRIC STUDIES OF CLOSE BINARY SYSTEMS

A Thesis Submitted to

The Gujarat University

for

THE DEGREE OF DOCTOR OF PHILOSOPHY

in

PHYSICS

by

WATSON P. VARRICATTU

PHYSICAL RESEARCH LABORATORY

NAVRANGPURA

AHMEDABAD 380 009

INDIA

January 1998

Contents

Acknowledgments

I would like to express my gratitude to Dr. N. M. Ashok, my supervisor, who has introduced me to this field. Throughout the course of my work, his comments and suggestions have been of valuable help to me. I have benefited immensely by my discussions with him. I also thank him for critically going through the thesis and giving many good suggestions. I have enjoyed working with Dr. T. Chandrasekhar and discussing with him. I thank him for the help and support that he has extended to me.

It was always a pleasant experience to discuss with Prof. J. N. Desai. The simplicity with which he used to talk about deep ideas has influenced me. I thank him for carefully going through the thesis and suggesting many improvements.

It would have been a difficult task to complete the collection of this large volume of data in a short time without the whole hearted help offered by my friends Kamath and Kunu. Their friendship and company, especially, in the long observing campaigns, were always pleasant support to me. Let me express my gratitude towards them for the various things that they have done for me.

I thank Prof. M. R. Deshpande and Prof. B. G. Anand Rao for their interest in the progress my work. Thanks are also due to Prof. U. C. Joshi, Dr. D. P. K. Banerji and Dr. H. O. Vats, for their concern over me at different stages of my work.

I greatfully acknowledge the co-operation and support of the staff members of the Mt. Abu Observatory Mr. Rajesh Shah, Purohit, Jinesh, Mathur, Narayan Singh, Padam Singh and Pitambar Singh for their help in the observation and the telescope operation. With their helpful nature, long observing campaigns were never felt straining. I thank Mr. A. K. Kothari and his team members at the Hill View guest house, and Chagan Bhai for making my stay comfortable during the observational trips. Let me also remember with thanks the help and company offered by C. K. Visvanath, A. H. Desai, D. B. Pancholi, S. L. Kayastha, Soumen

Mondal and P. K Kikani for staying awake with me throughout the nights and helping in the observations in the chilling nights at Gurushikhar. I thank Messrs. N. S. Jog, K. S. B. Manian, R. K. Mahadkar, S. D. Rawat, Mr. F. M. Pathan, Mrs. Mary and Mrs. Jani for offering me technical help at various stages of my work and to Mr. Stephan and Mrs. Meera for their support on various occasions. The works of Mr. Shroff, Punambhai Panchal, Jadavbhai and Atmarambhai at various stages of my works are greatfully acknowledged.

Let me thank Dr. Shyam Lal, Dr. A. Jayaraman, Prof. V. B. Sheorey, Prof. J. N. Goswami, Prof. R. Sreedharan and Dr. P. Sarma of P.R.L. and Dr. Harish Bhatt of the Indian Institute of Astrophysics, Bangalore for their interest in my career.

Mrs. Uma Desai of the Thaltej library and Mrs. R. Bharucha and the other staff members of the PRL library were always helpful in getting me the latest study materials whenever needed. My thanks to the staff members of the Thaltej and PRL Computer Centers and Administrative division for their service.

I have benefited very much through my discussions with Prof. K. D. Abhyankar of the Osmania University. I would like to thank Prof. R. E. Wilson of the Florida University for sending me the model for light curve analysis and Dr T. Hegedus of the Baja Observatory for providing the data on the moments of minima of RZ Cas. I thank Prof. E. Budding of Carter Observatory, NewZeland for useful interactions.

Friends have always encouraged me a lot throughout my life here. Memories of their pleasent company will always be fresh in my mind. Good amount of my free time here was spent in the cheerful company of Poulose, Biju and Clement. With them around, with their affectionate and helping nature, I never had to feel lonely. Frequent visits of Shibu John was always a happy experience. I thank Sam for his company on many field trips. I have benefited very much through my discussions with him. Let me express my gratitude to Aparna and Muthu for their warm friendship and caring nature. I also thank them for many help that

they have done for me. Let me acknowledge Shibu Mathew, Anshu, Abhijit and Nandu for their joyful company. It is a pleasure to say thanks to Joby, Vijaykumar, Seema, Mac., Prashant, Pravin, Puthar, Ban, Dulichand, Manish, Shikha, Siva, Raju K. P., Ram, Shajesh, Tharun, Anil, Santhanam and Pattu for their friendship and support.

I would feel delighted to remember my friends Mariam, Santhosh, Benno, Sankar, Tomy, Bijo, Raju, Suresh and Suresh Kumar for their concern over me.

I thank Mrs. Aruna Ashok, Abhijit, Ashwini and the family members of Clement, Pravin and Prashant for their nice hospitality. At this juncture, I have the warm memories of many of the happy evenings with my friends Jose and Delia.

My deep gratitude to my parents brother and sisters who kept their pleasures away and brought me up.

Finally let me express my thanks to the Physical Research Laboratory and the Dept. of Space, Govt. of India for funding my research and extending me all necessary facilities for carrying out my work.

Chapter 1

Introduction

A pair of stars of masses M_1 and M_2 bound together by their mutual gravitational attraction form a binary system. By Kepler's laws, the most general form of the orbit of such a pair of stars is an ellipse and the semi-major axis of the ellipse (a) and the orbital period (P) are related by the equation [1]

$$\frac{P^2}{4\ \pi^2} = \frac{a^3}{G\ M_1\ M_2} \tag{1.1}$$

where G is the gravitational constant. In a close binary system[2], the component stars are subjected to tidal force due to the proximity of each other and they get highly distorted from spherical shape. The tidal force varies as R^{-3} where R is the instantaneous separation between the components. If the orbit is eccentric, the stars will pulsate due to tidal forces of periodically varying amplitude throughout the orbit. Such pulsations are damped by viscous forces within the stars and the resulting dissipation of energy making the orbit circular. Similarly, if the spins of the stars are not synchronized with the orbital rotation, then also, the components will pulsate due to varying amount of tidal force. Exchange of angular momentum takes place between the orbital and the spin motions, which makes the stars CO-rotate with the orbital motion. Eventually the binary system settles down to a circular orbit, with the components spinning synchronously with the orbital rotation, which is the minimum energy state for a fixed angular momentum (Pringle & Wade 1985). Equation 1.1 relates the period of the binary system, which can

[1] Kepler's third law.

[2] The components are separated by only a few times their radii in a close binary system so that the evolution of each component is significantly affected by the proximity of the companion.

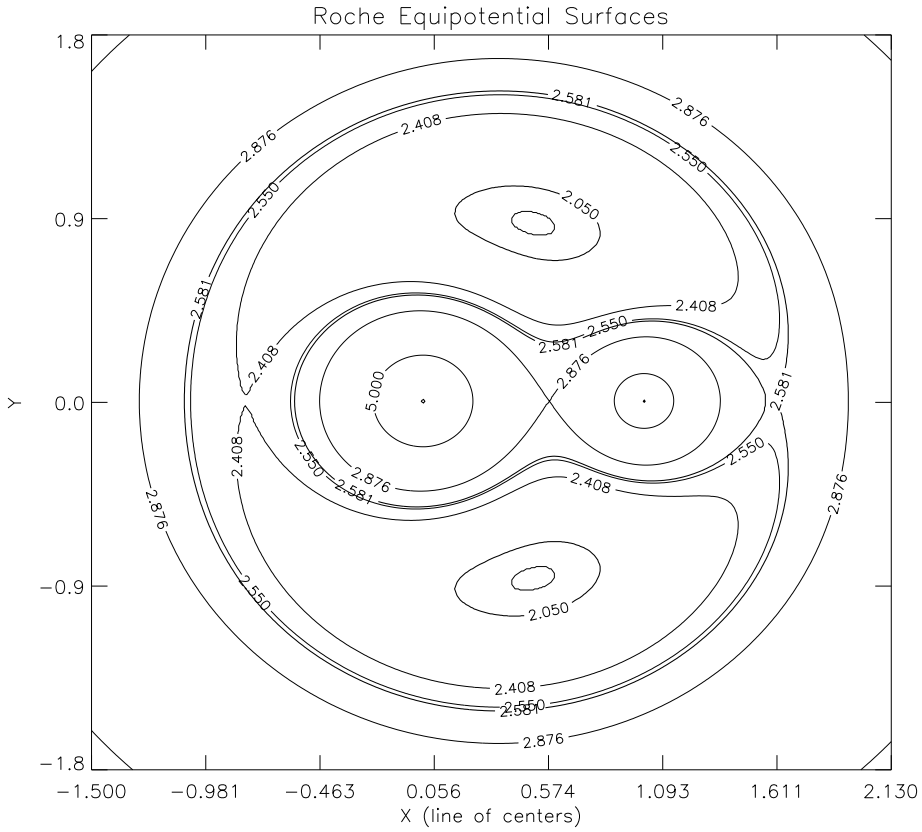

Figure 1.1: Roche Equipotential surfaces for $q = 0.5$. The Lagrangian points are labeled as L_i's. The dumbbell shaped configuration with $\Omega = 2.876$ contains the Roche lobes.

be directly measured, to the separation and the masses of the components, which have to be derived from other observables of a binary system like observed light and its variations due to mutual eclipses of the components, radial velocities of the components which are determined from the observed Doppler shift of the spectral lines, etc.

Rotational and tidal effects play significant roles in the structure and evolution of stars in a binary system. To understand these, let us consider any point mass (m) at p, at a distance r from M_1, co-rotating with the mass centers M_1 and M_2. It is assumed that for M_1 as well and M_2, all the masses are concentrated at their centers of masses. Consider rectangular Cartesian co-ordinates with the X axis along the line of centers of the stars, Y axis perpendicular to the X axis in the orbital plane and the Z axis, perpendicular to the orbital plane along the axis of rotation. Let M_1 and M_2 be separated by a distance R. We can calculate the total potential Ψ at p, taking into consideration the gravitational force on m due to M_1

and M_2 and the centrifugal force due to the rotation of m. This potential can be written as

$$\Psi = -\frac{GM_1}{r} - \frac{GM_2}{r'} - \frac{\omega^2}{2}\left\{\left\{x - \frac{M_2 R}{M_1 + M_2}\right\}^2 + y^2\right\} \tag{1.2}$$

where r' is the distance of p from M_2, ω is the angular velocity of the rotation of m about an axis through the center of gravity of the binary system and x and y are the distances along the X and the Y axis from the center of M_1. The first term on the right hand side of 1.2 is the gravitational potential at p arising from the mass M_1, the second term is arising from the mass M_2 and the third term is the potential due to the centrifugal force of rotation of m. On the surface of a star in the binary system, Ψ should have a constant value for maintaining a stable configuration. So we have to only look for a proper pair of surfaces with constant Ψ values to get information about the sizes and shapes of the component stars in a binary system.

Most of the binaries are so far from us that with any of the telescopes they appear as single stars. The angular separations of many of the close binaries are less than 1 milliarcsecond and we do not have any direct idea about the masses of the components. So for practical purposes, we have to represent Eq. 1.2 in a form where the above mentioned quantities do not enter directly and only those quantities which can be derived from the observations enter the equation. For this purpose, the potentials are represented in a dimensionless form as

$$\Omega = \frac{1}{r} + q\left\{\frac{1}{(1 - 2\,\lambda\, r + r^2)^{-1/2}} - \lambda\, r\right\} + \frac{(q+1)}{2}\, r^2\,(1 - \nu^2) \tag{1.3}$$

where all the masses are replaced by the mass ratio $q(= M_2/M_1)$ and the separation between the stars is taken as unity assuming circular orbits. r is also written in units of the separation between the stars. λ (= cosϕ sinθ) and ν (=cosθ) are direction cosines of p. The complete configuration of the system is represented by the value of q. So for a particular value of q, we can generate surfaces of constant Ω. A pair of such surfaces around the mass centers M_1 and M_2 will define the shape of the component stars in the system (Kopal 1959). Here Ω is only a linear function of the true potential, Ψ.

Fig. 1.1 shows the cross section of a set of such equipotential surfaces along the orbital plane. We see that towards the centers of the stars Ω has higher values since gravitational force dominates and for large values of Ω, the equipotentials around the mass centers M_1 and M_2 are nearly spherical. The equipotentials become more and more elongated for lower and lower values of Ω and for certain value of Ω, defined by q, the equipotentials around M_1 and M_2 touch each other at a point L_1 called *inner or first Lagrangian point* between M_1 and M_2 and a dumb bell shaped configuration results called the *inner critical surface*. The corresponding equipotentials around each mass are called the *Roche Lobes*. L_1 is a point of zero effective force and any particle, which crosses the Roche lobe of M_1 or M_2 through L_1 will find a net effective force pulling it towards the other star and it is accreted by that star. L_2, L_3, L_4 and L_5 are also Lagrangian points of zero effective force. The equipotential surface passing through L_2 is called *outer critical surface*. The Roche Lobes and Lagrangian points play significant roles in the evolution of the components of a binary system. Far away from the center of mass of the system, Ω will again take higher values since centrifugal potential will be high. The concept of Roche lobes comes to our aid in determining the parameters of the system.

Kopal (1959) classified the binary stars based on Roche model as *detached*, *semi-detached* and *contact* binaries. Detached systems are those in which the sizes of the component stars are smaller than their Roche lobes. They are relatively less distorted from spherical shape. When one of the stars fills its Roche lobe, the binary system is said to be in a semi-detached configuration. This often happens due to the evolutionary expansion of the star which is the more massive one among the two. The lobe-filling star then transfers mass to its companion which is still well within its Roche lobe, through L_1 point as described above. The lobe-filling star is highly distorted and has the shape of its Roche lobe and the companion will be relatively less distorted. When both stars fill their Roche lobes, a contact configuration results. Both the stars in such binary will be highly distorted with the system bound by a common envelope lying on one of the dumbbell shaped equipotential surfaces between the inner and outer critical surfaces, for a configuration stable

against mass loss.

1.1 *Photometric Studies of Eclipsing Binary Stars: A Brief History*

John Goodrike Junior of York, a deaf and dumb man of 18, was the first person to observe the periodic nature of the variation of light in a stellar system. He made the first observation of a minimum of Algol (β Per) on Nov. 12th, 1782, and made an estimate of the period to be close to 2 days and 21 hours. He proposed that this observed periodic change in light was caused by the periodic interposition of a large body revolving around Algol. Besides Algol, he also discovered the variability of β Lyrae & δ Cephi before his early death at the age of twenty two. Goodricke's suggestion was confirmed when Vogel in 1889 found Algol to be a spectroscopic binary whose conjunctions coincided with the minima of light. Thus Algol became the first known eclipsing binary and β Lyra, the second. The number of eclipsing binaries discovered increased fast after that, thanks to the untiring efforts of several dedicated observers. Schneller, in 1940, published a catalogue containing 1087 objects classified as eclipsing binaries and Kukarkin and Parenago in 1948, listed over 2000 eclipsing binaries (Kopal 1959). The present *General Catalogue of Variable stars* (Kholopov 1985) lists over 28400 variable stars in our Galaxy, good number of them being eclipsing binaries.

If the orbital plane of a binary system is along the line of sight or inclined within a certain angle with respect to the line of sight, defined by their separation and relative sizes, they will eclipse either fully or partially when they rotate around each other, causing variations in the observed light (light curve). During the eclipse one star scans the surface of its companion and studies of the light variations provide us valuable information about the sizes, shapes and circumstellar environments of the component stars in the system. The dimensions of the component stars can be derived with good accuracy, adopting a suitable model to

represent the stellar surfaces and dynamics of the system. Also for many of the stars, the temperature of one of the components is known from spectroscopy, and in that case, the temperature of the companion can be determined by analyzing the light curves. Analysis of the light curve provides the values of orbital inclination and the mass ratio. Combined with the spectroscopic results, these give the masses of the components, which otherwise are not measurable for single stars. Atmospheric properties of the stars like limb darkening, gravity darkening and bolometric albedo can also be derived from a light curve of good accuracy, ie., we will be able to resolve the binary system, with a good knowledge of the properties of the components, which otherwise would appear as a single star.

From the initial days of the study of binary stars, astronomers have tried different techniques to analyze the light curves. We can divide the history of the light curve analysis into two separate eras: the period dominated by purely geometrical models, when the process called *rectification* was the heart of the analysis technique, which lasted up to sixties & early seventies and the period of *physical models* which started in early seventies.

Russell model (Russell 1948 and references therein) was initially developed for spherical stars and later evolved to deal with more complicated ellipsoidal configurations. This model made use of rectification, where an observed light curve was corrected, so as to correspond to a binary configuration having spherical limb darkened stars in circular orbit. This rectified light curve was then analyzed to obtain the geometrical and photometric properties of the spherical stars, which could be corrected with transformation formulae, to relate back to those of real stars. The observed brightness variation outside the eclipse was used to derive information about the tidal deformation and its effect on the observed variations in the surface brightness over phase and the amount of reflected light and the light curve was then corrected for these effects. The fitting is carried out for the corrected curves. The main drawback was that the rectifiable models used only the eclipse portion to derive the binary system parameters. The portions of the light curves

between eclipse were not used to derive the system parameters, though they also contain valuable information. Deviations due to tidal deformation and reflection were considered as contaminants and were filtered out, rather than being used to derive information about the physics of the system.

Kopal (1959 and references therein) contributed considerably towards the development of the field of binary star light curve analysis. He encouraged the trend of representing the binary stars by Roche surfaces. He also utilized the method of rectification, but went a few steps ahead, and corrected the light curve of a binary star to spherical model from the Roche model distortions. His model was widely used and was found to be accurate for binary stars with $r/r_{lobe} \leq 0.8$. These models were of low accuracy for near-contact and contact binaries and inapplicable to over-contact systems. He also developed the method of analyzing the light curves in the frequency domain (Kopal 1979 and references therein).

Physical models are based on Roche equipotential surfaces to represent the star surfaces, and the fundamental idea that the surfaces of constant density coincide with the equipotential surfaces described in the previous section. The local gravity and the surface orientation are decided by the direction of the potential gradient at any point on the star. A first attempt was made by Lucy (1968) to deal with W UMa stars which are contact binaries, the components of which depart very much from spheres. The normal rectification methods failed to give reliable estimates of the stellar parameters for such systems. So Lucy proposed a model to deal with these systems which did not use rectification. But this method was applicable only to over-contact systems.

Several other models and programmes were developed afterwards for the efficient handling of the eclipsing binary light curves. Most of the them are *physical models* which make use of equipotentials to represent the star surfaces. Out of these, the model by Wilson and Devinney (1971) and improved by Wilson (1990) is the most widely used one for the analysis of the light curves of eclipsing binaries. This is the model used in the present study of the J and K light curves

of two eclipsing contact binaries: R CMa and RZ Cas. A brief description of this model and the parameters used is given in section 2.3. The models by Mochnacki & Doughty (1972), Linnell, A. P. (1984, 1989) are some of the other widely used physical models. There are some models, which are not based on equipotentials, but still popular because of their certain qualities. The models by Nelson, Davis and Etzel (NDE) (Nelson and Davis 1972, Etzel 1993) and Budding (1977) are the prominent among them, which are based on spheres. NDE model includes first order corrections for asphericity and gravity darkening. This model can be used for nearly spherical stars and is capable of dealing with eccentric orbits too. Budding's model can be efficiently used for spotted stars, which depart significantly from spherical geometry. Wood (1971) used triaxial ellipsoids for representing the component stars in the binary system. This model was widely used in seventies and early eighties (Wilson 1994).

1.2 The Algols

Algol binaries, numbering nearly 400 at present (Budding 1989), form a subgroup of the semi-detached class where the primary (bright star) is a late B to early F type Main Sequence star well within its Roche Lobe and the secondary (fainter star), which is the less massive one is a G or K type subgiant or giant whose surface is in contact with its critical Roche Lobe. This situation in Algols, where the less massive star is a giant or subgiant while the more massive companion is still on the Main Sequence is the famous *Algol paradox*. Crawford (1955) and Kopal (1955), independently suggested a solution to this paradox. According to them, the present secondary was initially the more massive one. Being more massive, it evolved faster, exhausting the hydrogen in its core and became a giant by expanding during the phase of shell hydrogen burning. During this phase of expansion, the star overfilled its Roche Lobe and transferred a good portion of the overflowing mass to its companion, through the L_1 point, to become the less massive one.

The present primary, which is the more massive one now, thanks to the mass transfer from its companion, is still in the core hydrogen burning stage. The cool star can be losing mass at a rate of $10^{-5} - 10^{-7}\ M_{\odot}\ year^{-1}$ for a very active system to less than $10^{-9} - 10^{-10}\ M_{\odot}\ year^{-1}$ for a typical Algol system (McCluskey 1993). Guiricin, Mardirossian & Mezzetti (1983), Budding (1989), Wilson, Van Hamme & Pettera (1985) and Sarma, Rao & Abhyankar (1996) have done detailed study of important properties of Algol binaries.

Many of the Algols show signatures of circumstellar matter due to mass transfer from the lobe-filling secondary to the primary. A few examples are listed in Olson (1982), Peters (1989) and Guinan (1989) where gas streams or disks around the gainers have been detected. Photometrically Algols show deep primary eclipses and shallow secondary eclipses at the optical wavelengths. Most of these are single lined spectroscopic binaries since the secondary lines are very weak and usually are blended with much more powerful lines of the primary.

Hall (1989) observed that the secondaries of Algol binaries are qualified to be included among the class of stars showing chromospheric activity. They satisfy the two main criteria which are believed to be responsible for chromospheric activity: rapid rotation and convection. He observed that as far as evolutionary stage is concerned, Algols are distinct from RS CVn binaries which are a prominent group among the stars showing chromospheric activity. Algols are in more advanced stage of evolution compared to RS CVn binaries. In both cases, the active stars are the more evolved ones. In Algols, the active subgiant is the less massive one due to large scale mass transfer, whereas in RS CVn s, except in very few cases, they are the more massive ones. In the plot of radius of the active component *vs.* rotation period, Hall found that both Algol secondaries and active components of the RS CVn binaries are indistinguishable. The equatorial velocities of all these stars were found to be higher than 5 $km\ s^{-1}$, which is the minimum level for chromospheric activity.

Core emission in Ca II H & K absorption lines is another indication of chromospheric activity. These emission lines are of chromospheric origin. These lines are observed in a few totally eclipsing Algols (U Cep, S Vel) during primary minimum when the primary is totally masked by the secondary. Hall (1989) concluded that this emission may not be observed in most of the Algols since at Ca II H & K wavelengths, most of the Algol primaries are brighter than the active secondaries by a few magnitudes, thus washing out the features of the secondary spectra.

1.2.1 Observations in the optical wavelengths

Most of the information that we have at present about the Algols has been derived from extensive photometric and spectroscopic studies in the optical wavelengths. Because of the deep primary minima and short periods, large number of these stars have good observational coverage in the optical photometric bands. The studies in the optical wavelengths have helped us in understanding the basic evolutionary processes leading to the formation of Algol binaries and the nature of the primary components in great detail.

Spectroscopic studies have helped in confirming the spectral and luminosity classes of the primaries with good accuracy. Along with the radial velocity curves and temperatures and relative sizes of the components derived from photometric light curve analysis, these studies have enabled the estimate of the absolute parameters of a large number of Algols. However, in the optical wavelengths, the depths of the secondary minima are very small in most of these systems (typically 0.03 to 0.08 magnitudes in V band). Alogls are usually observed as single lined spectroscopic binaries. The spectra of the secondary are extremely weak and blended with that of the primary. Recently with improved spectroscopic techniques, radial velocity curves of the secondary components of a few binaries have been obtained (Tomkin 1978, 1979, 1981, 1985, Popper & Tomkin 1984, Tomkin & Lambert 1978, and Maxted, Hill & Hilditch 1994) enabling accurate determination of the mass ratios of many Algols which is one of the most important parameters

in a binary system. They could derive relatively accurate masses of the components of δ Lib, U Sge, U Cep, R CMa, RZ Cas & S Cnc from their spectroscopic studies. Cool components of R CMa & S Cnc have 0.17 $M\odot$ which are the stars of lowest mass found in the Algols. In recent times, Doppler Tomography of some of the systems has enabled mapping of the gas streams. Doppler Tomography of the H_α difference profiles by Richards, Albright & Larissa (1995) has resolved the gas stream from the secondary to the primary due to Roche Lobe overflow of the secondary and the disk-like structures around the primary in 4 Algols, namely, U CrB, U Sge, RS Vul & β Per.

1.2.2 Near infrared observations of Algols

Infrared observations are helpful for studying the cool components of Algols and their circumstellar environments. The only existing near IR light curves of Algol systems are the 1.2 μm light curves of β Per (Chen & Reuning 1966) and UX Her (Lazaro *et al.* 1997). Analysis of the IR light curves of β Per by Richards (1990) has revealed time dependent changes in depths and phases of both eclipses, asymmetry in the secondary minima and cyclic variations in the mean temperatures of the secondary component. The overall variability found was similar to that seen in the optical light curves of RS CVn systems where star spots are believed to play a major role (McCluskey 1993). IR spectroscopy of UX Her by Lazaro *et al.* (1997) enabled the determination of the spectral type of the secondary by spectroscopic methods for the first time in Algols. Observations of 4 Algols (R CMa, TX UMa, δ Lib & TV Cas) and one RS CVn system (AR Lac) by Needham *et al.* (1980) could determine IR excess in these systems from the observed (K - L) and (L - M) colours. They attributed the excess to the plasma free - free emission from the gas streams and calculated the maximum rate of mass transfer. The observations were done at limited epochs and not aimed to construct the light curves. Smyth, Dow & Napier (1975) observed β Per at 2.2μm and 5.0μm over a few phases. Their observations

at 2.2μm didn't show any IR excess, but the observations at 5.0μm showed anomalous emission near the secondary minimum. Longmore & Jameson (1975) obtained infrared light curves of β Per at 2.2, 3.6, 4.8 and 8.6 μm. They modeled the system with a gas stream from the secondary to the primary with temperature and electron density in the ranges 5 - 20 $\times 10^3$ K and 5 - 30 $\times 10^{11}$ cm^{-3} respectively. They estimated a mass transfer rate of 1.8×10^{-8} $M_\odot$ $year^{-1}$.

1.2.3 Observations in the radio and X-ray wavelengths

We have already discussed that in Algols the secondaries are subgiants with convective envelopes which are rotating synchronously with the orbital motion. Due to synchronous rotation, all the secondaries are rotating much faster than normal giants of the same masses. Fast rotation and convection are known to be responsible for chromospheric activity in RS CVn binary systems, which are noted for the large scale spot activity. In the Sun also, it is the magnetic activity enhanced by differential rotation which is understood at present to be the cause for the spot activity and activities seen in the radio and X-ray wavelengths. This has inspired the radio and X-ray observations of Algols. Stars which show chromospheric activity display extremely strong radio emission (Morris & Mutel 1988). Algols are also observed to be showing similar levels of emission in the radio wavelengths as RS CVns. Observation of 11 Algols at 6cm by Mutel and Morris (1987) showed a median luminosity of 2.00×10^{16} $ergs$ $s^{-1} Hz^{-1}$. Morris and Mutel (1988) obtained a median luminosity of 2.5×10^{16} $ergs$ $s^{-1} Hz^{-1}$ for a set of 53 RS CVn binaries at the same wavelengths. Umana, Catalano & Rodono (1991) observed a selected list of 14 Algols with the VLA at 6 cm and detected 7 of them. The frequency distribution and the derived average Radio Luminosity (1.58×10^{16} $ergs$ $s^{-1} Hz^{-1}$) was similar to that of the RS CVns observed by Morris and Mutel (1988). This large radio luminosity was interpreted as of non-thermal original due to gyro-synchrotron emission from mildly relativistic electrons interacting with the magnetic field of the active component. Umana *et al.* (1993) obtained the radio spectra of 6 Algols

at 1.49, 5, 8.4 & 14.9 GHz with the VLA and found that the spectra are similar to RS CVns'. Hall (1989) observed that the only reason why less number of Algols are observed in the radio compared to other chromospherically active stars is that they are, on an average, at larger distances compared to other chromospherically active stars.

Strong soft X-ray emission is considered as a good characteristic of chromospherically active stars (Hall 1989). White & Marshall (1983) observed soft coronal X-ray emission from 9 Algols. Pallavicini *et al.* (1981) and Schmitt *et al.* (1990) observed strong soft X-ray emission from RS CVn systems. Schmitt *et al.* found that this is associated with an extremely strong corona with $T > 10^{7.5} K$. They also observed strong X-ray emission (less than average RS CVn s) from the Algol system RZ Cas. Pallavicini *et al.* (1981) observed X-ray emission from β Per too. Singh, Drake & White (1995) have done a study of coronal X - ray emission from 5 Algols with ROSAT and ASCA data. They found significant intensity variations, which were attributed to the chromospherically active secondary components.

1.3 Significance of the Present Work

It has already been pointed out in the previous sections that the secondaries of the Algol binaries are expected to show chromospheric activity, similar to RS CVn stars. Most of the information available about the Algols is mainly derived from observations in the optical wavelengths and a few observations done in the IR wavelengths give strong indications of RS CVn - type activities in Algols.

For a binary system of the Algol type, containing a B or A type main sequence star which is the brighter of the two and a G or K type subgiant star, the depth of the secondary minimum increases when we go from the optical to the near IR bands, because the relative contribution of the secondary component towards the total system light is higher in the near IR bands, compared to that in the optical bands. Observations at near infrared wavelengths of the Algols will help

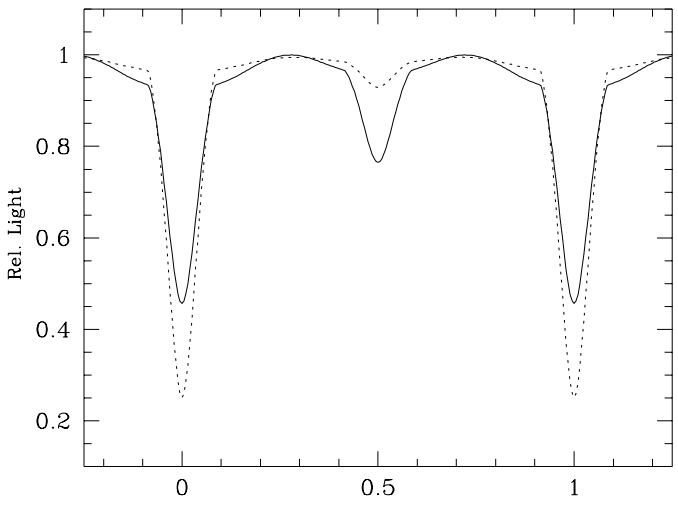

Figure 1.2: The dotted line shows the light curve of a typical Algol system in the V band. The continuous line represents the light curve in the K band.

in resolving the features of the surface of the secondary star with more confidence as the brightness of the secondary is relatively high at these wavelengths. A deep secondary eclipse will help detecting the presence of spots on the surface of the secondary star with better accuracy in a light curve analysis. Such a feature on the surface of the secondary will go unnoticed in the light curves in the optical bands where most of the system light comes from the primary component. Fig.1.2 shows simulated light curves showing the increase in the depth of secondary minima from the V to K band and section 2.3.4 demonstrates how spots on different locations of the secondary component will be better observed in an IR light curve compared to that in the optical. For the simulations a binary system with $q = 0.33107$, $i = 81^o.84$, $T_1 = 8720K$, $T_2 = 4317K$, $\Omega_1 = 4.3781$, $g_1 = 1$, $g_2 = 0.32$, $A_1 = 1.0$ and $A_2 = 0.5$ similar to RZ Cassiopeiae is chosen and light curves are generated in the J and the K bands. The adopted parameters are typical for the Algol system RZ Cas.

The study of period variations is an important tool to know about the different physical processes happening in a binary system. The nature of variations of the observed period monitored over a long period will tell us about mass transfer, apsidal rotation, presence of extra components in the system, magnetic activity etc. So the moments of occurrence of the primary minima determined from the

observed eclipses contribute to this information. The deep secondary minimum of an IR light curve will also enable us to determine the moment of secondary minimum more accurately, which will help us to look for the shift of the minima from $0^p.5$ which is indicative of elliptical orbit of the binary. Since the secondary eclipses of the optical light curves of most of the Algols are very shallow, this information is seldom available from the optical light curves of Algols.

1.4 Summary of the Thesis

The present work deals with study of two Algol binary systems in the near IR photometric bands J and K. An attempt is made to use the increased depth of the secondary minima in these bands to understand the nature of the secondary stars. We have also looked for the signatures of the activity of the secondary resulting from its fast rotation and the expected convective nature of its atmosphere.

Chapter 2 gives a brief description of the model and explains various parameters and their significance. Also given are the details of the observations and the method of analysis. Light curve simulations are carried out using the Wilson's model to show the effect of a high reflection albedo of the secondary star and to demonstrate how it can mimic the presence of a dark spot on the secondary star. It is also demonstrated how a dark spot on the secondary star will be better detected in the near IR bands.

Chapter 3 describes the observation and analysis of the J and K light curves of the Algol system RZ Cassiopeiae in detail. Complete light curves of this star are obtained in these bands for the first time, and analyzed with the Wilson's program and the system parameters are derived. Modeling is done for spots and the signatures of the probable presence of dark spot on the secondary are found.

One of the most famous members of the Algol family, R Canis Majoris, is studied in detail in Chapter 4. First near IR light curves of this star in the J and K

bands are obtained. The system parameters are determined from the analysis of the light curves. Optical light curves in the narrow and wide bands of U,B,V, H_β, H_α available in the literature are reanalyzed by Wilson's program. A comparative study is done with the results obtained from different photometric bands.

Chapter 5 gives a short summary of the results and lists some of the future work that need to be done to gain better understanding about Algol binary systems in general and these two interesting systems, RZ Cas and R CMa , in particular.

Chapter 2

Observation and Data Analysis

2.1 Observation

Observations were done from the Mt. Abu Observatory ($72^o\ 47'\ E, 24^o\ 39'\ N$, $1680m$) with the 1.2m (f/13) Gurushikhar IR telescope and a near IR photometer with an LN_2 cooled InSb detector attached to the Cassegrain focus. The details of the instrument can be seen in Ashok *et al.* (1994) & Sam Ragland (1996) some of which are presented in Table 2.1. For subtraction of the background, we alternated the beam between the star and the adjacent sky using a vibrating tertiary mirror and phase sensitive detection was used to enhance the signal to noise ratio. Typically we have used a chopping amplitude of $26''$ and a focal plane aperture of $26''$. Chopping was done at a frequency of 10 - 15 Hz. For both program stars and their comparison stars, an integration time of 20s was used for each data point acquired. After each observation of the star, the sky nearby is observed and subtracted from the observation of the star in order to remove any sky or instrumental gradient and instrumental offset, if present.

Light curves were obtained in the near IR bands J ($1.25\mu m$) and K ($2.2\mu m$) for two short period Algol systems RZ Cas and R CMa. Observations were done in the order C - V - V - C and the differential magnitudes are calculated (C refers to the comparison star and V, the variable star). The comparison stars were selected close to the binary under observation to minimize the effects of changing sky transparency and atmospheric extinction corrections. The check stars were observed

Table 2.1: Details of the instrument.

Components	Particulars	Values
1. Detector	Material	Photovoltaic InSb (0.5mm diameter)
	Spectral range	1 - 5 μm
2. Filter	Band (λ_{eff} μm)	Bandwidth (FWHM) μm
	J / 1.25	0.32
	H / 1.65	0.34
	K / 2.20	0.40
3. Focal Plane	size (mm)	Arcsec. on the sky
Aperture		(1.2m, f/13 beam)
	2	26.4
	3	39.6

two or three times during the night to keep watch on the stability of brightness of the comparison star. Most of the observations were done within airmass 2.0 except on very few occasions of observations of some eclipses, parts of which go beyond airmass of 2.0. Typical errors of observations are $\pm 0^m.03$ in the J band and $\pm 0^m.04$ in the K band. The atmospheric extinction coefficients were derived by fitting a straight line to the observed instrumental magnitudes of the comparison star and the airmass of observation. The observed magnitudes are corrected for extinction using the derived extinction coefficient for each night. Observed values of first order extinction coefficients varied from 0.08 - 0.15 in J band and 0.08 - 0.17 in the K band. Colour corrections are not applied since the observations are always done in single band at a time.

2.2 Data Analysis

The average observed relative magnitude at phase = 0.25 is subtracted from the respective light curves, and the relative magnitudes are converted to light values

and averaged in phase intervals of 0.01 to form normal points for the analysis. Each light value used for analysis is weighted by the number of points used for forming the corresponding normal point. Weighting is also applied according to the light level. The light curves are analyzed using the Wilson's model for eclipsing binary stars Wilson (1979). A brief description of the model is given in section 2.3.

2.3 The Model

The Wilson's model for eclipsing binary stars is *identical to*[1] the Roché Model. In this model the binary system is represented by two stars of temperatures $T_1 \& T_2$ and masses $M_1 \& M_2$ going around the common center of mass in a circular or elliptical orbit of eccentricity e. The plane of the orbit can be at any angle, i [2], with respect to the sky plane, which is normal to the line of sight of the observer. The surface of each of the component star is assumed to lie on one of the Roché equipotential surfaces Ω_1 or Ω_2. The stars can spin synchronously with the orbital rotation or can be non-synchronous represented by rotation ratios $F_1 \& F_2$ for the primary and the secondary respectively, where F is the ratio of the orbital rotation rate to the spin rate. The light emitted from different regions on the star surfaces is modified by the limb darkening of the star surfaces, parameterized by limb darkening coefficients $x_1 \& x_2$, which make the surface elements anisotropic radiators, gravity darkening (parameterized by $g_1 \& g_2$, the gravity darkening coefficients) and irradiation and heating of the star surface by the companion, commonly called reflection effect (parameterized by bolometric albedos of the star surfaces $A_1 \& A_2$). Total light from each star is represented by the monochromatic luminosities $L_1 \& L_2$. The equipotentials in this model are computed on the assumption of complete central

[1] Roché equipotentials are defined for circular orbits. In elliptical orbits, the field become non-conservative, but we can consider the system at each moment with variable separation and define instantaneous Roché equipotential surfaces which can be considered to represent the system over short fractions of the period, provided the stars are able to adjust themselves to the changing field over short time-scales. But, if the stars are not able to adjust themselves to the changing fields fast, the assumed figure will not be a correct representation of the stellar surface.

[2] $i = 90^o$ implies a totally eclipsing system along the line of sight and $i = 0^o$ implies a non eclipsing system whose orbital plane is perpendicular to the line of sight.

condensation for both the stars as described in chapter 1.

The surface potentials are defined by the equation

$$\Omega = \frac{1}{r} + q\left\{\frac{1}{(D^2 - 2\,\lambda\, r D + r^2)^{-1/2}} - \frac{\lambda\, r}{D^2}\right\} + \frac{1}{2}\,F^2\,(q+1)\,r^2\,(1-\nu^2) \qquad (2.1)$$

where $q = M_2/M_1$, λ and ν are direction cosines of any point at which we are calculating the Ω. Equation 2.1 is obtained when equation 1.3 modified to represent the component stars rotating non-synchronously in elliptical orbits. D is the instantaneous separation between stars, which vary from $1 - e$ at periastron to $1 + e$ at apstron. D = 1 for circular orbits. For a component for which the the axial rotation is synchronous with the orbital rotation, F = 1. Since equation 2.1 is formulated in such a way that we have to deal with only the mass ratio $q = M_2/M_1$ rather than individual masses, Ω is much simpler to handle than the original potential Ψ. Origin of the co-ordinates is at the center of mass of the component eclipsed during the primary minimum. Equation 2.1 is solved for $r(\theta, \phi, q, \Omega, F, D)$ by Newton - Raphson method. Next, the numbers proportional to the rectangular components of the gradient of potential at each point on the surface are calculated $(\partial\Omega/\partial x, \partial\Omega/\partial y, \partial\Omega/\partial z)$ which provide the local normals and surface potentials. These are proportional to the derivatives of Ψ. The flux in the observer's direction is calculated integrating the light contribution from all surface elements from both the stars, taking care of the phase and eclipse, orientation of the element with respect to the line of sight, limb darkening, gravity darkening, reflection effect and adopting a suitable model atmosphere for the star.

The model also has a provision to include any extra, non eclipsing source of light, the third light, l_3 and spots represented by the latitude, longitude, angular radius and temperature factor (T_{spot}/T_{star}) of the spot. Out of these L_1, L_2, l_3 & x_1, x_2 are wavelength dependent and the rest of the parameters are independent of wavelength. This model uses linear least - square analysis and differential corrections to arrive at the final parameters from an initial set of parameters. Wilson's program takes the model atmosphere of Carbon & Gingerich (1969) (Wilson & Devinney 1971, Wilson 1979, 1990, 1993).

2.3.1 *Limb Darkening*

In the stellar atmospheres, the density and temperature decreases upwards. So we find a particular surface element brighter, when we look at it in the direction of the local normal and the observed intensity reduces with increasing angle from the normal. Limb darkening is this variation in the intensity of light emitted by unit area of the stellar surface, depending on the angle at which we look at a particular surface element of the star. This is a manifestation of the departure of the stellar atmosphere from an ideal black body, the emission of the black body being isotropic and homogeneous. Limb darkening is dependent on the temperature of the star and the wavelength of observation.

Several laws have been proposed to model limb darkening. The first one is the *linear limb darkening law* according to which the light intensity varies linearly with the angle with respect to the normal to the surface ie.,

$$J_\lambda(\mu) = I_\lambda(\mu)/I_\lambda(1) = 1 - x_\lambda(1-\mu) \tag{2.2}$$

where $\mu = cos(\theta)$ and x_λ is the linear limb darkening coefficient. Al Naimiy (1978) obtained linear limb darkening coefficients by averaging the I_λ vs μ slopes from the Carbon & Gingerich (1969) model stellar atmosphere. He has derived the limb darkening coefficients for a range of temperatures (50000 K to 4000 K), wavelengths ($0.2\mu m$ to $2.2\mu m$) and surface gravities g ($2.0 \leq log(g) \leq 5.0$).

Often a two parameter limb darkening law is used for better representation of the actual emergent intensity of light over the stellar disk. A quadratic law for limb darkening can be written as

$$J_\lambda(\mu) = I_\lambda(\mu)/I_\lambda(1) = 1 - x_\lambda(1-\mu) - y_\lambda(1-\mu)^p \tag{2.3}$$

in which there are two limb darkening coefficients x_λ and y_λ and p is an integer.

Manduka, Bell & Gustafsson (1977), Wade and Rucinski (1985) and Claret and Gimenez (1992) studied the quadratic case with p = 2 and presented tables

of linear and quadratic limb darkening coefficients. Different stellar atmospheric models and computational methods are used to calculate these coefficients. Manduka, Bell & Gustafsson (1977) used the grids of model atmosphere for cool giants and super-giants by Bell *et al.* (1976). Wade and Rucinski (1985) obtained the coefficients using the model by Kurucz (1979).

Another successfully applied non-linear limb darkening law is the logarithmic law,

$$J_\lambda(\mu) = I_\lambda(\mu)/I_\lambda(1) = 1 - x_\lambda(1-\mu) - y_\lambda\ \mu\ ln(\mu) \tag{2.4}$$

by Klinglesmith and Sobieski (1970). Diaz-Cordores and Gimenez (1992) considered the non-linear square root law and compared the results

$$J_\lambda(\mu) = I_\lambda(\mu)/I_\lambda(1) = 1 - x_\lambda(1-\mu) - y_\lambda(1-\sqrt{(}\mu)) \tag{2.5}$$

with those obtained with the linear law (2.2) and quadratic law (2.3) with p=2. They found the square root law (2.5) to better represent the theoretical intensities of Kurucz (1979) models for stars hotter than 8500 K.

The value of limb darkening increases towards late type type stars and is higher for shorter wavelengths than for longer wavelengths. The limb darkening coefficient can be determined from a light curve of very good accuracy.

2.3.2 *Gravity Darkening*

In a close binary system, the shape of one or both of the stars will be highly distorted from spherical due to the mutual tidal interaction and the equipotential surfaces are closer along the polar directions than along the equatorial directions (Chapter 1). So the rate of flow of heat from the center will be different in different directions, being maximum towards the poles, making the poles hotter than the equator (Pringle & Wade 1985). This phenomenon is also termed *gravity brightening* by some authors. The effective temperature at the pole, $(T_e)_{pole}$, is related to the

surface average effective temperature $\bar{T_e}$ by

$$(T_e)_{pole} = \bar{T_e} \left\{ \frac{S}{\left[\int_{surface} (\nabla\phi)^g dS\right]} \right\}^{0.25} \tag{2.6}$$

(Wilson 1979), where S is the surface area of the star, $\nabla\phi$ is the local gradient of potential and g is the exponent of gravity darkening.

2.3.3 Reflection Albedo

In a close binary system, where, two hot bodies are separated by a distance of the order of a few times their radii, it is natural that the facing hemisphere of each star is strongly irradiated by the light from the facing hemisphere of the companion. This phenomenon is commonly called reflection effect in binary system. How much of this irradiated light is absorbed, depends very much on the properties of the atmosphere of the irradiated star and is commonly represented in the binary star light curve analysis methods by a parameter, the bolometric albedo, A, which is the local ratio of re-radiated to incident energy over all wavelengths. A is theoretically 1 for radiative atmospheres and 0.5 for convective atmospheres (Rucinski 1969). In Algols the primary component has a radiative atmosphere while the atmosphere of the secondary component is convective. Detailed treatment of the reflection effect is given in Wilson (1990). In a binary system of the Algol type, where a cooler star is in the company of a hotter star of nearly double its temperature, the surface of the secondary, facing the primary will be hotter compared to its rear surface due to the light incident from the primary. But the effect of the cool secondary on the primary is negligible. Also the light reflected (re-radiated) can change the shape of the light curve, especially outside the minima. Light curves are simulated to bring out the effects of the bolometric albedo of the secondary and the primary stars.

To learn the effect of a high albedo, light curves are simulated for a typical Algol binary, with $A_2 = 0.5$ and $A_2 = 1.0$. A binary star is considered with $i = 81^o.84$, $T_1 = 8720K$, $T_2 = 4317K$, $\Omega_1 = 4.3781$, $q = 0.33107$, $g_1 = 1.0$ and

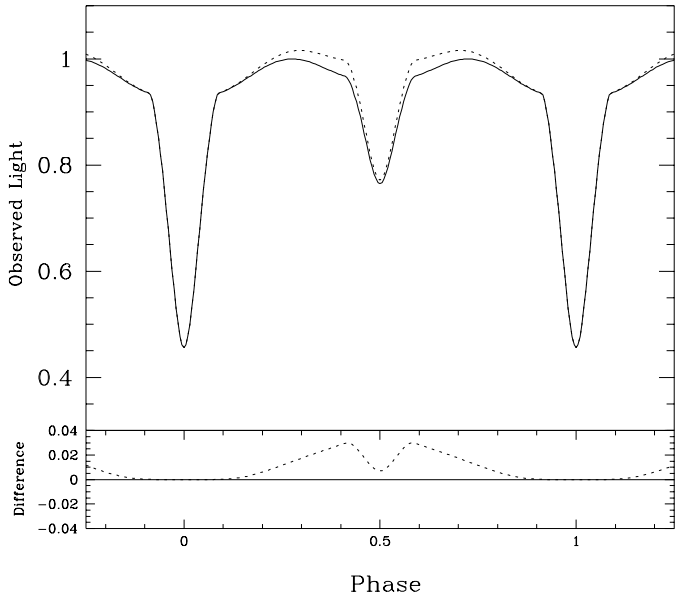

Figure 2.1: Effect of change of A_2 on the light curve of an Algol type star. The continuous line is the model for $A_2 = 0.5$ and the dotted line is for $A_2 = 1$. The bottom panel shows the difference between the two models on an expanded scale.

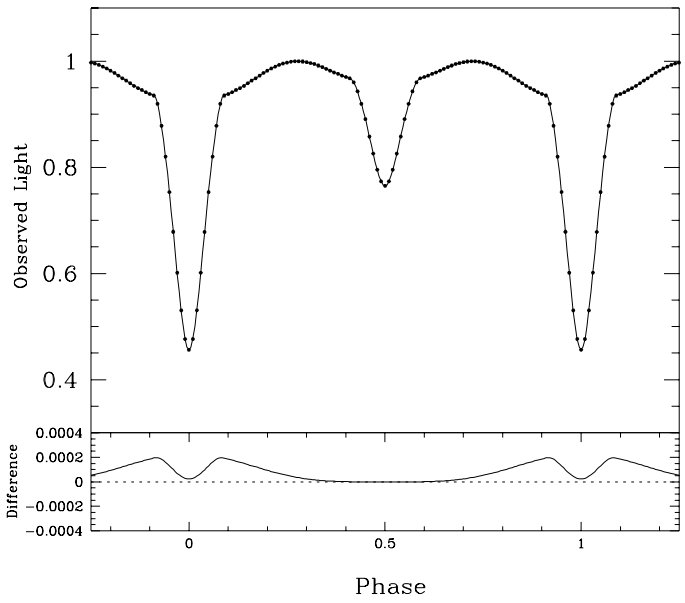

Figure 2.2: Effect of change of A_1 on the light curve of an Algol type star. The continuous line is the model for $A_1 = 1$ and the dotted line is for $A_1 = 0.5$. $A_2 = 0.5$ is adopted in both these cases. The bottom panel shows the difference between the two models on an expanded scale.

$g_2 = 0.32$. The system considered is similar to RZ Cassiopeiae. The limb darkening coefficients corresponding to the temperatures and surface gravities for the components of RZ Cas (Table 3.7) are adopted from Al Naimiy (1978). Fig. 2.1 shows the synthetic light curve at 2.2 μm with $A_2 = 0.5$ and $A_2 = 1.0$. The reflected light increases from the end of primary eclipse, where it is zero, and becomes maximum (the difference between models with $A_2 = 1.0$ & $A_2 = 0.5$ being 3 % of the total system light) just before the beginning of the secondary eclipse and again decreases towards secondary minimum. Here the bolometric albedo of the secondary star is a significant parameter and it can produce a visible change in the observed light curve. So the value of the A_2 has to be properly taken care of in the light curve analysis. The change in A_2 will not affect the light curve at the primary minimum. Fig 2.2 shows how a change in A_1 will affect the light curve. Here the reflected light increases from the end of secondary eclipses, where it is zero, toward the beginning of the primary eclipse (the difference between models with $A_1 = 1$ & $A_1 = 0.5$ being only 0.02 % for the system under consideration). Thus the effect of A_1 on the light curve will be negligible, and less by two orders of magnitude compared to the effect of A_2 in an Algol type system as evident from fig 2.1 and fig 2.2. This is because the temperature of the primary is much higher compared to that of the secondary in an Algol type system.

The version of the Wilson-Devinney program used in the present work uses improved treatment of the binary star Reflection Effect (Wilson 1990). This version requires bolometric limb darkening coefficients in addition to the effective wavelength specific limb darkening coefficients for the treatment of reflection. Van Hamme (1993) has derived the bolometric limb darkening coefficients and supplied tables of the linear and non-linear coefficients for logarithmic and square root laws for stars at different temperatures and surface gravities.

2.3.4 *Presence of Spots*

We have seen in section 1.2 that the secondaries of Algols are expected to show chromospheric activity. Presence of cool spots is one of the manifestations of chromospheric activity. Large scale spot activities are mainly noticed in the optical light curves of a particular group of chromospherically active binary stars called RS CVn binaries, in which the light curves are subjected to large distortions and the positions of these distortions on the light curves are found to be shifting with time. These are modelled with large spots or spot groups (magnetically activated similar to those seen in the sun, but on much larger scales) migrating on the star surface. These stars showed large values of fluxes in the radio and X-ray wavelengths (1.2.3) In this section, some simulations are presented, which will bring out the effect of a cool spot on the secondary in different wavelengths.

The parameters of RZ Cas as considered in section 2.3.3 are used for the simulations of spots. A cool spot of angular radius 25^o and with a temperature 75 % of T_2 is placed on the back surface of the secondary star (longitude $= 180^o$) at a latitude of $= 90^o$. Fig. 2.3, 2.4 and 2.5 show the simulated light curves in the U, V and K bands. The dotted line shows the model with cool spot, the continuous line shows the model without spots and $A_2 = 0.5$ and the dashed line represents the unspotted model with $A_2 = 1.0$. The difference between the spotted and unspotted models are shown at the bottom of each diagram on an expanded scale. The spot doesn't have any effect on the light curves during the secondary eclipse and it will affect the light curves only around the primary eclipse. The depth of the primary eclipse increased by only 0.38 % in the U band and 0.92 % in the V band, whereas the primary eclipse depth increased by 3 % in the K band. This spot can be detected in the K band whereas it will go un-noticed in the optical photometric bands. Also the spot produced a fall in the observed light from the end of the secondary eclipse towards the beginning of the primary eclipse. It is also noticeable that a high A_2 will be well noticed in all the wavelengths under consideration. Models with $A_2 = 1.0$ is higher than the one with $A_2 = 0.5$ by 2.2 % in the U band, 2.4 % in the V band

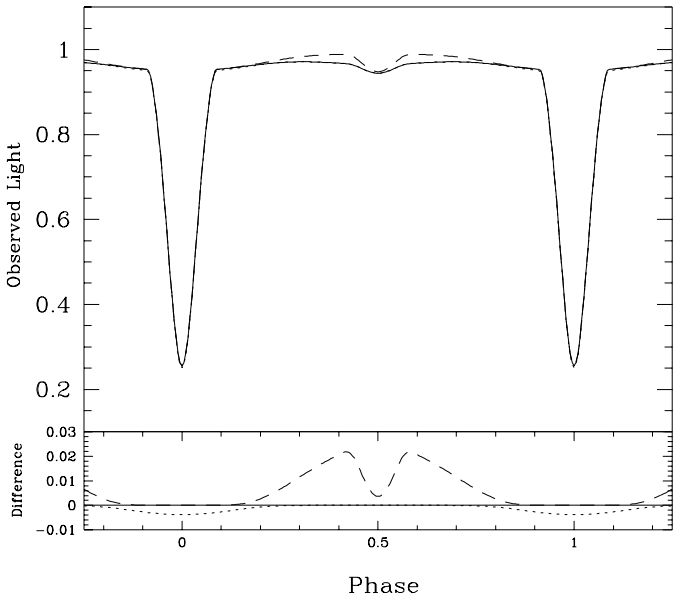

Figure 2.3: Effect of the presence of a cool spot on the secondary of a typical Algol binary in the U band. The continuous line shows the model with $A_2 = 0.5$ and without spot. The dashed line is the model for the same star with $A_2 = 1$. The dotted line is the model with a dark spot on the back side of the secondary. The difference of both these models with the model for a normal star with $A_2 = 0.5$ is shown in the bottom panel

and 3.0 % in the K band. With the adopted spot parameters, it is clear from Fig. 2.5 that in the region outside eclipse, a cool spot on the back side of the secondary can give a feeling of the presence of a high A_2 . So, without taking care of the presence of spot, if we fit the above light curve, with A_2 as a free parameter, the model will fit with a high A_2. Thus we can see that in a typical Algol, a cool spot on the secondary is likely to go un-detected in the optical bands, whereas it will have a very clear signature in the infrared light curves. Figs. 2.6 and 2.7 show the effects of cool spots at longitudes 270^o and 315^o respectively on the secondary star and the regions of the light curves affected by these spots in the K band.

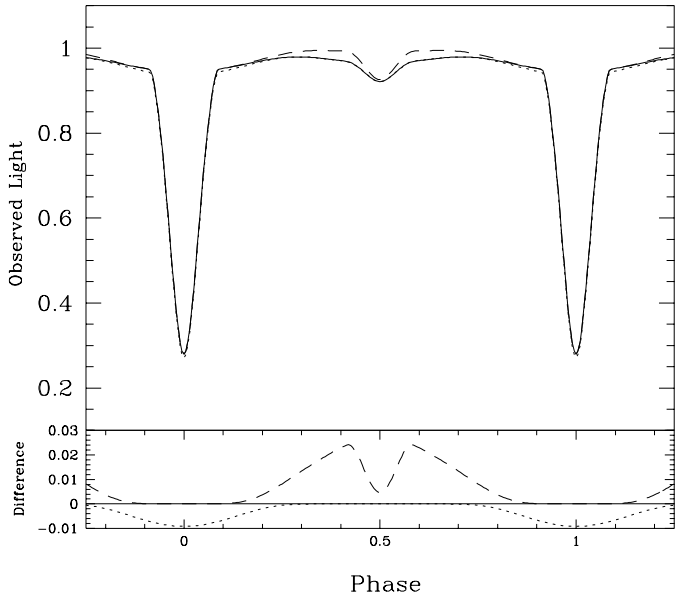

Figure 2.4: Effect of the presence of a cool spot on the secondary of a typical Algol binary in the V band. The continuous line shows the model with $A_2 = 0.5$ and without spot. The dashed line is the model for the same star with $A_2 = 1$. The dotted line is the model with a dark spot on the back side of the secondary. The difference of both these models with the model for a normal star with $A_2 = 0.5$ is shown in the bottom panel

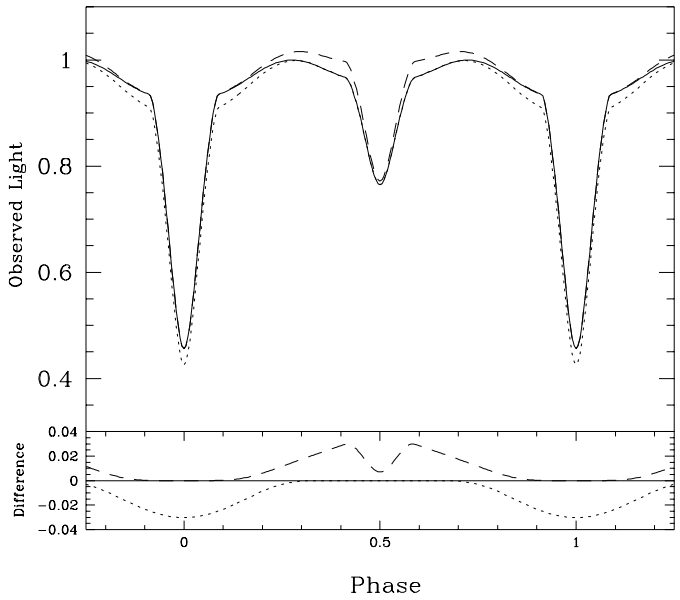

Figure 2.5: Effect of the presence of a cool spot on the secondary of a typical Algol binary in the K band. The continuous line shows the model with $A_2 = 0.5$ and without spot. The dashed line is the model for the same star with $A_2 = 1$. The dotted line is the model with a dark spot on the back side of the secondary. The difference of both these models with the model for a normal star with $A_2 = 0.5$ is shown in the bottom panel

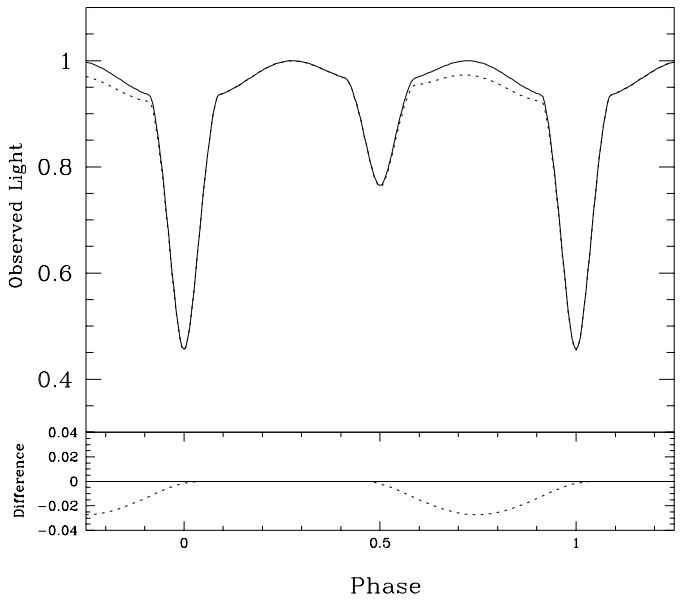

Figure 2.6: Effect of the presence of a cool spot on the secondary of a typical Algol binary in the K band at a longitude of 270^o. The continuous line is the model without spot and the dotted line is the light curve affected by spot. The difference between the two models is shown in the lower panel

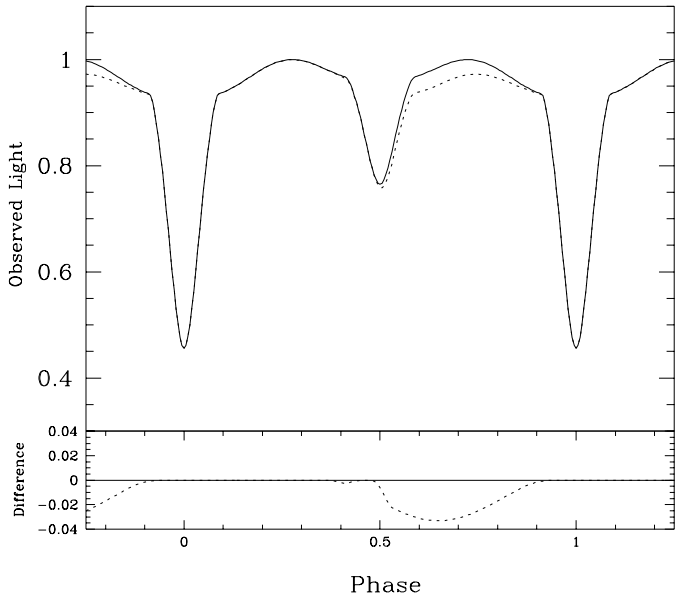

Figure 2.7: Effect of the presence of a cool spot on the secondary of a typical Algol binary in the K band at a longitude of 315^o. The continuous line is the model without spot and the dotted line is the light curve affected by spot. The difference between the two models is shown in the lower panel

Chapter 3

Near Infrared Photometric Studies of RZ Cassiopeiae

3.1 Introduction

RZ Cassiopeiae (RZ Cas, HD 17138, HR 815, SAO 12445, BD $+69^o$ 179) is a semi-detached eclipsing binary system of the Algol type. Its variability was discovered by G. Muller in 1906. Being a bright system with very deep primary eclipses in the optical wavelengths (V = $6^m.18$, ΔV = $1^m.5$) extensive photometric light curve study of this star has been done by many observers (Huffer 1955, Huffer & Kopal 1951, Chambliss 1976, Riazi, Bagheri & Faghihi 1994, Maxted, Hill & Hilditch 1994 and Narusawa, Nakamura & Yamasaki 1994).

This system was found to exhibit disturbances in the light curves, especially during the primary eclipse. The period was found to have frequent variations. Photometric analysis by all previous observers show this system to be a partially eclipsing one though many observers have observed primary minima with flat bottom lasting for several minutes (Szafraniec 1960, Arganbright, Osborn & Hall 1988, Hegedus 1989 and Narusawa, Nakamura and Yamasaki 1994). The colours of the system at the primary minima are also found to indicate partial eclipses only. Light curve distortions are observed at the primary minima, often as rise in flux near the mid eclipse. Olson (1982) described this as the probable indication of a disk-like bulge around the equator of the gainer (primary) and a gas stream from the subgiant secondary to the primary. He also proposed asymmetric distribution

of brightness of the disk due to the presence of a hot spot where the stream impinges on the disk. The cause of the flat minimum is not satisfactorily explained till now.

All the information about this bright binary system are derived from the photometric and a few spectroscopic investigations in the optical wavelengths. Observations in the radio (Drake, Simon & Linsky 1986, Umana, Catalano & Rodono 1991) and X-ray wavelengths (Mc Cluskey & Kondo 1984) gave strong indications of chromospheric activity in this system. X-ray observations by Schmitt *et al.* (1990) gave indications of a hot corona in RZ Cas and they calculated the coronal temperature to be $\sim 10^7$ K.

The depth of secondary minimum in the optical photometric bands ($\Delta V = 0^m.08$) is insufficient to get a clear picture of the features of the secondary star. So we have attempted to study the light curve of this system in the near infrared bands J and K, in which the secondary minima are much deeper compared to those in the optical bands, due to increased relative contribution of light from the secondary star towards the total system light. These are the first observations of this binary in the near infrared bands.

3.2 Observations

Observations were done with the 1.2 m Mt. Abu IR Telescope, India, and a near IR photo meter with an LN2 cooled In Sb detector during the period 6, Oct. 1995 to 28 Nov. 1996. The system is observed in the J band for 20 days and in the K band for 15 days. The details of the instrument are given in Ashok *et al.* (1994) and Sam Ragland (1996). HR 791 and ψ Cas were used as comparison and check stars respectively (*Bright Star Catalogue*). The details of RZ Cas, HR 791 and ψ Cas are given in Table 3.1. HR 791, though a spectroscopic binary star, was used as a comparison star for the optical observations of RZ Cas by several observers due to its similarity in spectral type and brightness to RZ Cas (Huffer 1955, Chambliss

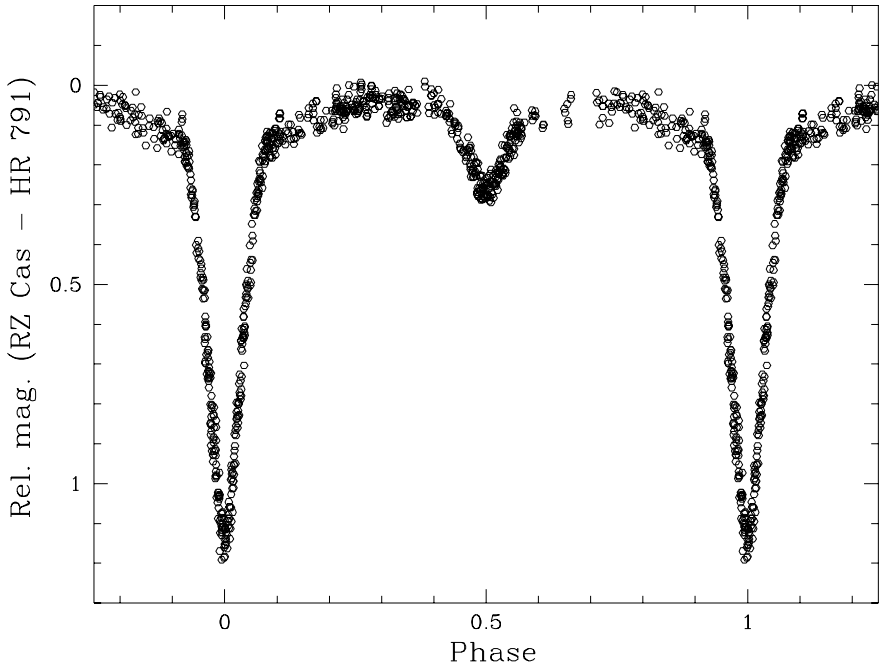

Figure 3.1: Complete observed points (rel. mag. RZ Cas - HR 791) in the J band.

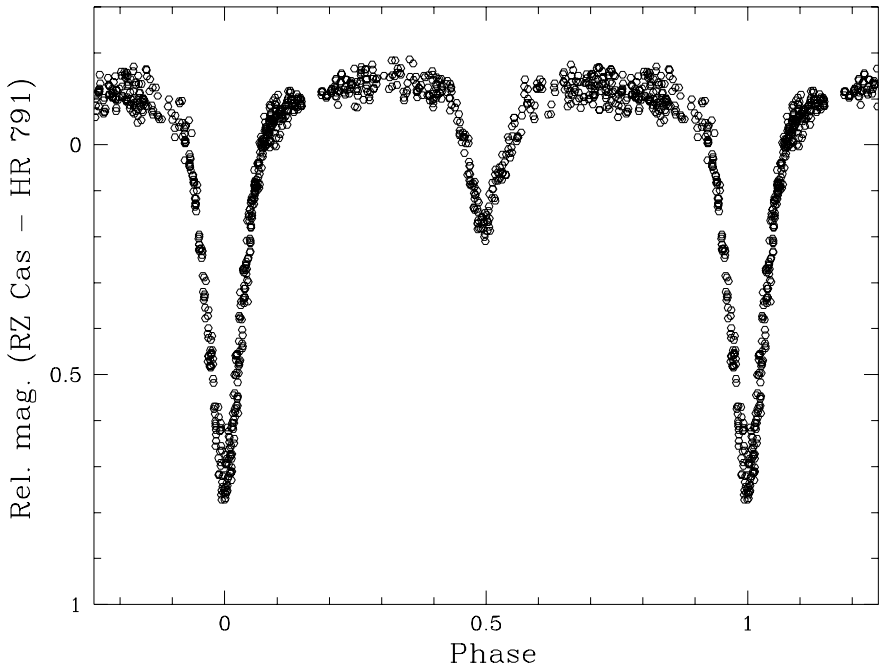

Figure 3.2: Complete observed points (rel. mag. RZ Cas - HR 791) in the K band.

Table 3.1: The co-ordinates, spectral types and magnitudes of RZ Cas, HR 791 & ψ Cas. *: Spectral type of the primary of RZ Cas (Maxted, Hill & Hilditch 1994)

Star Name	α_{2000}	δ_{2000}	V	B-V	U-B	Sp. type
RZ Cas	02 48 55.5	+69 38 03	6.18	+0.18	+0.10	A3* V
HR 791	02 44 42.7	+67 49 29	5.95	+0.10	+0.17	A5 III
ψ Cas	01 25 56.0	+68 07 48	4.74	+1.05	+0.94	K0 III

1976, Argenbright, Osborn & Hall 1988). Also in the JHK bands this star is bright enough for our system to get a good signal to noise ratio with the same integration time as used for RZ Cas.

There are no previous infrared observations existing for HR 791 to the best of our knowledge. The observed J, H and K band magnitudes of these stars are given in table 3.2. The J-H and H-K colours of HR 791 observed by us are typical for a star of spectral type A5 III as determined from optical observations. ψ Cas was observed by Neugebauer & Leighton (1969) in the 2μ Sky Survey. J-H and H-K colours of this star correspond to a star of spectral type K0 III as found by previous investigators. The observed J and K magnitudes of RZ Cas at phase = 0.25 and eclipse depths are given in Table 3.3. The primary standard used for photometry was HR 696 (Elias *et al.* 1982, Scott 1988). $BD\ +57^0\ 647$ (Scott 1988) was also observed. Typical errors of observations are $\pm 0^m.03$ in J band and $\pm 0^m.04$ in H and K bands.

The observations of RZ Cas and BS 791 are done in the sequence C-V-V-C with observations of the check star two to three times per night. V refers to the variable star under study and C, the comparison star. The extinction coefficients for each night are obtained by doing linear least square fit to the observed instrumental magnitudes of the comparison star and extinction correction is applied to

Table 3.2: Observed J, H & K magnitudes and colours of HR 791 & ψ Cas

Star Name	J	H	K	V - K	J - H	H - K
HR 791	5.71	5.67	5.63	0.32	0.04	0.04
ψ Cas	3.01	2.48	2.41	2.33	0.53	0.07

Table 3.3: Observed magnitudes and eclipse depths of RZ Cas in the J & K bands.

Photometric band	Magnitude at maximum brightness	Eclipse depth	
		Primary	Secondary
J	5.76	1.08	0.21
K	5.50	0.87	0.30

the observed relative magnitudes of RZ Cas. We have not applied colour corrections as observations were always done in single band. 839 and 947 individual observations of RZ Cas were obtained in the J and K band respectively with good coverage of phase. The epochs of observations, phases and the observed relative magnitudes are given in Appendices 1 and 2 respectively. Fig. 3.1 & 3.2 show the observed light curves of RZ Cas in the J and K bands.

Seven epochs of primary minima (5 in J band and 2 in K band) and 3 epochs of secondary minima (1 in J band and 2 in K band) are observed. Epochs of minima are calculated using the method given by Kwee & van Woerden (1956). The epochs of secondary minima are determined with similar accuracies that of the epochs of primary minima due to the enhanced depths of the secondary minima in the J and K bands compared to those in the optical bands. The epochs determined, errors, bands of observations, number of points and type of minima (primary (PM)

Table 3.4: Observed epochs of minima of RZ Cas

Epoch of minimum(HJD)	Band	No. of Pts.	Minima type
2450017.4178±0.0007	K	69	SM
2450032.3587±0.0008	K	71	PM
2450035.347 ±0.001	J	35	SM
2450037.1411±0.0005	J	35	PM
2450062.2402±0.0005	J	49	PM
2450092.1244±0.0004	J	33	PM
2450093.3174±0.0003	J	37	PM
2450114.2288±0.0005	K	27	SM
2450117.2228±0.0005	J	50	PM
2450387.3514±0.0004	K	27	PM

or secondary (SM)) are given in Table 3.4. None of the minima shows flat bottom. We have derived a new ephemeris for RZ Cas by doing a linear least square fit to our observed epochs of primary minima.

$$JD\ Hel.\ Min\ I = 2450020.4070\ (\pm 0.0005)\ + 1^d.1952592\ (\pm 0.000004)\ E_0 \qquad (3.1)$$

The phases for constructing our J and K light curves are calculated according to this new ephemeris. All the secondary minima appeared at phase 0.5 implying a circular orbit.

3.3 *Light Curve Analysis*

The Wilson - Devinney model is used to analyze the light curves and the physical parameters of RZ Cas are derived. The J and K light curves observed in the present programme are analyzed and the results are compared with the results of our analysis of the UBV light curves (obtained by Chambliss 1976) done as a part of the present study.

3.3.1 *Analysis of the J and K band light curves*

The observed relative magnitudes are converted to light units. The average relative magnitude (RZ Cas - HR 791) at phase = 0.25 in each band is subtracted from the observed light curve in the corresponding band and the resulting relative magnitude values are converted into relative light values. The light curves are then averaged in phase intervals of $0^p.01$. 92 and 95 normal points are formed in J and K bands respectively. Each data point is weighted with the number of individual points averaged to form the normal point.

The Wilson's program needs a set of parameters reasonably near the solution to start with. We have adopted the values given by Chambliss (1976) as starting set of parameters for the analysis of J band data. The output values of the J band analysis are used as starting values for the analysis of the K band data. *Mode 5* (for the semi-detached systems) is selected and differential corrections are applied to the light curves. The program parameter $noise = 2$ is selected so that observational scatter is assumed to depend upon light levels. Both the light curves are analyzed separately as well as simultaneously. The mass ratio, q, which is one of the most important parameters of the Roché model, for RZ Cas is determined by Maxted, Hill & Hilditch (1994) with good accuracy from the radial velocity curves of both the primary and the secondary. The value of q obtained by Maxted, Hill & Hilditch $(q = 0.331)$ is close to those used by previous observers. (Chambliss 1976 (0.35), Duerbeck & Hanel 1979 (0.35), Narusawa, Nakamura & Yamasaki 1994 (0.319)). So we have adopted q as determined by Maxted, Hill & Hilditch as a fixed parameter in the light curve fitting. F_2, the ratio of the axial rotation to the mean orbital rotation for the secondary star was adopted to be 1. Since the secondary is a lobe-filling component in the close binary system, it is justifiable to consider it to be a synchronous rotator. The corresponding parameter, F_1, for the primary, though left as a free parameter in the initial iterations with 1.000 as the starting value, didn't vary by more than its probable error. So the value of F_1, was fixed to be 1.000 in further iterations. g_1 and g_2, the gravity darkening coefficients for

star 1 and 2 were fixed to their theoretical values 1.00 and 0.32 respectively for the primary and the secondary (Von Zeipel 1924, Lucy 1967).

The primary is known to be an A3 V star from previous photometric and spectroscopic studies (Maxted, Hill & Hilditch 1994). So we have fixed the average effective temperature of the primary, T_1, to be 8720 K, corresponding to an A3 V star (Lang 1992) in the analysis. The secondary temperature T_2 is left as a free parameter throughout the analysis. Small change in the value of limb darkening is found to have only mild effect on the light curve. So the values of the limb darkening were fixed to their theoretical values. The linear law was adopted to represent the limb darkening effect. Wavelength specific limb darkening coefficients were taken from the tables of Al Naimiy (1978) and bolometric limb darkening coefficients for the treatment of the reflection effect were taken from Van Hamme (1993). The number of reflections, NREF, was taken as 1 during the initial iterations and was changed to 2 near the minima. Increasing the number of reflections from 1 to 2 had only a minor effect on the corrections to the parameters. The control integer in the model IPB is selected to be 0 so that the luminosity of the secondary L_2 is calculated from the temperatures $T_1 \& T_2$ and the luminosity of the primary star L_1, system geometry and the radiation laws. L_1 is left as a free parameter. Model atmosphere corrections are applied to the primary star luminosity. For calculating L_2 the secondary is considered as a black body since its temperature is below 5000 K and the atmospheric model used by Wilson's programme (Carbon & Gingerich 1969) is recommended for atmospheres only above 5000 K. We tried to explore the possibility of the presence of a third component in the system, releasing the corresponding component l_3 as a free parameter during the initial iterations. The analysis didn't give any signature of third light. Corrections for l_3 fluctuated around the starting value 0.000. So after a few iterations l_3 is fixed to 0.000. In the *Mode 5* for Algol type systems, the potential representing the secondary surface, Ω_2, is determined within the programme from the lobe-filling condition for the given mass ratio. The corresponding potential for the primary surface, Ω_1, is released as a free parameter during the analysis. The bolometric albedos for the

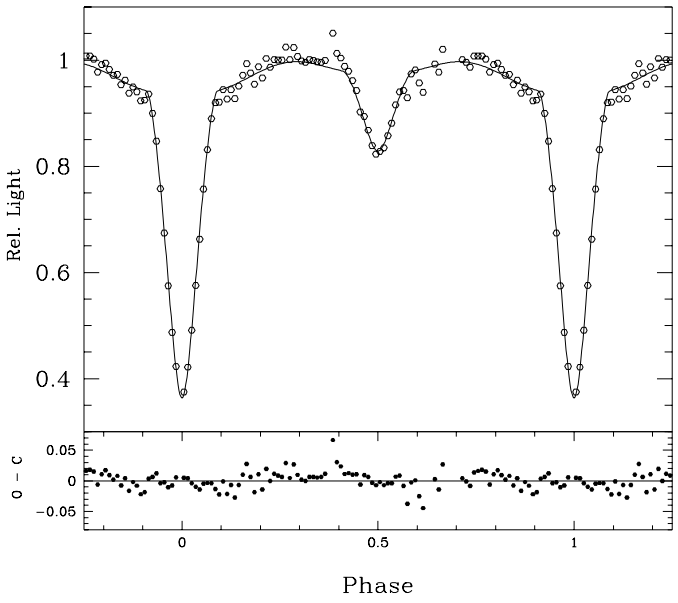

Figure 3.3: J band light curve of RZ Cas. The circles show the normal points formed from the observed light curve and the continuous line shows the model fit with $A_2 = 0.5$. The bottom panel shows the deviations of the observed points from the model.

primary and secondary surfaces, $A_1 \& A_2$, which parameterize the reflection effect, were fixed to their theoretical values 1.00 and 0.50 for the radiative and convective stellar atmospheres respectively.

Table 3.5 shows the results of the light curve fits in J & K bands with the complete set of parameters. (In the tables, a superscript *f* implies that the corresponding parameter was not adjusted during the analysis). Fig. 3.3 and Fig. 3.4 show the model fits in the J & K bands respectively along with the normal points formed for the analysis and the residuals of the fit. The fit is poor outside the primary minima, where systematic residuals are found. The light curves are divided into eight sectors based on the phases of minima and eclipse duration ($0.17 \times$ Period) and the residuals for all sectors are calculated. The arithmetic mean and the r.m.s. values of the residuals (observed - model) in the different sectors of the light curve are given in Table 3.8. This table brings out clearly the poor fit and the asymmetry in the light curve, especially in the regions before and after the secondary minima (the model that we have adopted is symmetric). The large positive residual near the region of beginning and the negative residual near the end of the secondary

Table 3.5: Elements obtained from the analysis of J and K band data with $A_2 = 0.5$. f: fixed parameter.

Parameter	J Band	K Band	J & K Combined	
			J Band	K Band
T_1^f	8720 K	8720 K	8720 K	
T_2	4163 ± 30 K	4249 ± 36 K	4190 ± 25 K	
q^f	0.331	0.331	0.331	
i	$82^o.55 \pm 0.11$	$81^o.81 \pm 0.11$	$82^o.25 \pm 0.08$	
Ω_1	4.236 ± 0.051	4.384 ± 0.050	4.329 ± 0.052	
Ω_2	2.5339	2.5339	2.5339	
$r_{1\ pole}$	0.255 ± 0.003	0.246 ± 0.003	0.250 ± 0.002	
$r_{1\ point}$	0.261 ± 0.004	0.251 ± 0.003	0.255 ± 0.002	
$r_{1\ side}$	0.258 ± 0.004	0.249 ± 0.003	0.252 ± 0.002	
$r_{1\ back}$	0.260 ± 0.004	0.250 ± 0.003	0.254 ± 0.002	
$r_{2\ pole}$	0.2684	0.2684	0.2684	
$r_{2\ point}$	0.3886	0.3886	0.3886	
$r_{2\ side}$	0.2796	0.2796	0.2796	
$r_{2\ back}$	0.3123	0.3123	0.3123	
x_1^f	0.250	0.150	0.250	0.150
x_2^f	0.470	0.320	0.470	0.320
$x_{1\ bol}^f$	0.573	0.573	0.573	
$x_{2\ bol}^f$	0.528	0.528	0.528	
g_1^f	1.00	1.00	1.00	
g_2^f	0.32	0.32	0.32	
A_1^f	1.000	1.000	1.000	
A_2^f	0.500	0.500	0.500	
$L_1/(L_1+L_2)$	0.804 ± 0.006	0.680 ± 0.006	0.793 ± 0.004	0.692 ± 0.005
$L_2/(L_1+L_2)$	0.196 ± 0.011	0.320 ± 0.016	0.207 ± 0.008	0.308 ± 0.011
l_3^f	0.000	0.000	0.000	0.000

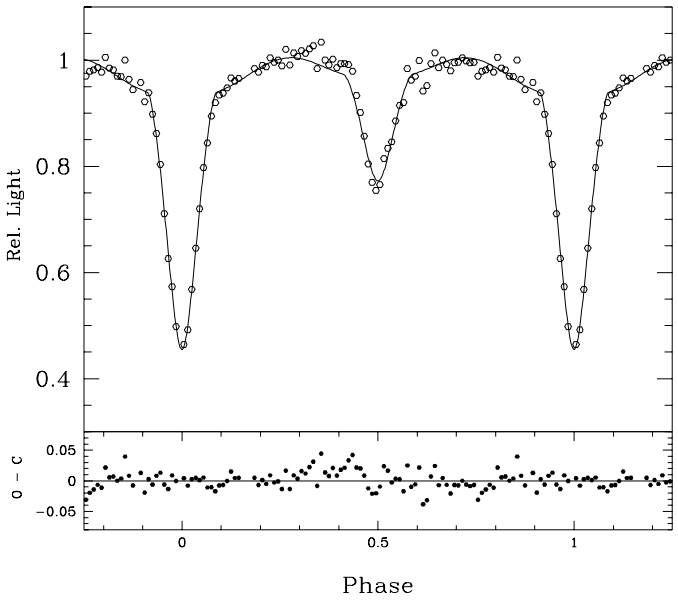

Figure 3.4: K band light curve of RZ Cas. The circles show the normal points formed from the observed light curve and the continuous line shows the model fit with $A_2 = 0.5$. The bottom panel shows the deviations of the observed points from the model.

eclipse are noticeable in the arithmetic mean of residuals of both the light curves. The effect is more pronounced in the J band than in the K band. The average value of T_2 derived is 4190 K, which is less than the T_2 derived by Maxted, Hill & Hilditch (1994) and Narusawa, Nakamura and Yamasaki (1994). It is less by 300 K from the value of T_2 derived by our own analysis of the Chambliss' optical light curves (section 3.3.2). The T_2 derived by Chambliss himself is above 5000 K, much higher than our value, but the model used by him is different and he has adopted 9700 K for T_1 which is higher than the value used by us for T_1 (8720 K).

We have attempted to fit the light curves with Ω_2 as a free parameter, adopting the *mode* 2 of the program, looking for the possibility of a detached configuration. But most of the time Ω_2 went below the critical value which is an unphysical situation according to the adopted model where the secondary star becomes bigger than its Roché lobe. So as in the case of all of the previous investigations, this study also reveals that the system is in the semi-detached state.

3.3.2 *Analysis of the UBV light curves*

The light curves published by Chambliss (1976) in the optical bands U, B and Y bands (similar to the standard UBV filters) are of very good accuracy. Chambliss has analyzed the light curves by Wood's method, where the stars are treated as triaxial ellipsoids and Narusawa, Nakamura and Yamasaki (1994) have analyzed these light curves with the program LIGHT2 of Hill (1979). No solutions of these light curves has been done with the Wilson's method. So we have analyzed the light curves with Wilson's program. We have used the normal points given in the Tables VI, VII and VIII of Chambliss. The UBY light curves were analyzed separately as well as together and the derived values of the parameters are given in Table 3.6. We have adopted the limb darkening coefficients in the three bands as given by Narusawa, Nakamura and Yamasaki (1994) as fixed parameters. q is fixed to the value 0.331 as derived by Maxted, Hill & Hilditch (1994). $T_1 = 8720K$ is adopted, which is typical for an A3V star (Lang 1992). A_1 is fixed to its theoretical value of 1 for a star of the mass and temperature as that of the primary. A_2 when left as a free parameter, always stayed near its expected value 0.5 and so it is fixed to the theoretical value. Chambsiss has used a low value of A_2 (0.2) in his analysis. Maxted, Hill & Hilditch obtained high values of A_2 in the U and B bands contrary to what we found. The value of the inclination, i, derived from all the three bands are matching very well among themselves, but, they are larger by 1^o than what was obtained by Chambliss. The T_2 shows different values in the three wavelengths, with the maximum at B. The value of T_2 derived by us (4507 K from the combined fit) is less than that obtained by Chambliss (1976). He obtained a gradually reducing T_2, from 5511 K in the U band to 5006 K in the V band with an average of 5248 K in the UBV bands and a difference of 500 K in the T_2 derived from the U and the V bands. Chambliss has adopted a high value of T_1 (9700 K). Our analysis of these UBV light curves yielded T_2 = 4507 K in the UBV combined analysis and on individual analysis, T_{2V} is found to be less tha T_{2U} by 140 K. This difference is only slightly more than that permitted by the error limits in the value

Table 3.6: Parameters derived from the analysis of the UBV light curves. (f: Parameter not adjusted during the analysis.)

Parameter	U Band	B Band	V Band	U, B & V Combined		
				U Band	B Band	V Band
T_1^f	8720 K	8720 K	8720 K	8720 K		
T_2	4665 ± 64 K	4712 ± 62 K	4525 ± 40	4507 ± 22 K		
q^f	0.331	0.331	0.331	0.331		
i	$83^o.36 \pm 0.10$	$83^o.31 \pm 0.07$	$83^o.24 \pm 0.08$	$83^o.20 \pm 0.03$		
Ω_1	4.378 ± 0.019	4.361 ± 0.0097	4.370 ± 0.013	4.362 ± 0.005		
Ω_2	2.5339	2.5339	2.5339	2.5339		
$r_{1\ pole}$	0.2465 ± 0.0011	0.2475 ± 0.0002	0.2470 ± 0.0008	0.2475 ± 0.0001		
$r_{1\ point}$	0.2515 ± 0.0013	0.2526 ± 0.0002	0.2520 ± 0.0009	0.2525 ± 0.0001		
$r_{1\ side}$	0.2490 ± 0.0012	0.2501 ± 0.0002	0.2496 ± 0.0008	0.2501 ± 0.0001		
$r_{1\ back}$	0.2507 ± 0.0012	0.2518 ± 0.0002	0.2513 ± 0.0009	0.2518 ± 0.0001		
$r_{2\ pole}$	0.2683	0.2683	0.2683	0.2683		
$r_{2\ point}$	0.3886	0.3886	0.3886	0.3886		
$r_{2\ side}$	0.2795	0.2795	0.2795	0.2795		
$r_{2\ back}$	0.3123	0.3123	0.3123	0.3123		
x_1^f	0.515	0.554	0.475	0.515	0.554	0.475
x_2^f	0.900	0.800	0.700	0.900	0.800	0.700
$x_{1\ bol}^f$	0.573	0.573	0.573	0.573		
$x_{2\ bol}^f$	0.537	0.537	0.537	0.537		
g_1^f	1.00	1.00	1.00	1.00		
g_2^f	0.32	0.32	0.32	0.32		
A_1^f	1.000	1.000	1.00	1.000		
A_2	0.500	0.500	0.500	0.500		
$L_1/(L_1+L_2)$	0.960 ± 0.005	0.957 ± 0.004	0.931 ± 0.003	0.970 ± 0.001	0.968 ± 0.001	0.932 ± 0.002
$L_2/(L_1+L_2)$	0.040 ± 0.006	0.043 ± 0.004	0.069 ± 0.004	0.030 ± 0.001	0.032 ± 0.001	0.068 ± 0.002
l_3^f	0.000	0.000	0.000	0.000	0.000	0.000

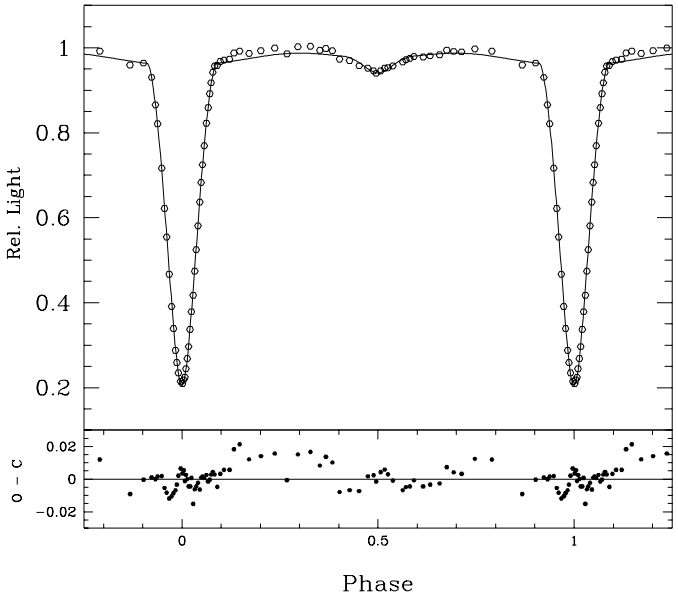

Figure 3.5: U band light curve of RZ Cas and the residuals. The circles show the normal points formed from the observed light curve and the continuous line shows the model fit with $A_2 = 0.5$. The bottom panel shows the deviations of the observed points from the model.

of T_2 derived by us. Fig. 3.5, 3.6 and 3.7 show the model light curves derived in the U, B and V bands along with the normal points given by Chambliss (1976). As noticed by Chambliss, we can see that the residuals are not random and are distributed systematically above or below the model curve in different regions of the light curves. The phases of deviations are well correlated in all the three bands. The observed secondary eclipses appear broader than the secondary eclipse of the fit which is more pronounced in the V band light curve. There are small positive residuals around the primary minimum, which are reducing to negative values at phase ~ 0.03 on both sides of the primary minimum in the U band and at phase ~ 0.22 in the V band and again increasing to positive values when the stars come out of the eclipse. The presence of circumstellar gas around the primary star can be the reason for this particular distribution of the residuals around the primary minima and the apparently broader secondary eclipse.

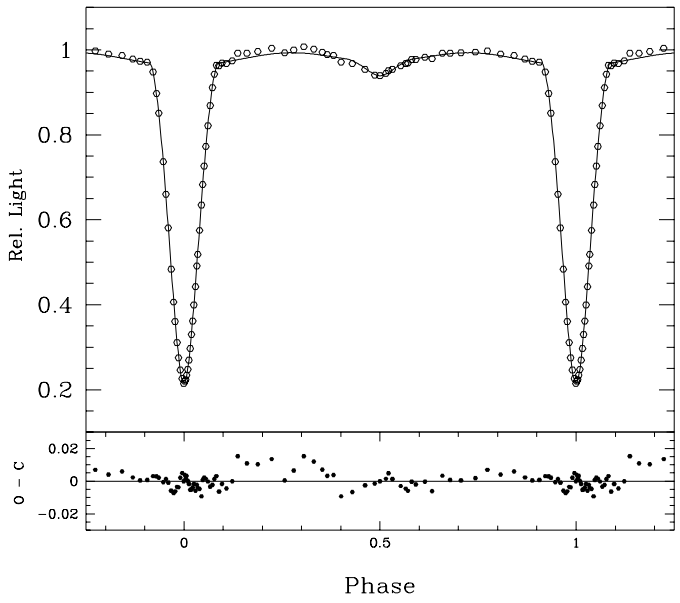

Figure 3.6: B band light curve of RZ Cas and the residuals. The circles show the normal points formed from the observed light curve and the continuous line shows the model fit with $A_2 = 0.5$.

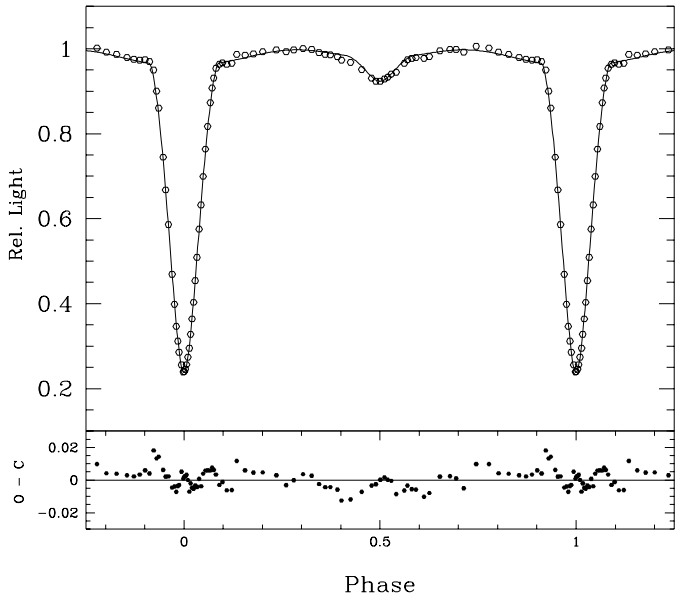

Figure 3.7: V band light curve of RZ Cas. The circles show the normal points formed from the observed light curve and the continuous line shows the model fit with $A_2 = 0.5$. The bottom panel shows the deviations of the observed points from the model.

3.3.3 *Analysis of the J and K band light curves with A_2 as a free parameter.*

We have discussed in section 2.3.3 that A_2 is a parameter which can produce significant changes in the estimated light output from the secondary star, whereas A_1 is a weak parameter. Since the nature of the observed light curves outside the eclipses resembled the presence of a high bolometric Albedo for the secondary star, light curve fitting was again done with A_2 as a free parameter. A_1 was fixed to its theoretical value 1.00. In both J & K light curve analysis and in the combined analysis, A_2 when released as a free parameter, converged to a value greater than 0.7. The problem of finding high A_2 in the light curves of Algol secondaries was faced in the light curve analysis of many Algols by different investigators. Van Hamme & Wilson (1993) obtained values of $A_2 \sim 0.7$ & ~ 0.8 respectively for S Cnc and TT Hya. They have called for a revised treatment of reflection from convective atmospheres. In the case of RZ Cas, Maxted, Hill & Hilditch obtained high A_2 in the analysis of the U and B light curves. The complete set of fitted parameters, with A_2 as a free parameter are given in Table 3.7.

The value of T_2 derived from the analysis of J & K light curves is less than that derived from the light curves in UBV bands by more than 200 K. This is more than what is allowed by error limits. This situation didn't improve much with A_2 as free parameter. This problem of finding different values of T_2 at different wavelengths is observed frequently in the analysis of the light curves of many Algols (Chambliss 1976, Van Hamme & Wilson 1986, 1990, 1993). In the present study, in R CMa also, T_2 is different at different wavelengths. In the Wilson's programme, the control parameter IPB can be selected as 1 so that L_2 is determined independently of T_2, so that we can assign same value of T_2 to all the light curves and adjust L_2 as a free parameter. We have not adopted this method in the present study, instead looked for alternate methods to solve it which will be explained in the next section.

The orbital inclination derived from the J and K light curves is less than that derived from the UBV light curves by $\sim 1^o$. The fitted light curves are shown

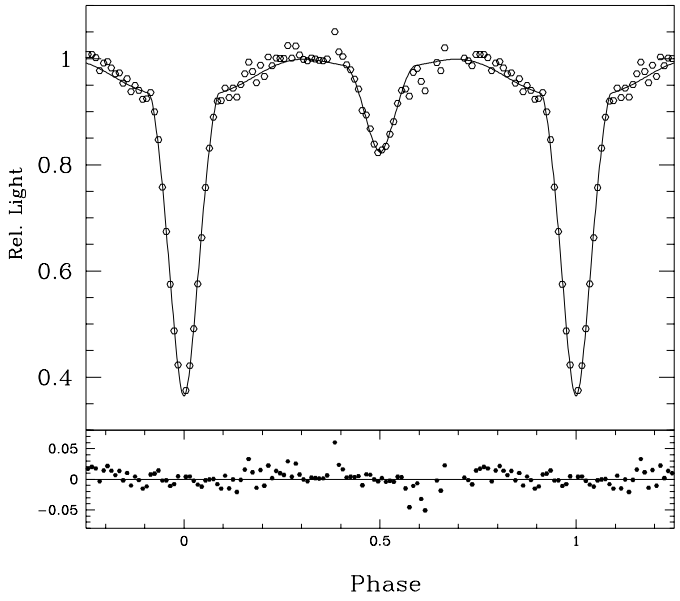

Figure 3.8: J band light curve of RZ Cas. The circles show the normal points formed from the observed light curve and the continuous line shows the model fit with A_2 as a free parameter. The bottom panel shows the deviations of the observed points from the model.

in Fig. 3.8 and Fig. 3.9. The model light curves shown are generated with the parameters obtained in the J & K individual analysis. We can see that the fit has improved slightly with a high value of A_2. But still systematic residuals are present in the region outside eclipse. But here we end up in some new problems. The secondary is a sub giant star of mass 0.73 $M_\odot$ and theoretically it is expected to have a convective atmosphere. According to Rucinski (1969), the bolometric albedo of such an atmosphere should be 0.5. In the analysis of the UBV light curves, we do not find any signature of an A_2 higher than 0.5. In our re-analysis of the UBV light curves of Chambliss (1976), A_2, when released as a free parameter, oscillated around the value 0.5 and the programme gave a good fit to the observed light curves for $A_2 = 0.5$. In all the existing models of binary star light curve analysis, the reflection effect is treated bolometrically and the parameter A is wavelength independent. So it is puzzling to see how the light curves of a star in different wavelengths can have different bolometric albedos. This will lead us to the following conjectures:

- If the higher A_2 (compared to the theoretical value and what we derived from the optical observations) that we find in the J & K bands is real, then we have

Table 3.7: Elements obtained from the analysis of J and K band data with A_2 as free parameter

Parameter	J Band	K Band	J & K Combined	
			J Band	K Band
T_1^f	8720 K	8720 K	8720 K	
T_2	4204 ± 32 K	4317 ± 38 K	4257 ± 26 K	
q^f	0.331	0.331	0.331	
i	$82^o.48 \pm 0.11$	$81^o.84 \pm 0.11$	$82^o.21 \pm 0.07$	
Ω_1	4.280 ± 0.040	4.404 ± 0.066	4.370 ± 0.044	
Ω_2	2.5339	2.5339	2.5339	
$r_{1\ pole}$	0.2526 ± 0.0026	0.2449 ± 0.0039	0.2470 ± 0.0003	
$r_{1\ point}$	0.2581 ± 0.0028	0.2498 ± 0.0043	0.2520 ± 0.0003	
$r_{1\ side}$	0.2554 ± 0.0027	0.2474 ± 0.0041	0.2495 ± 0.0003	
$r_{1\ back}$	0.2573 ± 0.0028	0.2490 ± 0.0042	0.2512 ± 0.0003	
$r_{2\ pole}$	0.2684	0.2684	0.2684	
$r_{2\ point}$	0.3886	0.3886	0.3886	
$r_{2\ side}$	0.2796	0.2796	0.2796	
$r_{2\ back}$	0.3123	0.3123	0.3123	
x_1^f	0.250	0.150	0.250	0.150
x_2^f	0.470	0.320	0.470	0.320
$x_{1\ bol}^f$	0.573	0.573	0.573	
$x_{2\ bol}^f$	0.528	0.528	0.528	
g_1^f	1.00	1.00	1.00	
g_2^f	0.32	0.32	0.32	
A_1^f	1.000	1.000	1.000	
A_2	0.72 ± 0.06	0.74 ± 0.07	0.73 ± 0.04	
$L_1/(L_1+L_2)$	0.796 ± 0.005	0.671 ± 0.009	0.782 ± 0.004	0.680 ± 0.003
$L_2/(L_1+L_2)$	0.204 ± 0.008	0.329 ± 0.022	0.218 ± 0.011	0.320 ± 0.012
l_3^f	0.000	0.000	0.000	0.000

Table 3.8: Average residuals at different parts of the light curves

Phase interval	J Band		K Band	
	Arithmetic Mean	r.m.s	Arithmetic Mean	r.m.s
$A_2 = 0.5$				
0.000 - 0.085	-0.00132	.01880	-0.00235	0.00842
0.085 - 0.250	-0.00127	.02358	+0.00108	0.00658
0.250 - 0.415	+0.01491	.02647	+0.01261	0.01924
0.415 - 0.500	+0.00290	.01928	+0.00870	0.02466
0.500 - 0.585	-0.00127	.01951	+0.00382	0.01483
0.585 - 0.750	-0.00040	.02113	-0.00527	0.01657
0.750 - 0.915	+0.00316	.02414	-0.00016	0.01679
0.915 - 1.000	+0.00159	.02094	+0.00017	0.00904
$A_2 = free\ parameter$				
0.000 - 0.085	-0.00192	.00572	-0.00125	0.00719
0.085 - 0.250	+0.00275	.01494	+0.00279	0.00747
0.250 - 0.415	+0.01243	.02028	+0.00685	0.01533
0.415 - 0.500	+0.00207	.00572	+0.00654	0.01965
0.500 - 0.585	-0.00768	.01715	+0.00084	0.01604
0.585 - 0.750	-0.00817	.02117	-0.01082	0.01913
0.750 - 0.915	+0.00625	.01285	+0.00167	0.01786
0.915 - 1.000	+0.00087	.00846	+0.00120	0.00916

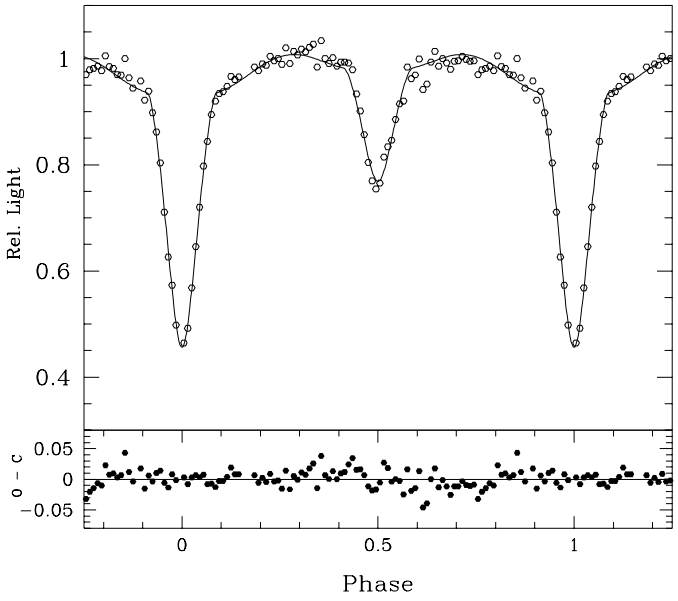

Figure 3.9: K band light curve of RZ Cas. The circles show the normal points formed from the observed light curve and the continuous line shows the model fit with A_2 as a free parameter. The bottom panel shows the deviations of the observed points from the model.

to reconsider the treatment of reflection in the existing models, *ie.*, whether we should think about a wavelength dependent reflection effect *viz.*, absorption in certain wavelengths and re-emission in certain other wavelengths locally.

- Is our concept about the atmosphere of the secondary star, that it is convective, right? Since we are finding a higher albedo A_2 in the J & K bands, should we think that the atmosphere is not totally convective? Or should we think that A_2 may not be 0.5 for a convective atmosphere?[1]. Then why do we see an albedo of 0.5 in the UBV bands which agrees very well with the theoretical value for a convective atmosphere? So the discrepancy in the value of A_2 that we see is unlikely to be an indication of the departure of the photosphere from convective nature. This will be addressed in the next chapter, in the light curve analysis of R CMa

- Is the high A_2 that we obtained from the analysis of the J & K light curves resulting from any other parameter not properly taken care of in the analysis or in the model ? One possibility is the presence of a cool spot on the back

[1]This question was previously raised by Van Hamme & Wilson (1993)

side (longitude = 180^o) of the secondary star. This can reproduce the slope seen outside the minima similar to that produced by a high A_2 as described in section 2.3.4 where light curves are simulated to show how a high A_2 and the effect of a cool spot of suitable size and temperature located at the above longitude on the secondary star can mimic each other in the region outside the eclipse in an IR light curve. So an attempt is made to model the light curves with a single spot on the back of the secondary star and the results are presented in section 3.3.4. The presence of a gas stream in the system, oriented towards the pole of the primary due to the bipolar magnetic field of the primary can also can mimic a high A_2, since we may see parts of the primary through the stream before and after the primary eclipse. This can also reproduce the asymmetry of the light curve, seen as a maculation at around phase 0.6 due to absorption of the light from the secondary star by the stream which is deviated from a radial path due to Coriolis force. The modeling of a stream is not attempted in this thesis.

3.3.4 Model with a single spot on the secondary star

In the previous section we have looked at the possibility of explaining the distortions in the light curve outside the minima by invoking a cool spot on the secondary star. Accordingly a dark spot was adopted on the secondary star. To begin with the spot parameters were selected by trial and error. The iteration was started with a suitable set of numbers for the spot parameters. The spot parameters were kept fixed and the iterations were done for the set of system parameters $i, T_2, A_2, \Omega_1 \& L_1$. It was noticed that, as expected from the simulations, A_2 came down to a value near 0.5. The secondary temperature T_2 also increased by more than 130 K in both J & K. Thus the situation of the discrepancy of T_2 being less in the present analysis of the J and K light curves has reduced with the inclusion of a cool spot on the secondary star [2]. After attaining convergence in the system param-

[2]This is obviously expected since we are fixing the temperature of the primary and darkening some portion of the secondary star. So to keep the luminosity of the model fit in agreement with

Table 3.9: RZ Cas: Elements obtained from the analysis of J and K band data with a dark spot on the secondary star. f: Parameter not changed during the analysis.

Parameter	J Band	K Band	J & K Combined	
			J Band	K Band
T_1^f	8720 K	8720 K	8720 K	
T_2	4349 ± 30 K	4415 ± 44 K	4359 ± 28 K	
q^f	0.331	0.331	0.331	
i	$82^o.10 \pm 0.09$	$81^o.54 \pm 0.11$	$82^o.01 \pm 0.08$	
Ω_1	4.413 ± 0.047	4.401 ± 0.053	4.408 ± 0.045	
Ω_2	2.5339	2.5339	2.5339	
$r_{1\ pole}$	0.244 ± 0.003	0.245 ± 0.003	0.245 ± 0.002	
$r_{1\ point}$	0.249 ± 0.003	0.250 ± 0.004	0.250 ± 0.002	
$r_{1\ side}$	0.247 ± 0.003	0.248 ± 0.003	0.247 ± 0.002	
$r_{1\ back}$	0.249 ± 0.003	0.249 ± 0.003	0.249 ± 0.002	
$r_{2\ pole}$	0.2684	0.2684	0.2684	
$r_{2\ point}$	0.3886	0.3886	0.3886	
$r_{2\ side}$	0.2796	0.2796	0.2796	
$r_{2\ back}$	0.3123	0.3123	0.3123	
x_1^f	0.250	0.150	0.250	0.150
x_2^f	0.470	0.320	0.470	0.320
$x_{1\,bol}^f$	0.573	0.573	0.573	
$x_{2\,bol}^f$	0.528	0.528	0.528	
g_1^f	1.00	1.00	1.00	
g_2^f	0.32	0.32	0.32	
A_1^f	1.000	1.000	1.000	
A_2	0.56 ± 0.05	0.49 ± 0.06	0.53 ± 0.04	
$L_1/(L_1+L_2)$	0.768 ± 0.006	0.661 ± 0.008	0.767 ± 0.004	0.664 ± 0.004
$L_2/(L_1+L_2)$	0.232 ± 0.012	0.339 ± 0.020	0.233 ± 0.008	0.334 ± 0.010
l_3^f	0.000	0.000	0.000	0.000
Phase Shift	0.0000 ± 0.0001	0.9999 ± 0.0002	0.0000 ± 0.0001	
Spot Parameters:				
Latitude^f	80.00	80.00	80.00	
Longitude^f	175.41	182.64	174.72	
Ang. Rad.^{f}	20.43	20.48	20.53	
Temp. f.^{f}	0.739	0.783	0.743	

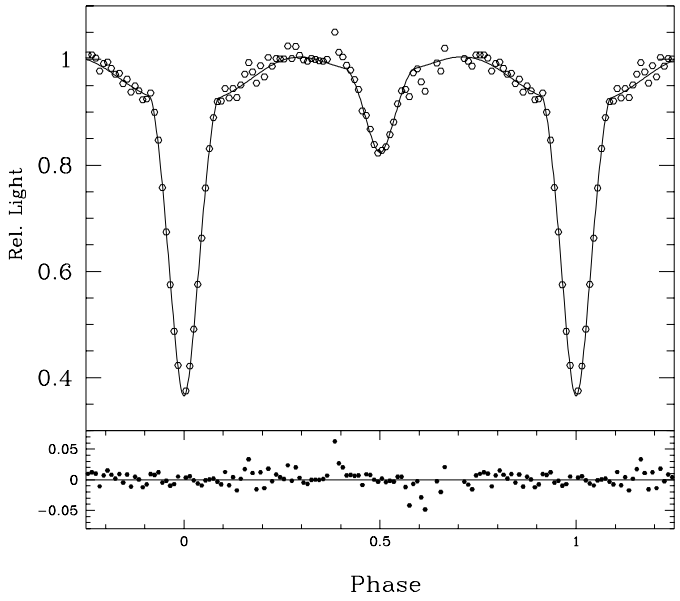

Figure 3.10: J band light curve of RZ Cas. The circles show the normal points formed from the observed light curve and the continuous line shows the model fit with one cool spot at the back side of the secondary. The bottom panel shows the deviations of the observed points from the model.

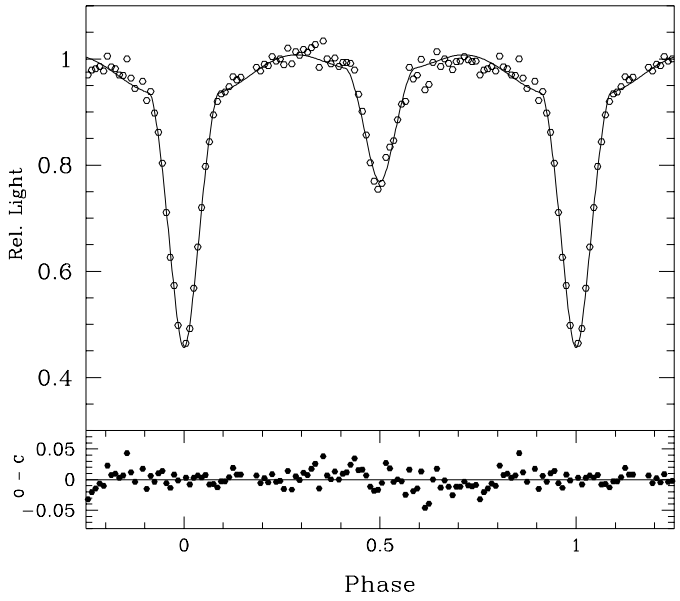

Figure 3.11: K band light curve of RZ Cas. The circles show the normal points formed from the observed light curve and the continuous line shows the model fit with one cool spot at the back side of the secondary. The bottom panel shows the deviations of the observed points from the model.

eters, we released the spot parameters free and tried fitting for the spot. Though convergence was obtained for each spot parameter separately, the error estimates of the spot parameters were high when all the spot parameters are released free simultaneously. So the spot parameters were fixed to the converged values and system parameters were again fitted for. The derived system parameters are given along with the adopted spot parameters in Table 3.9. The fitted light curves and residuals in the J & K bands are shown in Fig.3.10 and Fig.3.11 respectively. The model with the spot better represents the observed light curves especially in the J band. Since the spot is assumed to be present on the less luminous secondary star, its effect will go un noticed in the UBV bands as shown in the section 2.3.4 where the U and V light curves are simulated with and without cool spots on the secondary star. That can be one of the reasons, why the presence of spots, if any, went unnoticed in the previous optical observations. Since the convergence of the spot parameters were not satisfactory, at this stage, we would like to propose the spot model only as one of the strong possibilities to explain the discrepancies that we noticed between the analysis of the JK and UBV light curves and to explain some of the distortions seen in the J and K light curves. The large scale activity of the system in the radio and X-ray wavelengths due to chromospheric and coronal activities and the very fact that the secondary star is a late type fast rotator with a convective envelope encourage us to put more faith in the presence of a cool spot on the secondary star. It is encouraging to note that Maxted, Hill & Hilditch (1994) raised the possibility of a dark spot on the secondary to explain the difference in light levels at quadratures seen in the UBV light curves of Chambliss (1976). Umana, Catalano & Rodono (1991) observed RZ Cas with the VLA at 6cm and derived a brightness temperature of 4.26×10^8 K and 11.1×10^8 K from two observations. Assuming the radio emission to be arising from the gyrosynchrotron radiation from mildly relativistic electrons interacting with the magnetic field of the active component, they derived the mean magnetic field to be 15 - 150 Gauss for a set of seven Algols. Umana *et al.* (1993) obtained radio continuum

the observed total luminosity, the temperature of the secondary will increase.

spectra of RZ Cas along with 5 other Algols at VLA frequencies 1.49, 5, 8.4 and 14.9 GHz. The observed spectra were similar to that of RS CVns. RZ Cas was detected in the X-Ray wavelengths also. Schmitt *et al.* (1990) observed soft X-ray emission from RZ Cas. Singh, Drake & White (1995) observed X-ray emission from RZ Cas along with 4 other Algols. The emission is interpreted as of coronal origin. RZ Cas showed variable levels of emission. All these observations give us strong faith on the chromospheric activity of the secondary of RZ Cas. More observations of the light curves in the near IR bands with better accuracy will help us to confirm the presence of spot and observe its migration if any.

We have already shown through Table 3.8 that there is a fall in the observed light when the system comes out of the secondary eclipse. This maculation type of phenomenon is seen more prominent in the J band and is very weak in the K band light curve. The depression of light in the J band can be fitted well with a spot on the inner surface of the secondary at a longitude greater than 315 as shown in Fig. 2.6. But before proceeding further, let us have a closer look at this maculation type of phenomena. Arévalo & Lázaro (1990) in their J & K light curves of the short period RS CVn system XY UMa observed an asymmetric secondary minimum with the intensity lower in the ascending branch of the secondary eclipse where it emerges out of the eclipse. They commented that it may be the effect of absorption by a gas stream from the secondary directed towards the pole of the primary. Budding & Zeilik (1987) have noticed maculation minima at phases 0.27 and 0.56 in the V band light curve of XY UMa and have modeled it with two spots on the secondary. They have analyzed the light curves of 10 short period RS CVn systems and found maculation minima between phases 0.56 and 0.65 in 5 systems (XY UMa (0.56), SV Cam (0.60), CG Syg (0.61), ER Vul (0.65) and UV Psc (0.61)). A closer look at the $1.2\mu m$ light curve of β Per by Chen and Reuning (1966) and the model fit by Richards, Mochnacki & Bolton (1988) reveals that there is a mild rise in flux around the beginning of the secondary eclipse and most of the observed values are lying below the model curve when the system emerges out of the secondary eclipse. The same $1.2\mu m$ light of Chen and Reuning (1966) is

analyzed by Wilson *et al.* (1972) along with UBV light curves observed by them. The normal points formed by them and the model fits reveal the above mentioned asymmetry of the secondary minimum of β Per very clearly. This asymmetry is present, though to a lesser extent, in their V light curve too. At this juncture, we have to think as to whether we should expect spots at around the same position in many of these stars and if yes, why a preference to certain longitudes? As Arévalo & Lázaro (1990) pointed out, absorption by a properly oriented gas stream can produce this type of an effect around the phases mentioned above. Both RS CVn s and Algols are systems in which mass transfer is possible (through Roché lobe overflow in Algols and magnetically driven stellar wind in RS CVn s). Such a stream can also mimic a high bolometric albedo of the secondary in Algols, since outside the eclipse when we move towards the primary eclipse we will start seeing more and more of the primary's surface through the gas stream. This can produce a depression of the light curve when we move towards the onset of the primary eclipse, where as a high A_2 will cause a rise in light value when we move towards the secondary eclipse. If we look at the region outside the light curve, these two effects can mimic the same shape except for the fact that the rise in flux caused by a high A_2 will be symmetric with respect to the secondary minimum, whereas, an asymmetry can be present in the change in shape of the light curve due to a gas stream because of Coriolis deviation of the stream. Repeated observations of the the complete light curves of these systems are necessary to look for the migration of these maculation type of phenomena. In those systems, where more than one spot are modelled on the same star, if one spot is moving and this particular one is not, then we have to doubt the presence of this spot which produces the maculation at around phase 0.56 - 0.65 or if it is confirmed to be a spot by further observations, we have to look for processes which hold it at a particular location on the star. In this study, we have not fitted this depression in the J band light curve with a spot on the secondary.

3.4 Colours and spectral types of individual components

Study of photometric light curves allows us to determine the colours of individual components of the binary system. The magnitudes and colours of the individual components of RZ Cas are derived adopting the following procedure. First the model fits were done to the J & K light curves observed by us and the UBV light curves of Chambliss (1976). Wilson's program gives the light contributions from individual components along with the total system light at each phase. These light values at phase 0.25 along with the observed magnitudes at that phase were used to calculate the magnitudes of the component stars [3].

The distance towards RZ Cas is estimated to be 73 pc. We have calculated the probable effects of interstellar extinction on the estimated magnitudes and colours of the components of RZ Cas and on the spectral types derived from these colours.

The normal interstellar extinction law is adopted.

$$R = A_v / E(B-V) \tag{3.2}$$

A value of 3.1 is adopted for R. If we adopt the average value of $A_v = 1.9$ mag / kpc. (Allen 1973), we will get an E(B-V) of 0.047. Since the observed E(B-V) in the system is only 0.03, we have adopted that value. The observed system magnitudes at U, B, V, J & K bands are corrected for interstellar extinction with the values of A_λ derived from this observed E(B-V) and the relations given in Savage and Mathis (1979). These values of the corrected system magnitudes are used to derive the magnitudes and colours of the components. The magnitudes and colours of RZ Cas and the components with and without interstellar extinction correction are

[3]The magnitudes calculated will be affected by the departures in the shape of the stars from spherical symmetry and associated gravity darkening and contamination by reflection effect. These effects will be negligible for the primary of an Algol type system, where the distortion of the primary's surface is small and the reflected component of the light is $\sim 0.03\%$ of the intrinsic contribution of the light from the primary component. But for the secondary star, the above mentioned effects (reflected component is more than 2% at $0^p.25$ of the intrinsic contribution) can cause observable contamination in the calculated colours, though very little. Also a disk, stream or spot, not properly taken care of in the model can contaminate the derived colours.

given in Table 3.10.

3.4.1 Primary

Chambliss (1976) has classified the primary star as A2 V from his photometric analysis. Spectroscopic investigation by Duerbeck & Hanel (1979) has revealed the primary component to be an A3 V star with reasonably good accuracy. Narusawa, Nakamura and Yamasaki (1994) have shown the primary to be an unreddened main sequence A3 star with solar type composition by the comparison of the IUE spectrum of RZ Cas with the standard star spectra and from the Strömgren (u-b), (v-b) and (b-y) indices. The UV colours derived by them ((2740-V), (2365-V) and (1565-V)) were representative of an A4 - A5 V star. But the authors have cautioned about taking these colours very seriously due to the uncertainty in the information of the phase of eclipse of RZ Cas at the time of the IUE observations. Also the presence of a stream or hot spot can contaminate the observed UV colours.

We have derived the colours of the primary star from our photometric analysis as mentioned above. Magnitudes and colours of the system and individual components are given in the Table 3.10. The U-V colour of the primary, when not corrected for interstellar extinction, corresponds to an A3 - A3.5 V star. Similarly the uncorrected B-V, V-J, V-K and J-K colours of the primary match with the colours of an A4 V star. All the U-V, B-V, V-J, V-K and J-K colours of the primary match with that of an A3 V star when corrected for interstellar extinction. The intrinsic colours given by Johnson (1966) are used for comparison. Considering the various points discussed above, we assign A3 V as the spectral and luminosity classes for the primary component. We have adopted 8720 ± 100 K (corresponding to an A3 V star) as the temperature of the primary star (Lang 1992).

Table 3.10: Magnitudes and colours of RZ Cas and its components

Photometric band	System	Primary	Secondary	System	Primary	Secondary
	without interstellar extinction correction			After correcting for interstellar extinction		
U	6.40	6.46	9.65	6.24	6.26	9.49
B	6.32	6.39	9.51	6.19	6.24	9.36
V	6.18	6.27	8.91	6.08	6.17	8.81
J	5.76	6.04	7.37	5.73	6.01	7.34
K	5.50	5.98	6.63	5.49	5.96	6.62
U-B	0.08	0.07	0.14	0.05	0.05	0.13
U-V	0.22	0.18	0.74	0.16	0.12	0.68
B-V	0.14	0.12	0.61	0.09	0.07	0.55
V-J	0.42	0.23	1.54	0.35	0.16	1.49
V-K	0.68	0.30	2.28	0.59	0.21	2.19

Table 3.11: V - J, V - K & J-K Colors for Sub giants (Calculated from Johnson 1966)
.

Spectral type	U - V	B - V	V - J	V - K	J - K
G5	1.21	0.79	1.33	1.75	0.42
G8	1.35	0.85	1.40	1.90	0.50
K0	1.61	0.93	1.55	2.07	0.52
K2	1.96	1.04	1.72	2.37	0.65
K3	1.79	1.00	1.93	2.64	0.71
K4	1.99	1.07	2.12	2.90	0.78
K5	2.76	1.35	2.38	3.21	0.83
K7	2.95	1.42	2.55	3.47	0.92
M0	3.05	1.48	2.77	3.70	0.93
M1	3.07	1.52	2.98	3.94	0.96
M2	3.10	1.56	3.23	4.19	0.96

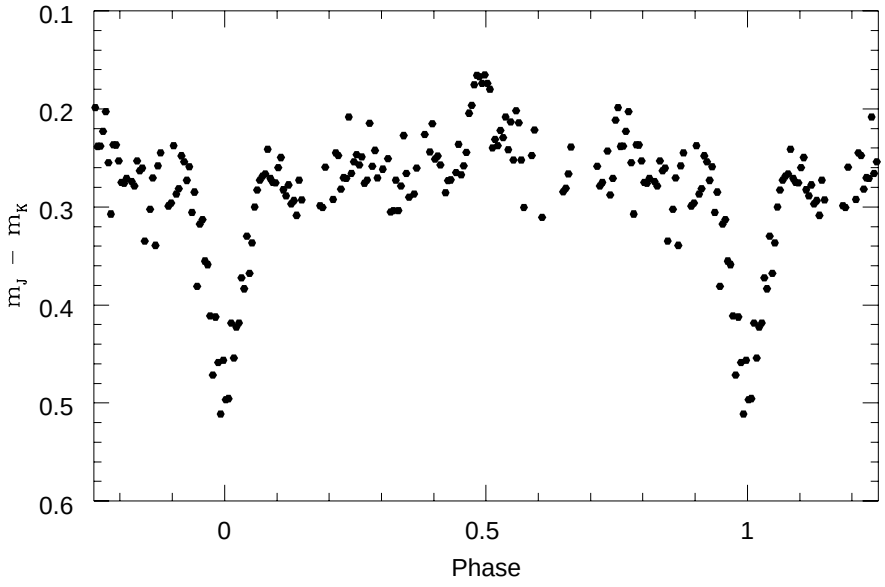

Figure 3.12: The J - K colour curve of RZ Cas

3.4.2 Secondary

Chambliss (1976) has derived the spectral type of the secondary to be G5 V from his photometric study. Surface gravity and mean radius obtained by Chambliss were indicative of luminosity class III and IV respectively. The magnitudes and colours of the secondary were derived in the present work from the photometric analysis as described in the previous section. The secondary is a subgiant and no literature is available compiling the intrinsic colours of subgiants of different spectral types. So the subgiant colours are taken as an average of the colours of main sequence and giant stars of the same spectral type. We have used the intrinsic colours given by Johnson (1966) for our comparisons. The V-J , V-K & J-K colours for a subgiant, calculated based on the table of intrinsic colours of Johnson are given in Table 3.11.

The V-J colour (corrected for interstellar extinction) of 1.49 observed by us implies a G9 IV secondary whereas the V-K colour (2.19) represents a K1 subgiant secondary. The J-K colour gives us a secondary star of K3 IV, but this again has to be treated with caution considering the observational errors in these bands and the small value of the colour in this band as seen in Table 3.10. The T_2 derived from

the light curve analysis in the J & K bands are typical for a K3 - K4 IV star and is lower than the temperature corresponding to our observed V - J and V - K colours and that derived from the analysis of the UBV light curves. Since the secondary is better observed in the J and K bands, we are taking the temperatures and colours in these bands to be representing the component in a better way than those derived from the optical light curves. At present we can classify the secondary as K1 - K4 IV star. But the discrepancy in the optical and near IR colours and temperatures of the secondary, and their systematic variation points to the fact that there is some factor in this system which we have not properly taken care of in the model. Further observations of this system with a view to resolve the presence of any circumstellar matter in the system can help to determine the spectral type of the components more accurately.

Fig. 3.12 shows the observed J - K colour curve of RZ Cas. The J - K colour of the system at the primary minimum is 0.50, whereas the colour of the K3.5 IV secondary component is 0.74. The observed J - K colour of the system at the secondary minimum is 0.17 while the colour of the A3 V primary star is 0.07. The differences in the colours are more than the observational errors. The observed colours at the minima confirm the partial nature of the eclipses.

3.5 Period Variations

The period variations of RZ Cas have inspired the interest of many people over the years (Herczeg & Frieboes-conde 1974, Bruke & Roland 1965, Hegedus, Szatmáry & Vinkó 1992). Kopal (1965) included RZ Cas among the list of binary systems that exhibit apsidal motion in an elliptical orbit with an eccentricity $e = 0.13$. The spectroscopic study of Horak (1952) showed a nearly circular orbit. Robinson (1965) suggested that the period might have exhibited several sudden discontinuous changes. Bruke & Roland (1966) pointed out a possible abrupt change of period around 1954. Herczeg & Frieboes - Conde (1974) interpreted the changes in

O-C of the moments of primary minima as due to a set of period discontinuities with constant period between the jumps. They showed that some of the apparently major period changes (like the one near JD 2438300) were caused by a rapid succession of minor displacements of the epoch of primary minimum which summed up to a measurable phase shift before the period assumed its new value. They didn't find any evidence of apsidal motion as expected in an elliptical orbit suggested by Kopal (1965). Heckathorn (1966) observed secondary minima at exactly phase 0.500 whereas Robinson (1967) observed a small shift of secondary minimum. Maxted, Hill & Hilditch (1994) observed changes in the observed spectra

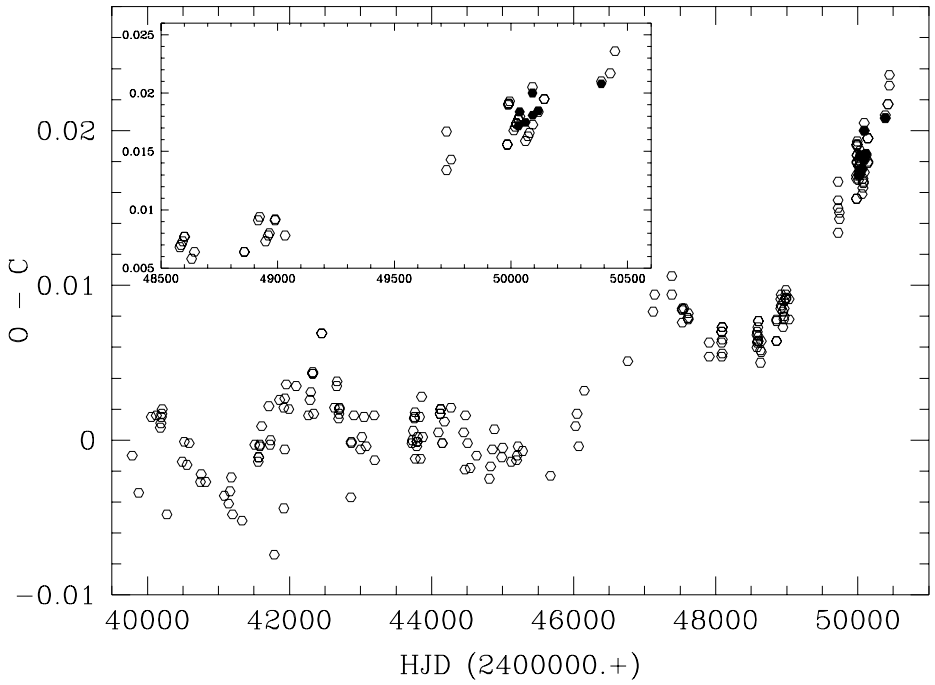

Figure 3.13: O - C curve of RZ Cas

associated with the period changes in RZ Cas. Narusawa, Nakamura & Yamasaki (1994) observed that no major period changes have happened in this system after HJD 2448581. They derived linear ephemeris for the moments of minima of RZ Cas for the interval HJD 2447370 - 2448220 and for the observed epochs of minima after HJD 2448581 and observed that a period increase of 1.7×10^{-5} has happened in the system during the interval HJD 2448220 - 2448581.

The O - C curve of RZ Cas showing recent epochs of primary minima are shown in Fig.3.13. The values of the O - C are generated with the linear epoch (Kholopov *et al.* 1985).

$$JD\ Hel.\ Min\ I = 2443200.3063\ + 1^d.195247\ E_0 \tag{3.3}$$

The epochs of 7 primary minima observed in the current work are represented as filled hexagons. The recently reported epochs of minima by Narusawa *et al.* (1997) and Hill and Osborn (1997) are also included. The present epochs of minima show that no major period change has happened in the system since HJD 2448581. From the O - C curve shown in Fig.3.13 it is clear that the period change was not abrupt and was continuous in the interval HJD 2448220 - 2448581.

3.6 Absolute dimensions

Absolute dimensions of RZ Cas are calculated combining the separation between the components and mass ratio from the previous spectroscopic studies and the results of our photometric light curve analysis. The derived absolute dimensions are given in Table 3.12. The masses and radii derived in this study are higher than those derived by Chambliss (1976), but are in good agreement with those derived by Maxted, Hill & Hilditch (1994). The T_2 derived is smaller than that derived in both the studies mentioned above. Chambliss has used a higher value of T_1 for his analysis. The T_2 obtained by him from the V band light curve is less than that was derived from his U band by $\sim$ 500 K. The mean T_2 derived in this study from the IR bands is lower than the mean T_2 of Chambliss by $\sim$ 1000 K. Only a part of the excess T_2 (a few hundreds of K) of Chambliss can be attributed to the higher T_1 used by him. T_2 (UBV) derived from the same light curves of Chambliss in the present study is higher than the T_2 (JK) by $\sim$ 300 K. Also T_2 (UBV) derived by Maxted, Hill & Hilditch is higher than T_2 (JK) by $\sim$ 500 K. We cannot account for this difference in T_2 derived from the optical and near IR light curves unless some physical process within the system are invoked. The significance of the physical

Table 3.12: Absolute Dimensions of RZ Cas

Parameter	Primary	Secondary
Mass ($M_\odot$)	2.21 ± 0.26	0.73 ± 0.07
Mean Radius ($R_\odot$)	1.69 ± 0.06	1.95 ± 0.06
Mean Temperature	8720 ± 100 K	4257 ± 26 K
($L/L_\odot$)	14.90 ± 1.06	1.12 ± 0.01
Mean log(g)	4.33 ± 0.02	3.72 ± 0.01
M_{bol}	1.81 ± 0.05	4.66 ± 0.3

parameters in the context of the evolutionary status of the system is treated in the next section.

3.7 *Evolutionary Status*

The first hand clues about the evolutionary status of any star can be obtained from its position in the H-R diagram. Also the star's location in the Mass-Luminosity, Mass-Radius and Temperature-Radius diagrams will tell us whether the star is following normal pattern of evolution or is departing from the normal path. These in turn, help us to understand the different physical processes and their impact on the fate of the binary system in a better way.

The H-R diagram and the position of the components of RZ Cas are shown in Fig.3.14. The H-R diagram is adopted from the grids of Schaller *et al.* (1992). The continuous line is the model for the stars of Zero Age Main Sequence (ZAMS) and the dotted line is for the stars at the Terminal Age Main Sequence (TAMS) for different masses from 0.08 $M_\odot$ to 15 $M_\odot$ from Schaller *et al.* (1992). The broken line is adopted from Lang (1992).

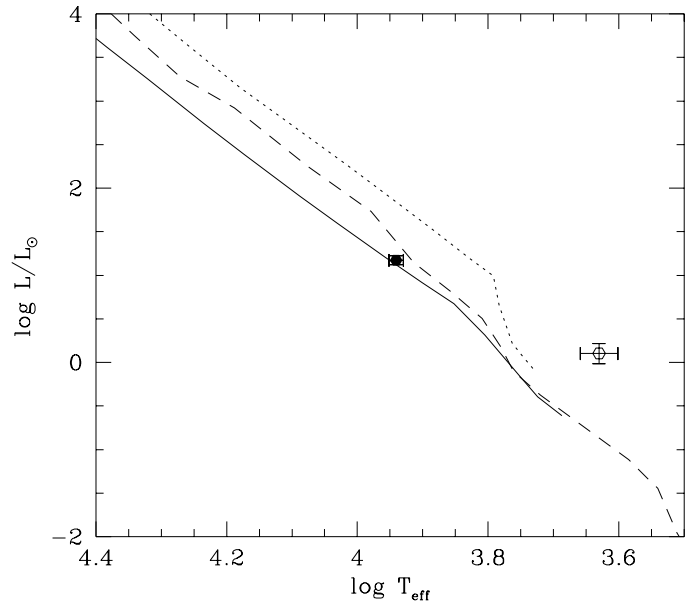

Figure 3.14: HR diagram and the position of the components of RZ Cas. The filled circle represents the primary star and the open circle, the secondary star.

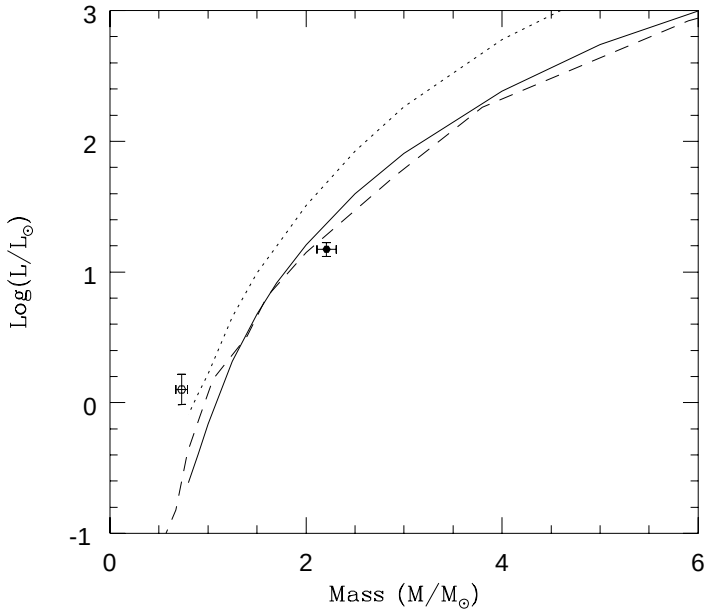

Figure 3.15: Mass Luminosity Diagram for Main Sequence stars. Lines and symbols are same as in 3.14

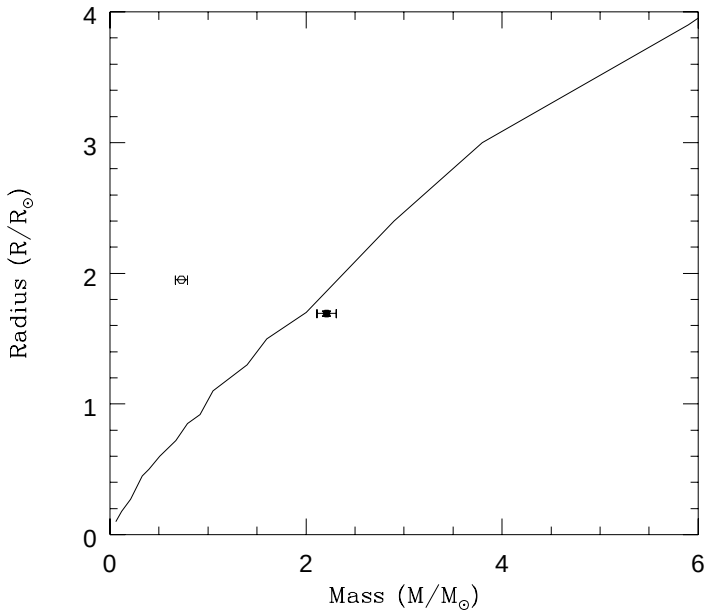

Figure 3.16: Mass-Radius Diagram for Main Sequence stars The primary of RZ cas is shown as a filled circle and the secondary as an empty circle.

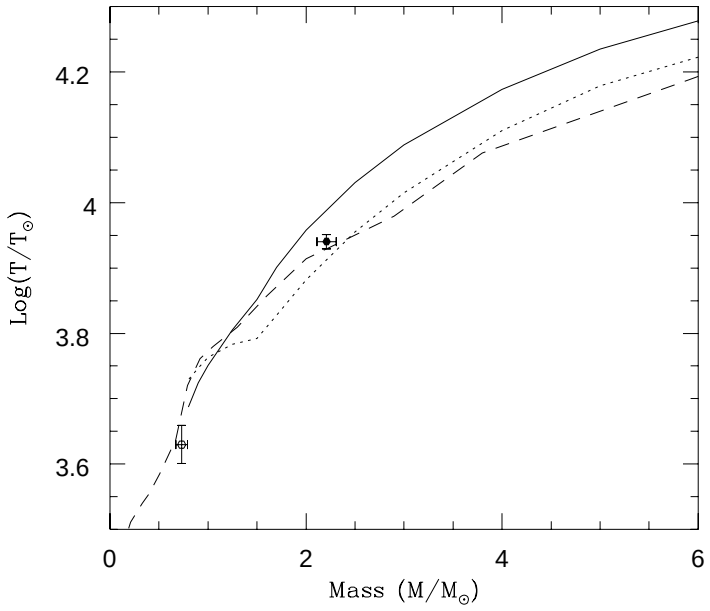

Figure 3.17: Mass-Temperature Diagram for Main Sequence stars. Lines and symbols are same as in 3.14

We can see that the primary lies close to the ZAMS branch of the HR diagram and its luminosity is normal for a main sequence star of the same temperature. The secondary is over-luminous for its spectral type and it lies above the TAMS branch implying a star evolved out of the Main Sequence stage to become a subgiant.[4] Fig.3.15 shows the position of the components on the Mass - Luminosity diagram for the main sequence stars. We can find that the primary is close to main sequence though slightly under-luminous for a ZAMS star of the same mass contrary to what was found by Duerbeck & Hanel (1979). (They found a primary over-luminous for its mass and interpreted as probably evolving out of the main sequence.) This behavior of the primary, being under-luminous, is noticed in several Algols (Sarma, Rao & Abhyankar 1996). The secondary is over-luminous for the main sequence luminosity. Fig.3.16 shows the Mass - Radius diagram for Main Sequence stars adopted from the tables of Lang (1992). The primary is seen to be slightly smaller for its mass and the secondary is much bigger for a main sequence star. Fig.3.17 shows the RZ Cas components on the Mass-Temperature diagram derived from the model of Schaller *et al.* (1992). The primary and the secondary are seen to be of lower temperatures for their masses. The departure of the secondary from the Main Sequence limits in the above diagrams can be interpreted as due to its evolution out of the main sequence and the mass loss. We have to treat the departures of the primary with caution. The luminosity of the primary is below both the ZAMS and TAMS in the Mass - Luminosity diagram, whereas its temperature is lower than ZAMS and higher than TAMS in the Mass - Temperature diagram. So the primary cannot be taken as a star evolving out of the Main Sequence. We have to treat these deviations from the perspective of the effects of mass transfer to a star, which has already started nuclear burning at a much lower mass.

[4]These sub giants are stars from which the outer envelopes are removed on their way to the giant branch due to Roche Lobe overflow or large scale stellar wind. These stars are over-luminous for a Main Sequence star of the same spectral type, but under-luminous for a giant of the same spectral type.

3.8 Conclusions

- The secondary temperature derived from the infrared bands is less than that derived from the optical bands by $\sim 300K$ even after adopting the same size for the primary star for the analysis of the optical and the infrared light curves.

- The bolometric albedo of the secondary surface is higher in the IR Bands (> 0.7) whereas in the optical bands it is near the theoretical value (0.5) for a convective atmosphere as expected for a sub giant star of its mass. This is indicative of deficiency in bolometric treatment of reflection effect in light curve modeling. Local absorption at one wavelength and re-emission at a different wavelength can be a possible reason for the departure of the albedo from its theoretical value. This can also tell us about the probable presence of a cool dark spot on the surface of the secondary star or a stream of mass transfer from the lobe-filling secondary to the primary star.

- Secondary eclipse is asymmetric, both in J and K bands, especially near the end of the eclipse where it shows a depression and large scatter, the effect being more prominent in the J band light curve. This is probably due to the presence of gas streams. This type of phenomenon is seen in the IR light curves of many short period RS CVn systems. This was also noticed before in the optical and near-infrared light curves of β Per.

- Though some observers have seen a flat bottom of the primary minimum lasting for up to 21 minutes, none of the minima observed in the present study showed flat bottom. The observed eclipse depths and colours at the minima in the IR bands also rule out any probability of a total eclipse. We can now confidently tell that RZ Cas is a partially eclipsing system. The observed flat bottom which appears randomly can be a manifestation of the presence of circumstellar matter in motion. The system has not undergone any major period change during the last 5 years.

- The secondary minima appear at $0^p.5$ and the primary and the secondary eclipses have the same duration implying a circular orbit.

Chapter 4

Infrared and Optical Light Curve Analysis of R Canis Majoris

4.1 Introduction

R Canis Majoris (R CMa, HR 2788, HD 57167, $BD\ -16^o\ 5898$) is a short period semi-detached eclipsing binary of the Algol type. Its variability was discovered by Swayer in 1887. Being the member with the lowest total mass (1.24 $M_\odot$) and hosting the lightest secondary (0.17 $M_\odot$), R CMa enjoys a special status in the semi-detached family. Due to its brightness ($V = 5^m.7$), this binary is well observed and most of the observers found the system to be showing variability in its photometric and spectroscopic behaviors. Kopal (1955) proposed a new subclass of semi-detached binary stars of 10 objects including R CMa, called 'R CMa type', characterized by components which are very less massive for their luminosities. But further studies of these binaries by several other investigators argued that there was no need for a separate subclass as proposed by Kopal. Photoelectric photometric study of R CMa by Koch (1960) and Kitamura & Takahashi (1962) showed that both the components of the system are over-luminous for their masses. Smak (1961) and Sahade (1963) interpreted the over-luminosity as due to both the components being in the He burning stage. Sahade (1963) suggested that the secondary is overflowing its Roche lobe. Sato (1971), Guinan (1977), Batten, Fletcher & Mann (1978) and Hall & Neff (1979) showed that R CMa is not anomalous for Algol type and suggested that there is no need of a separate subclass 'R CMA type'. Sato

(1971) carried out extensive photometric studies of this system in the UBV and H_β bands. He concluded that R CMa is an ordinary semi-detached binary except for some peculiarities caused, probably, by gaseous envelopes surrounding the stars. Tomkin (1985), from spectroscopic studies, also concluded that R CMa need not be considered in a different class among semi-detached systems. He found that the system has an evolved and lobe filling secondary of lower mass among the components, overluminous for a dwarf star of the same mass, which is the chief identity of Algols.

Tomkin (1985) was the first to determine the mass ratio of R CMa spectroscopically. The radial velocity curves of both the components were obtained and the mass ratio was derived (q = 0.158). Assuming $i = 80^o$ the relative radii of the components were estimated as 0.325 and 0.219 for the primary and the secondary respectively, which matched well with the photometric estimates by Sato (1971) and Guinan (1977). The size of the secondary was found to be matching with the Roche lobe radius of 0.226 for the secondary for a mass ratio of 0.158. Large residuals were found in the solution of the primary radial velocity curve, more than the observational errors, which were interpreted as arising from the probable presence of circumstellar matter.

Radhakrishan, Sarma & Abhyankar (1985) conducted photometric study of R CMa in the UBV bands using the Russell - Merrill method. They derived a mass ratio of 0.13 ± 0.01 which is close to the value of mass ratio derived by Tomkin (1985). They found the secondary to be over-luminous by $5^m.0$ and hotter for its spectral type. Budding *et al.* (1994) obtained B and V light curves of R CMa and derived the system parameters. Sarma, Rao & Abhyankar (1996) analyzed the UBV and H_α light curves using Wilson's model. The luminosity of the primary and the secondary derived by them were large for their masses. They concluded that the overluminosity of the secondary is because it has evolved out of the main sequence stage and that of the primary, due to the helium enriched material that it has gained from the secondary due to mass transfer.

Kitamura and Takahashi (1962) have observed this star in the broad bands similar to the UBV system at the central wavelengths $3950\mathring{A}, 4650\mathring{A}$ & $5550\mathring{A}$ respectively. They found a maculation type of effect with observed light at the second quadrature lower than the first quadrature by $0^m.012, 0^m.008$ and $0^m.016$ in the U, B and V bands respectively. This was not observed in the optical band light curves of Guinan (1977). Most of the published light curves are variable and have asymmetries of some kind or the other and the characteristics of the radial velocity curve was also found to vary with time. Especially the secondary minima were found to show asymmetry by almost all the observers. Also the analysis of different light curves are found to show slightly different values for the parameters derived. Guinan (1977) assigned these differences to the difference in the character of the light curves obtained at different epochs due to the variable amount of gas in the system.

The IRAS source 07127 - 1617 is identified with R CMa. This source is detected only at 12μ with a flux of 0.65 Jy. Taking 28.3 Jy as the zero magnitude flux (Biechman $etal.$ 1988), it corresponds to magnitude [12] = 4.1. We have calculated the expected 12μ magnitude of R CMa adopting the V magnitudes and spectral types of individual components given by Sarma, Rao & Abhyankar (1996) and using intrinsic V - [12] colours listed by Cohen *et al.* (1987). The calculated 12μ magnitude for the system is [12] = 4.54. Considering the uncertinty in the spectral classification of the secondary component, which contributes significantly at 12μ, the difference of 0.43 mag. cannot be considered as a firm detection of excess radiation. At present, we interpret the observed 12μ emission as originating in stellar components.

4.2 Observations

R CMa was observed from November 1995 to January 1997 from the Mt. Abu Observatory. BD -15^o 1734 was observed as the comparison star and HR 2853 the

check star. The details of R CMa and the comparison and check stars are given in Table 4.1. BD -15^o 1734 was used as comparison star for the observations of R CMa by several observers before (Koch 1960, Kitamura & Takahashi 1961, Wood 1946, Guinan 1977, Edalati, Khalesse & Riazi 1989 and Sato 1971) and is established to be a non-variable in the optical photometric bands. This star is close to R CMa in spectral type and is located near it in the sky. There are no IR observations existing for BD -15^o 1734 and HR 2853.

The magnitudes of BD -15^o 1734 and HR 2853 are calculated using the observations of standard stars from the list of Koornneef (1983a,b). The observed J, H & K magnitudes of BD -15^o 1734 and HR 2853 are given in Table 4.2. BD -15^o 1734 is of spectral type A3 V (Kitamura & Takahashi 1962). The V - J and V - K colours of this star derived from our J and K observations match with this spectral type within error limits. BS 2853 is listed by *Bright Star Catalogue* as an A5n star whereas *The Hipparchos Input Catalogue* lists it as an F2 V star with B - V = $0^m.314 \pm 0.02$. The B - V colour of this star corresponds to a spectral type of F0.5 V. Our observed J - K colour is suggestive of an A9.5 V star and considering the errors of observations in the J and K bands we adopt the spectral type as derived from B - V colour and consider this star to be normal.

Light curves of R CMa are obtained in the J and K bands with 837 points in the J band and 972 points in the K band respectively. Figs. 4.1 & 4.2 show the complete light curves in the J and K bands of R CMa in terms of the observed relative magnitudes. Appendices 3 and 4 list the observed relative magnitudes (R CMa - BD -15^o 1734), Heliocentric Julian Days (HJD) and phases of observation. These are the first light curves of R CMa in the near IR bands J and K. The observed magnitudes of R CMa at phase = 0.25 and eclipse depths in the J and K bands are given in Table 4.3. The only observations of R CMa done before in the near infrared bands, JHKLM, are by Needham *et al.* (1980). From the observed (K - L) and (L - M) indices, they estimated the mass transfer rate in R CMa to be $4.6 \times 10^{-10}\ M_\odot\ year^{-1}$. Their observations covered only very limited phases and were

Table 4.1: The co-ordinates and spectral types of R CMa, BD -15^o 1734 & HR 2853

Star Name	α_{2000}	δ_{2000}	V	B-V	U-B	Sp. type
R CMa	07 19 28.1	-16 23 42	5.69	+0.34	+0.04	F1 V + K 3-4 IV
BD -15^o 1734	07 16 14.4	-15 35 08	5.46	+0.08	+0.06	A3 V
HR 2853	07 27 08.0	-17 51 52	5.60	+0.31		F2 V

Table 4.2: Observed J, H & K magnitudes and colours of BD -15^o 1734 and HR 2853.

Star Name	J	H	K	V - J	J - H	H - K
BD -15^o 1734	5.40	5.41	5.38	0.06	-0.01	0.03
HR 2853	5.01	4.87	4.82	0.59	0.14	0.05

Table 4.3: Observed magnitudes and eclipse depths of R CMa in the J & K bands.

Photometric band	Magnitude at phase = 0.25	Eclipse depth	
		Primary	Secondary
J	5.04	0.52	0.19
K	4.80	0.48	0.28

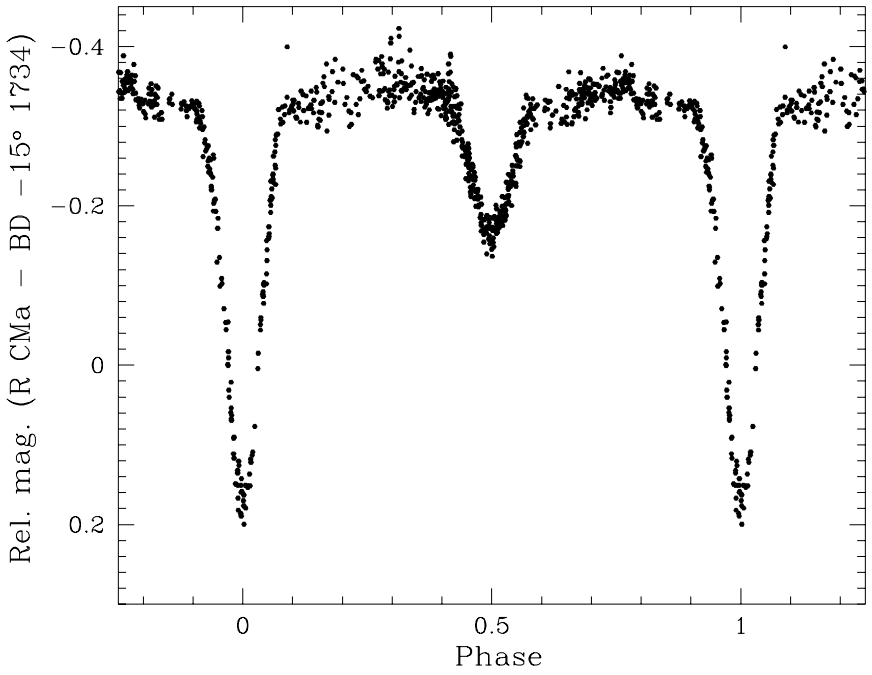

Figure 4.1: J band light curve of R CMa. Observed relative magnitudes (R CMa - BD−15°1734) are shown.

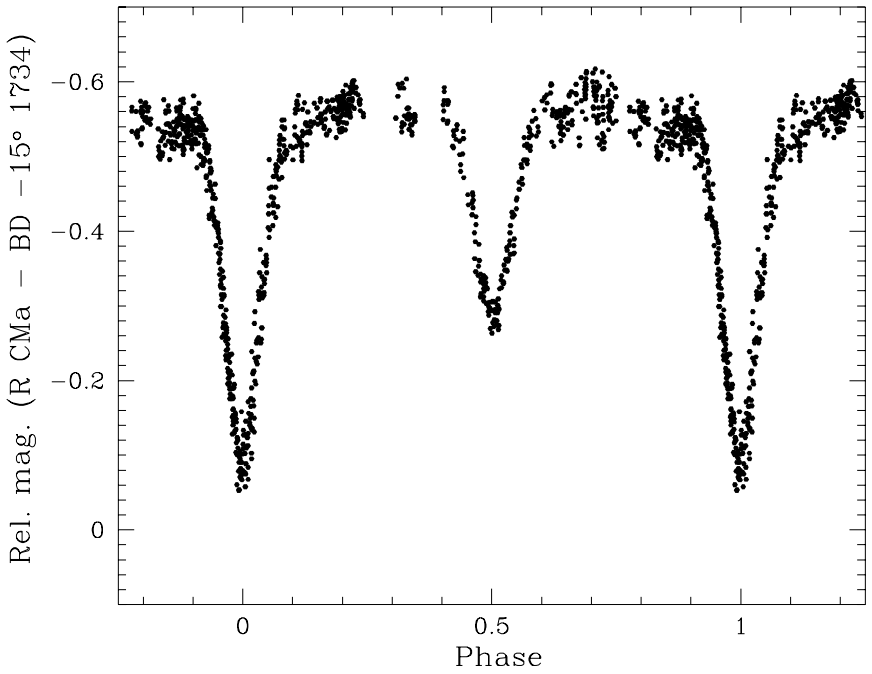

Figure 4.2: K band light curve of R CMa. Observed relative magnitudes (R CMa - BD−15°1734) are shown.

Table 4.4: Observed epochs of minima of R CMa

Epoch of minimum(HJD)			Band	No. of Pts.	Analysis method	Minima type
2450034.4301	±	0.00098	J	34	K	SM
2450088.3859	±	0.0005	J	62	K	PM
2450092.35933	±	0.00007	J	64	L + K	SM
2450096.3408	±	0.0002	J	32	L + K	PM
2450116.21785	±	0.00005	K	38	L + K	SM
2450117.354498	±	0.000004	K	23	L + K	SM
2450145.1819	±	0.0003	K	82	L + K	PM
2450154.2663	±	0.0009	K	24	L + K	PM
2450439.39475	±	0.00008	K	64	L + K	PM

insufficient to form a light curve for analysis.

Five epochs of primary minima (2 in the J band and 3 in the K band) and 4 epochs of secondary minima (2 in the J band and 2 in the K band) are observed. The epochs of minima are determined using Kwee - van Woerden (1924) method or by fitting a series of Legendre polynomials. Whenever the light curves were low in scatter, Kwee - van Woerden method was used to find the epochs of minima. When scatter of points in an observed light curve was high, the eclipse region was first fitted with a series of Legendre Polynomials and then Kwee - van Woerden method was applied to the fitted polynomial to find the epoch of minimum. The calculated epochs of minima are given in Table 4.4 along with the method used and number of points. K implies Kwee - van Woerden method and L + K implies fitting a series of Legendre Polynomials and then applying Kwee - van Woerden method.

A new linear ephemeris is derived for R CMa from our light curve observations by doing a linear least square fit to the observed epochs of primary minima

and the eclipse number.

$$JD\ Hel.\ Min\ I = 2450065.666391\ (\pm 0.0005)\ + 1^d.1359499\ (\pm 0.000004)\ E_0 \quad (4.1)$$

The phases of eclipse corresponding to the epochs of observations are calculated using this ephemeris. All the observed minima, primary and secondary, are found to be due to partial eclipses as seen by all the previous observers.

4.3 Light Curve Analysis

The light curves are analyzed using the Wilson's light curve interpretation program (Wilson 1979). A short description of this model is given in section 2.3.

4.3.1 Analysis of the J and K light curves

The average of the relative magnitudes between phases 0.24 and 0.26 of the J & K light curves are subtracted from the corresponding light curves, the relative magnitudes are averaged in phase intervals of 0.01 and converted to relative light values to create the normalized light curve for the analysis. 98 normal points are formed in the J band and 87 points in the K band. Each point is weighted according to the number of points used to form the normalized point for the analysis. The weighting is also applied according to the inverse of the light values (selecting noise = 2 in the model input data set) so that maximum weightage will come to the region of eclipse.

The value of $q(0.158)$ derived by Tomkin (1985) is used as a fixed parameter for all our analysis of the light curves of this star. This value of q matches well with the estimates of Guinan (1977) (0.15, assuming M_1 to be 1.7 $M_\odot$ for an F1 V star and 0.165 assuming the secondary to be lobe-filling). Sarma, Rao & Abhyankar (1996) have also used this value of q for their analysis of optical light curves. The J & K light curves are analyzed in the 'mode 5' of the Wilson's programme assuming a semi-detached configuration of the Algol type, with phase of

minimum, $i, T_2, \Omega_1 \& L_1$ as free parameters. The model parameter IPB = 0 is selected so that the secondary luminosity is coupled to its temperature. The gravity darkening co-efficient and the bolometric albedo of the primary are selected according to the theoretically expected values for an F1 V star with radiative atmosphere ($g_1 = A_1 = 1.0$). Corresponding gravity darkening co-efficient $g_2 = 0.32$ is adopted for the secondary star assuming it to have a convective atmosphere. Primary is considered as a star with a radiative envelope for fixing the gravity darkening co-efficients considering its spectral type. Its derived mass (1.07 $M_\odot$) is however less for a star with a radiative envelope and a convective core (DeLore & Doom 1992). A linear law is adopted for treating the limb darkening and the co-efficients of limb darkening are adopted from Al - Naimiy (1978) for the stars of surface temperatures and gravities corresponding to the primary and the secondary respectively. Similarly the bolometric limb darkening co-efficients are adopted from Van Hamme (1993). Both the component stars are assumed to rotate synchronously in circular orbits. The model fits are done for the normalized light curves only. The light curves are analyzed initially with $A_2 = 0.5$, the expected value for a star with a convective atmosphere. We have seen through chapters 2 and 3 that in Algols, A_2 is not a parameter, the variation of which from the theoretical value can be ignored. So analysis is also done with A_2 as a free parameter. When A_2 is left as a free parameter, the J band fit converged with a value around 0.5 within error limits. So we have adopted $A_2 = 0.5$ as a fixed parameter in the final run of the J band fit. The K band curve showed a high A_2 and the sum of residuals in K was found to be lesser for the model with A_2 as a free parameter than for the model with $A_2 = 0.5$. The fitted values are given in Table 4.5. The normal points and the model fits in the J and K bands are shown in Figs. 4.3 and 4.4 respectively. The fits are shown for the model with A_2 as a free parameter. Both the light curves are found to be asymmetric with the asymmetry more in the J band than in the K band. The second quadrature (average of relative magnitude values in the phase interval 0.72 to 0.78) is fainter than the first quadrature (average of relative magnitude values in the phase interval 0.22 to 0.28) by $0^m.015$ in the J band and by $0^m.019$ in the K band.

Table 4.5: Analysis of J and K band light curves of R CMa. f: fixed parameter.

Parameter	J Band $A_2 = 0.5$	K Band	
		$A_2 = 0.5$	$A_2 = free$
T_1^f	7310 K	7310 K	7310 K
T_2	4580 ± 25 K	5128 ± 46 K	5158 ± 47 K
q^f	0.158	0.158	0.158
i	$79^o.37 \pm 0.09$	$79^o.55 \pm 0.098$	$79^o.47 \pm 0.1$
Ω_1	3.566 ± 0.036	3.580 ± 0.055	3.612 ± 0.053
Ω_2	2.1234	2.1234	2.1234
$r_{1\ pole}$	0.293 ± 0.003	0.292 ± 0.005	0.289 ± 0.004
$r_{1\ point}$	0.300 ± 0.003	0.298 ± 0.005	0.296 ± 0.005
$r_{1\ side}$	0.297 ± 0.003	0.296 ± 0.005	0.293 ± 0.005
$r_{1\ back}$	0.299 ± 0.003	0.298 ± 0.005	0.295 ± 0.005
$r_{2\ pole}$	0.2173	0.2173	0.2173
$r_{2\ point}$	0.3202	0.3202	0.3202
$r_{2\ side}$	0.2260	0.2260	0.2260
$r_{2\ back}$	0.2579	0.2579	0.2579
x_1^f	0.315	0.198	0.198
x_2^f	0.450	0.270	0.270
$x_{1\ bol}^f$	0.464	0.464	0.464
$x_{2\ bol}^f$	0.537	0.530	0.530
g_1^f	1.00	1.00	1.00
g_2^f	0.32	0.32	0.32
A_1^f	1.000	1.000	1.000
A_2	0.500^f	0.500^f	0.84 ± 0.16
$L_1/(L_1+L_2)$	0.823 ± 0.004	0.729 ± 0.008	0.723 ± 0.008
$L_2/(L_1+L_2)$	0.177 ± 0.007	0.271 ± 0.017	0.277 ± 0.017
l_3^f	0.0000	0.0000	0.0000
Phase shift	0.0007 ± 0.0003	-0.0005 ± 0.0003	-0.0005 ± 0.0003

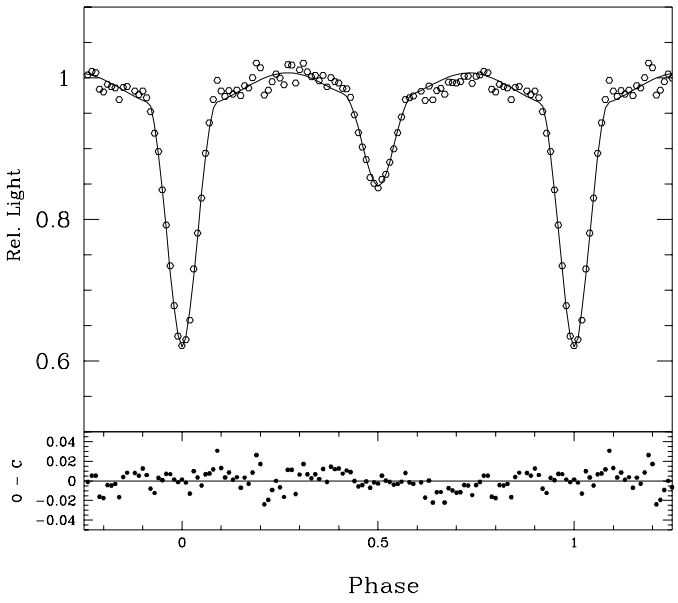

Figure 4.3: J band light curve of R CMa. The circles show the normalized light curve and the continuous line is the model fit. The bottom panel shows the difference between the model and the observed data. The fit shown is with $A_2 = 0.5$

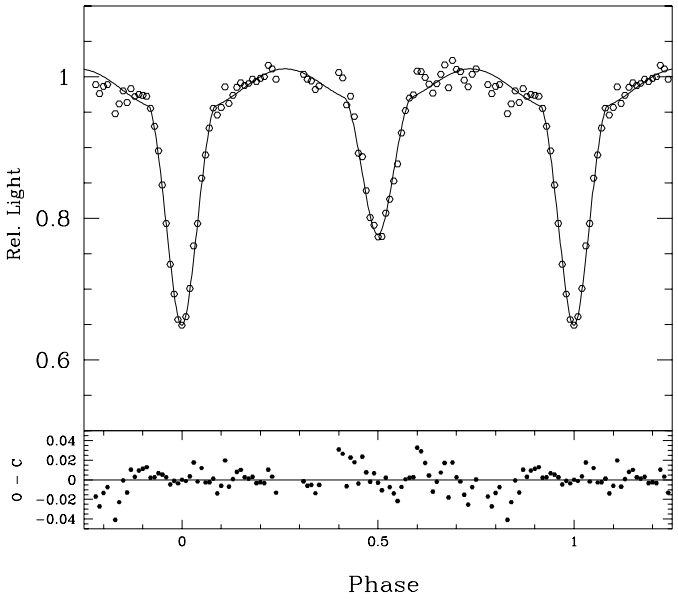

Figure 4.4: K band light curve of R CMa. The circles show the normalized light curve and the continuous line is the model fit. The bottom panel shows the difference between the model and the observed data. The fit shown is with A_2 as free parameter.

Table 4.6 shows the arithmetic mean and rms of *normal points - model* in different regions of the light curves. The light curves are divided into 8 sectors considering the duration of eclipses ($0.15 \times$ Period) and the phases of beginning and end of eclipses. It is clear from the table that in both the bands, the secondary eclipses are asymmetric. The primary eclipses do not have any asymmetry. It is also clear that there is a rise in flux in the J band before the beginning of the secondary eclipse and a fall in flux after the secondary eclipse. The arithmetic mean of the residuals has maximum positive value in the phase interval 0.25 - 0.425 and maximum negative value in the phase interval 0.575 - 0.75 in the J band. This effect is more pronounced in the J band light curve of RZ Cas. For reasons described in section 3.3.4, we have not attempted to fit this depression in the light curves with a spot on the secondary. But in the K band, the normal points after the secondary eclipse are lying above the model, but, most of the normal points between phases 0.65 and 0.9 are lying below the model fit.

The T_2 derived from the J band data is higher than that obtained from the analysis of the UBV data by $(\sim 300K)$ and this is discussed in the next section. The T_2 derived from our K band light curve is higher than the T_2 from J band by $(\sim 550K)$. The primary eclipse is found to be shallower by 0.02 and 0.03 magnitudes and the secondary eclipse deeper by 0.03 and 0.07 magnitudes in the J and K band respectively than what was expected from the observed depth of eclipse and the temperatures of the components in the V band. This will give the net effect of a secondary of higher temperature in the analysis of the light curves in these bands compared to the derived temperature of the secondary from the V light curve.

4.3.2 *Analysis of the optical light curves*

Making conclusions about an eclipsing binary, by analysis of the light curve in only one particular wavelength can always be biased as there can be emission or absorption features in the system in that particular wave band. It is also important that the analysis of the light curves under study be treated with the same model

Table 4.6: Average values of residuals at different parts of the J and K light curves

Phase interval	J Band		K Band	
	Arithmetic Mean	r.m.s	Arithmetic Mean	r.m.s
$A_2 = 0.5$				
0.000 - 0.075	+.00123	.00716	+.00263	.00757
0.075 - 0.250	+.00387	.01439	-.00071	.00828
0.250 - 0.425	+.00537	.01059	+.00560	.01694
0.425 - 0.500	-.00155	.00483	+.00978	.01581
0.500 - 0.575	+.00071	.00410	-.00714	.01058
0.575 - 0.750	-.00926	.01145	+.00538	.01667
0.750 - 0.925	-.00100	.00933	-.00820	.01739
0.925 - 1.000	+.00087	.00616	+.00131	.00400
with A_2 as free parameter				
0.000 - 0.075	+.00145	.00678	+.00319	.00781
0.075 - 0.250	+.00469	.01466	+.00071	.00833
0.250 - 0.425	+.00525	.01037	+.00251	.01577
0.425 - 0.500	-.00133	.00445	+.00871	.01380
0.500 - 0.575	+.00087	.00422	-.00824	.01122
0.575 - 0.750	-.00935	.01150	+.00292	.01549
0.750 - 0.925	-.00018	.00934	-.00662	.01716
0.925 - 1.000	+.00065	.00613	+.00115	.00420

and technique, so that all the different effects in the system are treated in a similar manner at all the wavelengths. With this view we have analyzed the U, U_n, B, B_n, V, V_n, $H_{\beta w}$ and $H_{\beta n}$ light curves of Guinan (1977) with the Wilson's program and done a comparative study of the results with the results of the analysis of our J & K light curves. The results are also compared with Guinan's results and the results derived by the previous studies of several other optical light curves. These light curves were obtained during the period from Dec. '67 to April '68. This data has a good coverage of the optical bands for our analysis. Also this set of data is not yet analyzed with the Wilson's program. Guinan has used the method of rectification for the analysis of these light curves. He found that the secondary minima in the V and $H_{\beta n}$ bands are asymmetric with the descending branch steeper than the ascending branch while Koch (1960), Kitamura & Takahashi (1962) and Sato (1971) found asymmetric secondary minima in all the bands of their light curves. The results derived by Guinan (1977) in these two bands were significantly different from the results obtained from the analysis of the light curves in the other bands as evident from Table VII of Guinan (1977). He observed that this difference was due to the V and $H_{\beta n}$ light curves being 1 - 2 % brighter near the shoulders of the primary minima than the other curves. He attributed the difference in these bands to the presence of variable amount of circumstellar gas in the system. He observed that the $H_{\beta n}$ is sensitive to the emission or absorption in the H_β line while V band is most sensitive to the continuous emission of a gas in the temperature range 4000 - 5000 K.

As in the case of the analysis of the IR light curves, the stars were considered as rotating synchronously in circular orbits. $g_1 \& g_2$ are fixed to 1.0 and 0.32 respectively. The values of limb darkening co-efficients, monochromatic and bolometric, were taken from Al Naimiy (1978) and Van Hamme (1993) respectively for the stars of corresponding wavelengths and surface gravities. Linear law was adopted for the limb darkening. A bolometric albedo of 1.0 is assumed for the primary star. Initially, the light curves are analyzed with A_2 = 0.5 as expected for a star with a convective envelope. The region outside the eclipse in most of these light curves

showed the signatures of a high albedo. So the fitting was also done, with A_2 as a free parameter. The results are given in subsequent sections.

Sato (1971) has done extensive photometric study of R CMa in the UBV bands. His V light curve is composed of a set of 622 individual observations with very good coverage of all phases. He has analyzed the light curves using the method of Russell & Merrill (1952) that makes use of rectification. Since R CMa is reported to host variable amount of gas, we decided to analyze Sato's V light curve with the Wilson's model and compare the results with our results from the analysis of Guinan's (1977) V light curves. This comparative study is expected to bring out the short term variations seen in the light curves of R CMa.

Analysis of the V light curves

Analysis, carried out in this study, of the V and V_n band light curves, observed by Guinan (1977) and V light curve observed by Sato (1971) are presented in this section. A comparative study of our results with those obtained by Guinan and Sato is also done.

The complete light curves of Guinan were used for analysis and no binning in phase was done. The light values and the model fits with A_2 as free parameter are shown in Figs. 4.5 and 4.6 for V and V_n light curves respectively. Elements derived from the analysis of the V light curves are presented in Table 4.7. One interesting thing that is noticed from Table 4.7 is the high bolometric albedo of the secondary in both the V and V_n light curves. In both these light curves of Guinan (1977), when A_2 is left as a free parameter, the fits converged to values higher than 0.5. Analysis of the K band light curve observed by us also yielded a high A_2 whereas J band yielded a normal atmosphere with $A_2 = 0.5$. The problem of finding unexpected high A_2 was discussed in the case of RZ Cas where the J and K band light curves showed high A_2 while the optical light curves were normal with $A_2 = 0.5$ as expected for a low mass star with a convective atmosphere. There

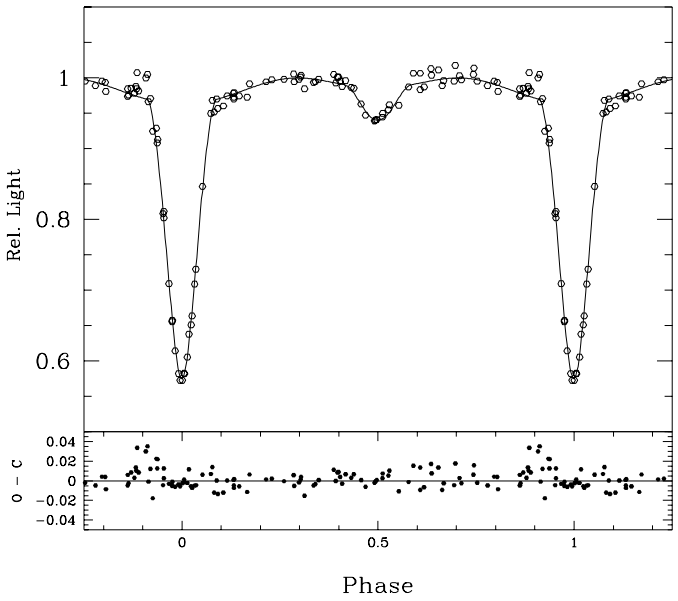

Figure 4.5: V band light curve of R CMa observed by Guinan. The top panel shows the observed data and the model fit. The bottom panel shows the difference between the observations and the model. The fit shown is with A_2 as a free parameter.

we had considered some alternative explanations too. Here an attempt is made to understand the reason for this high A_2, ie., whether it can be a property of the photosphere [1] or not and, if not, what can be the reason?

First of all, we have to realize that if the high value of A_2 is of photospheric origin, it should be seen in all the light curves of our study. The simulations presented in section 2.3.3 show that in Algols, A_2 is a significant parameter irrespective of the wavelength and in a light curve analysis, a high value of A_2 will show up clearly. So the very fact that we do not see a high value of A_2 in many of the optical light curves and in our J band light curve raises doubts on the photospheric origin of this abnormality. Another important fact is that this high value of A_2, if of photospheric origin, cannot change over a period of a few years. To understand this, and to look for the time variability of any other system parameter which can be present, we have analyzed the V light curve of Sato (1971).

Sato's V light curve was obtained during the period HJD 2439116 - 2439876 and Guinan's, during the period HJD 2439827 - 2439986. Sato had used Russell

[1] originating from the bolometric albedo not being 0.5 for a convective atmosphere or the atmosphere of the secondary itself not being convective.

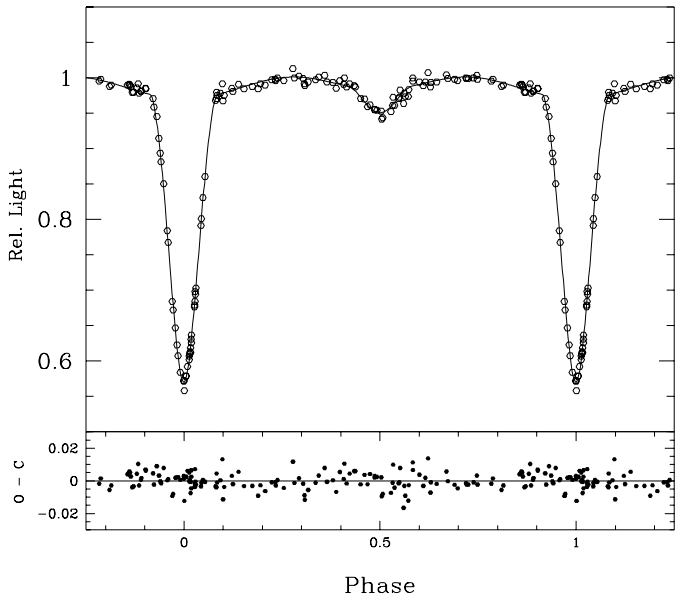

Figure 4.6: V_n band light curve of R CMa observed by Guinan. The top panel shows the observed data and the model fit. The bottom panel shows the difference between the observations and the model. The fit shown is with A_2 as a free parameter.

- Merril rectification method to analyze the light curve. We have normalized this light curve as described in section 4.3.1. Binning was done in a phase interval of 0.01 and 99 normal points were formed. The light curve was analyzed using Wilson's program. The fitted light curve is shown in Fig. 4.7 and the parameters are given in Table 4.7. We can see that the value of T_2 derived from all these three V light curves are in very good agreement. So during this period, we can rule out any possible changes in the apparent temperature of the secondary due to mechanisms like large scale spot activity. The values of Ω_1 and i also agree well among the light curves. But the difference in derived values of A_2 is noticeable. Both V and V_n light curves of Guinan (1977) showed a high A_2 whereas Sato's V light curve converged with with A_2 = 0.5 and didn't show any signature of high bolometric Albedo. From this we can conclude that the apparently high A_2 that we see in many of the subgiants may not be of photospheric origin. One possibility is a changing phenomenon like a gas stream which can be present in one epoch due to Roche lobe overflow from the secondary due to some instability.

Another interesting phenomenon which is noticed is the systematically high

Table 4.7: Elements obtained from the analysis of V band data of R CMa. f: fixed parameter.

Parameter	V Light curves of Guinan				V Light curves of Sato
	V_{broad}		V_{narrow}		V_{broad}
	$A_2 = 0.5$	$A_2 = free$	$A_2 = 0.5$	$A_2 = free$	$A_2 = 0.5$
T_1^f	7310 K	7310 K	7310 K	7310 K	7310 K
T_2	4223 ± 60 K	4192 ± 59 K	4240 ± 35	4240 ± 33 K	4250 ± 39 K
q^f	0.158	0.158	0.158	0.158	0.158
i	$79^o.80 \pm 0.09$	$79^o.54 \pm 0.09$	$79^o.60 \pm 0.04$	$79^o.50 \pm 0.05$	$79^o.35 \pm 0.05$
Ω_1	3.402 ± 0.032	3.470 ± 0.034	3.478 ± 0.017	3.506 ± 0.018	3.434 ± 0.017
Ω_2	2.1234	2.1234	2.1234	2.1234	2.1234
$r_{1\,pole}$	0.308 ± 0.003	0.301 ± 0.003	0.301 ± 0.002	0.298 ± 0.002	0.305 ± 0.002
$r_{1\,point}$	0.316 ± 0.003	0.309 ± 0.004	0.308 ± 0.002	0.306 ± 0.002	0.313 ± 0.002
$r_{1\,side}$	0.313 ± 0.003	0.306 ± 0.003	0.306 ± 0.002	0.303 ± 0.002	0.310 ± 0.001
$r_{1\,back}$	0.315 ± 0.003	0.308 ± 0.003	0.307 ± 0.002	0.305 ± 0.002	0.312 ± 0.002
$r_{2\,pole}$	0.2173	0.2173	0.2173	0.2173	0.2173
$r_{2\,point}$	0.3202	0.3202	0.3202	0.3202	0.3202
$r_{2\,side}$	0.2260	0.2260	0.2260	0.2260	0.2260
$r_{2\,back}$	0.2579	0.2579	0.2579	0.2579	0.2579
x_1^f	0.630	0.630	0.640	0.640	0.630
x_2^f	0.850	0.850	0.942	0.942	0.850
$x_{1,bol}^f$	0.464	0.464	0.464	0.464	0.464
$x_{2,bol}^f$	0.530	0.530	0.530	0.530	0.530
g_1^f	1.00	1.00	1.00	1.00	1.00
g_2^f	0.32	0.32	0.32	0.32	0.32
A_1^f	1.000	1.000	1.000	1.00	1.000
A_2	0.500^f	0.92 ± 0.08	0.500^f	0.71 ± 0.05	0.500^f
$L_1/(L_1+L_2)$	0.963 ± 0.004	0.963 ± 0.004	0.969 ± 0.002	0.969 ± 0.002	0.961 ± 0.002
$L_2/(L_1+L_2)$	0.037 ± 0.004	0.037 ± 0.004	0.031 ± 0.002	0.031 ± 0.002	0.039 ± 0.003
l_3^f	0.0000	0.0000	0.0000	0.0000	0.0000
Phase shift	-0.0003 ± 0.0002	-0.0003 ± 0.0002	-0.0004 ± 0.0001	-0.0004 ± 0.0001	0.0065 ± 0.0001

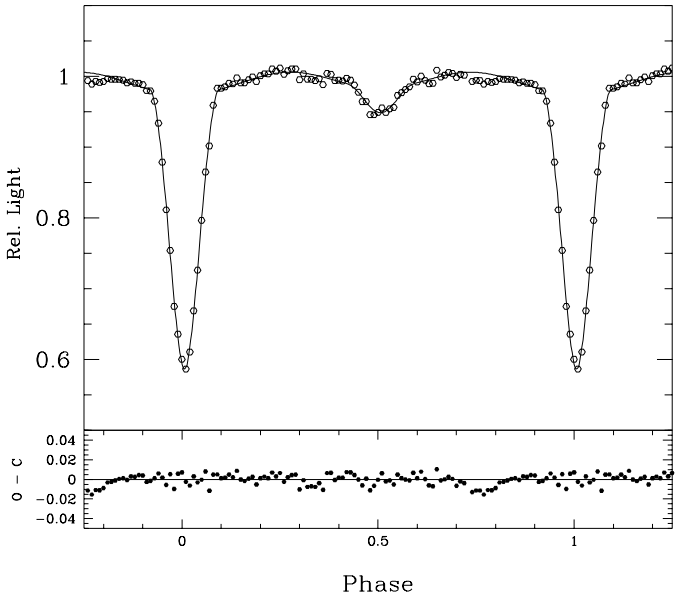

Figure 4.7: V band light curve of R CMa observed by Sato. The top panel shows the observed data and the model fit. The bottom panel shows the difference between the observations and the model.

A_2 in the broad band light curves compared to the narrow bands. We have got 5 such sets of light curves here namely, (V, V_n), ($H_{\alpha w}$, $H_{\alpha n}$), ($H_{\beta w}$, $H_{\beta n}$), (B, B_n) and (U, U_n). In all these sets, except (U, U_n) where the light curves are too much scattered, it is the broad band light curve which is having a higher A_2 compared to the narrow bands. This is seen very well in Table 4.13 where the results from the analysis of all the light curves in the present study are compiled. This can give us some clues about the reason for the observed high A_2 in many Algol systems.

Analysis of the H_β, B and U light curves

The broad band and *narrow* band light curves in the H_β, B and U light curves of Guinan(1977) are analyzed in the same way as the V light curves. The complete light curves of Guinan were used and no normalization was done. The light curves are analyzed separately and the analysis was done with $A_2 = 0.5$ and with A_2 as a free parameter. The analysis is done with IPB = 0 with L_2 coupled to T_2. q and T_1 are fixed to their pre-determined values and A_1, limb darkening and gravity darkening co-efficients are fixed to their theoretical values. The results of

Table 4.8: Analysis of $H_{\beta w}$ and $H_{\beta n}$ band data of R CMa. f: parameter fixed during the analysis.

Parameter	$H_{\beta w}$		$H_{\beta n}$	
	$A_2 = 0.5$	$A_2 = free$	$A_2 = 0.5$	$A_2 = free$
T_1^f	7310 K	7310 K	7310 K	7310 K
T_2	4291 ± 48 K	4300 ± 45 K	4328 ± 45	4328 ± 44 K
q^f	0.158	0.158	0.158	0.158
i	$79^o.33 \pm 0.06$	$79^o.21 \pm 0.06$	$79^o.52 \pm 0.06$	$79^o.36 \pm 0.06$
Ω_1	3.487 ± 0.024	3.534 ± 0.024	3.385 ± 0.018	3.428 ± 0.017
Ω_2	2.1234	2.1234	2.1234	2.1234
$r_{1\ pole}$	0.300 ± 0.002	0.296 ± 0.002	0.309 ± 0.002	0.305 ± 0.002
$r_{1\ point}$	0.307 ± 0.002	0.303 ± 0.002	0.318 ± 0.002	0.313 ± 0.002
$r_{1\ side}$	0.305 ± 0.002	0.300 ± 0.002	0.315 ± 0.002	0.310 ± 0.001
$r_{1\ back}$	0.306 ± 0.002	0.302 ± 0.002	0.317 ± 0.002	0.312 ± 0.001
$r_{2\ pole}$	0.2173	0.2173	0.2173	0.2173
$r_{2\ point}$	0.3202	0.3202	0.3202	0.3202
$r_{2\ side}$	0.2260	0.2260	0.2260	0.2260
$r_{2\ back}$	0.2579	0.2579	0.2579	0.2579
x_1^f	0.651	0.651	0.651	0.651
x_2^f	0.960	0.960	0.960	0.960
$x_{1\ bol}^f$	0.464	0.464	0.464	0.464
$x_{2\ bol}^f$	0.531	0.531	0.531	0.531
g_1^f	1.00	1.00	1.00	1.00
g_2^f	0.32	0.32	0.32	0.32
A_1^f	1.00	1.00	1.00	1.00
A_2	0.500^f	0.83 ± 0.05	0.500^f	0.76 ± 0.05
$L_1/(L_1+L_2)$	0.970 ± 0.002	0.969 ± 0.003	0.971 ± 0.002	0.970 ± 0.002
$L_2/(L_1+L_2)$	0.030 ± 0.003	0.031 ± 0.003	0.029 ± 0.003	0.030 ± 0.003
l_3^f	0.0000	0.0000	0.0000	0.0000
Phase shift	0.0000 ± 0.0002	0.0000 ± 0.0002	-0.0002 ± 0.0002	-0.0002 ± 0.0002

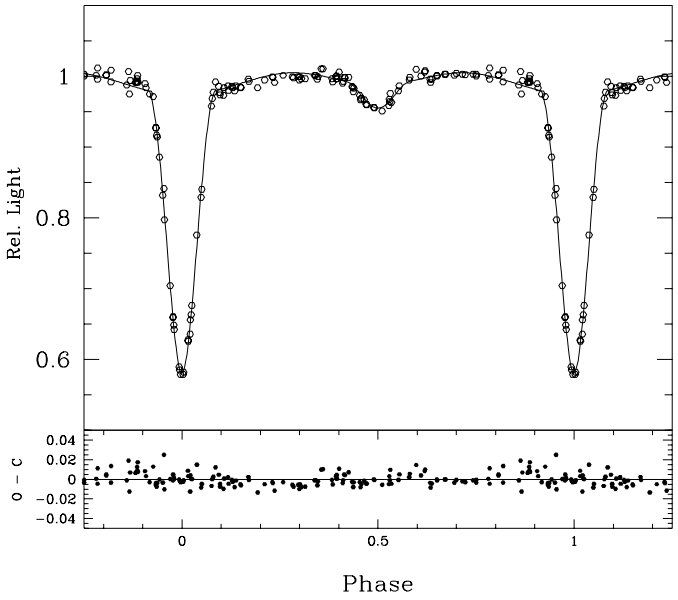

Figure 4.8: $H_{\beta w}$ band light curve of R CMa observed by Guinan. The top panel shows the observed data and the model fit with A_2 as a free parameter. The bottom panel shows the difference between the observations and the model.

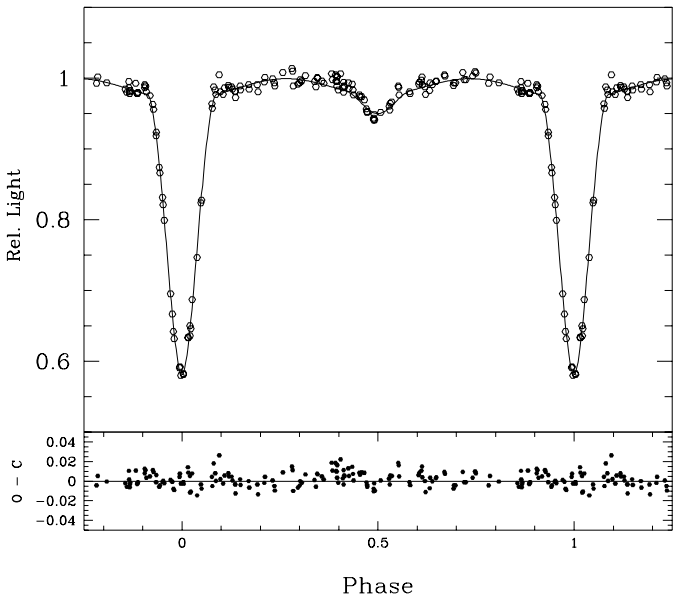

Figure 4.9: $H_{\beta n}$ light curve of R CMa observed by Guinan. The top panel shows the observed data and the model fit. The bottom panel shows the difference between the observations and the model. The fits shown are with A_2 as a free parameter.

Table 4.9: Elements obtained from the analysis of broad band and narrow band B light curves of R CMa

Parameter	B		B_{narrow}	
	$A_2 = 0.5$	$A_2 = free$	$A_2 = 0.5$	$A_2 = free$
T_1^f	7310 K	7310 K	7310 K	7310 K
T_2	4403 ± 64 K	4393 ± 63 K	4103 ± 64	4103 ± 63 K
q^f	0.158	0.158	0.158	0.158
i	$79^o.72 \pm 0.08$	$79^o.63 \pm 0.07$	$79^o.61 \pm 0.03$	$79^o.55 \pm 0.05$
Ω_1	3.418 ± 0.028	3.443 ± 0.022	3.452 ± 0.014	3.474 ± 0.017
Ω_2	2.1234	2.1234	2.1234	2.1234
$r_{1\ pole}$	0.306 ± 0.003	0.304 ± 0.002	0.303 ± 0.001	0.301 ± 0.002
$r_{1\ point}$	0.314 ± 0.003	0.312 ± 0.002	0.311 ± 0.001	0.309 ± 0.002
$r_{1\ side}$	0.311 ± 0.003	0.309 ± 0.002	0.308 ± 0.001	0.306 ± 0.002
$r_{1\ back}$	0.313 ± 0.003	0.311 ± 0.002	0.310 ± 0.001	0.308 ± 0.002
$r_{2\ pole}$	0.2173	0.2173	0.2173	0.2173
$r_{2\ point}$	0.3202	0.3202	0.3202	0.3202
$r_{2\ side}$	0.2260	0.2260	0.2260	0.2260
$r_{2\ back}$	0.2579	0.2579	0.2579	0.2579
x_1^f	0.690	0.690	0.715	0.715
x_2^f	0.990	0.990	0.990	0.990
$x_{1\ bol}^f$	0.464	0.464	0.464	0.464
$x_{2\ bol}^f$	0.537	0.537	0.530	0.530
g_1^f	1.00	1.00	1.00	1.00
g_2^f	0.32	0.32	0.32	0.32
A_1^f	1.00	1.00	1.00	1.00
A_2	0.500^f	0.72 ± 0.09	0.500^f	0.62 ± 0.07
$L_1/(L_1 + L_2)$	0.975 ± 0.003	0.975 ± 0.003	0.987 ± 0.002	0.987 ± 0.002
$L_2/(L_1 + L_2)$	0.025 ± 0.003	0.025 ± 0.003	0.013 ± 0.002	0.013 ± 0.002
l_3^f	0.0000	0.0000	0.0000	0.0000
Phase shift	-0.0001 ± 0.0002	-0.0001 ± 0.0002	-0.0002 ± 0.0001	-0.0002 ± 0.0001

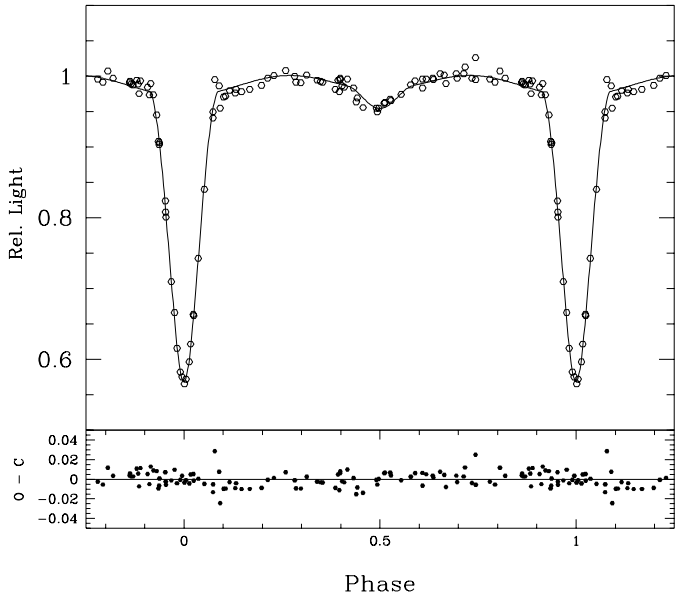

Figure 4.10: B band light curve of R CMa observed by Guinan. The top panel shows the observed data and the model fit with A_2 as a free parameter. The bottom panel shows the difference between the observations and the model.

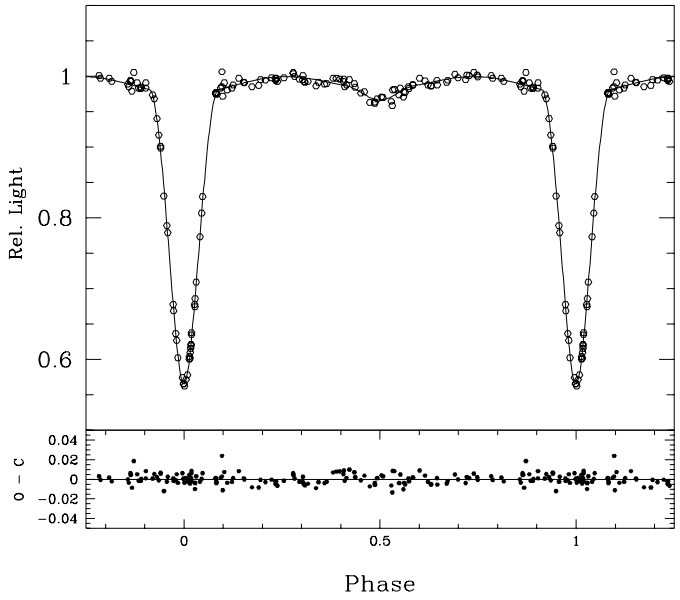

Figure 4.11: B_n light curve of R CMa observed by Guinan. The top panel shows the observed data and the model fit with A_2 as a free parameter. The bottom panel shows the difference between he observations and the model.

Table 4.10: Elements obtained from the analysis of U and U_n band light curves of R CMa

Parameter	U		U_n	
	$A_2 = 0.5$	$A_2 = free$	$A_2 = 0.5$	$A_2 = free$
T_1^f	7310 K	7310 K	7310 K	7310 K
T_2	4152 ± 141 K	4124 ± 151 K	4353 ± 92	4299 ± 98 K
q^f	0.158	0.158	0.158	0.158
i	$79^o.47 \pm 0.08$	$79^o.44 \pm 0.09$	$79^o.65 \pm 0.09$	$79^o.47 \pm 0.10$
Ω_1	3.454 ± 0.029	3.461 ± 0.031	3.388 ± 0.035	3.431 ± 0.035
Ω_2	2.1234	2.1234	2.1234	2.1234
$r_{1\ pole}$	0.303 ± 0.003	0.302 ± 0.003	0.309 ± 0.003	0.305 ± 0.003
$r_{1\ point}$	0.311 ± 0.003	0.310 ± 0.003	0.318 ± 0.004	0.313 ± 0.004
$r_{1\ side}$	0.308 ± 0.003	0.307 ± 0.003	0.315 ± 0.004	0.310 ± 0.004
$r_{1\ back}$	0.310 ± 0.003	0.309 ± 0.003	0.317 ± 0.004	0.312 ± 0.004
$r_{2\ pole}$	0.2173	0.2173	0.2173	0.2173
$r_{2\ point}$	0.3202	0.3202	0.3202	0.3202
$r_{2\ side}$	0.2260	0.2260	0.2260	0.2260
$r_{2\ back}$	0.2579	0.2579	0.2579	0.2579
x_1^f	0.767	0.767	0.767	0.767
x_2^f	1.000	1.000	1.000	1.000
$x_{1\ bol}^f$	0.464	0.464	0.464	0.464
$x_{2\ bol}^f$	0.524	0.524	0.524	0.524
g_1^f	1.00	1.00	1.00	1.00
g_2^f	0.32	0.32	0.32	0.32
A_1^f	1.000	1.000	1.000	1.000
A_2	0.500^f	0.67 ± 0.13	0.500^f	1.00 ± 0.11
$L_1/(L_1+L_2)$	0.991 ± 0.003	0.991 ± 0.004	0.984 ± 0.004	0.986 ± 0.004
$L_2/(L_1+L_2)$	0.009 ± 0.004	0.009 ± 0.004	0.016 ± 0.004	0.014 ± 0.004
l_3	0.0000^f	0.0000	0.0000	0.0000
Phase shift	-0.0003 ± 0.0003	-0.0007 ± 0.0002	-0.0007 ± 0.0002	-0.0007 ± 0.0002

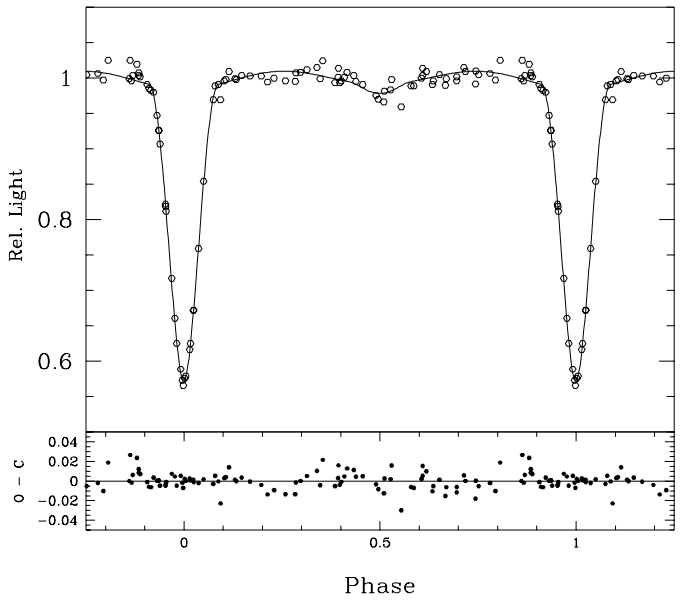

Figure 4.12: U band light curve of R CMa observed by Guinan. The top panel shows the observed data and the model fit with A_2 as a free parameter. The bottom panel shows the difference between the observations and the model.

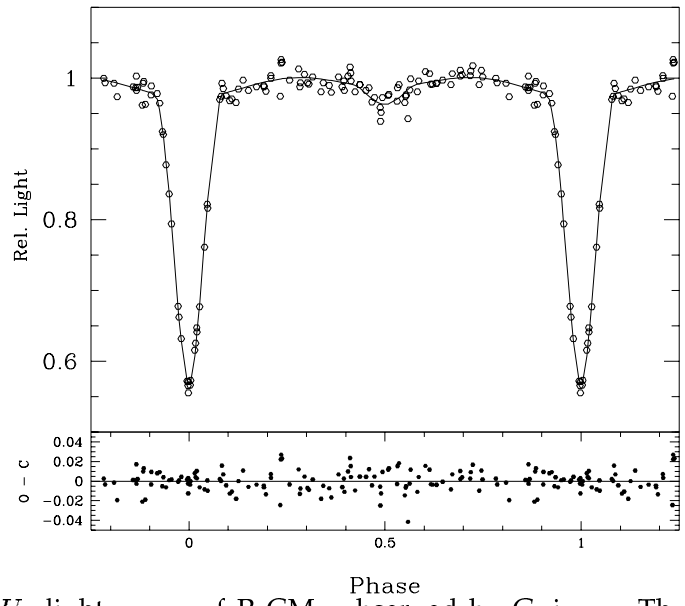

Figure 4.13: U_n light curve of R CMa observed by Guinan. The top panel shows the observed data and the model fit with A_2 as a free parameter. The bottom panel shows the difference between the observations and the model.

the analysis are given in Tables 4.8, 4.9 and 4.10 for the H_β, B and U light curves respectively. The light curves and the model fits are shown in Figs. 4.8, 4.9, 4.10, 4.11, 4.12 and 4.13 respectively.

The inclination derived from these light curves match well with that derived from all the other light curves in the present study and is also in very good agreement with that derived by Sarma, Rao & Abhyankar (1996). The errors in T_2 in these bands are comparatively larger than that in the other bands. The secondary minima are shallow in these bands and the light curves are more scattered especially in the U bands. The values of L_1 and L_2 derived from the B and V bands match well with the values derived by Budding *et al.* (1994). But the values of L_1 are higher than that derived by Sarma, Rao & Abhyankar. Budding *et al.* have used a lower value of T_2 and higher value of T_1. The inclination derived by them is higher than that derived in this study.

Analysis of the H_α light curves

The motivation behind taking up this light curve for our analysis was to study the system at a wavelength between the V and J bands and to look for the properties of the system. Edalati, Khalesse & Riazi (1989) observed R CMa in the $H_{\alpha w}$ and $H_{\alpha n}$ filters at $6583\ \mathring{A}(FWHM = 238\mathring{A})$ and $6569\ \mathring{A}(FWHM = 38\mathring{A})$ respectively. They found the system with small light variations outside the minima implying small reflection and ellipticity effects. The light curves were analyzed in the frequency domain. They obtained the H_α indices of the system at various phases (Table IV of Edalati, Khalesse & Riazi 1989) and didn't find any changes in the indices at primary and secondary eclipses beyond the error values. Also the secondary minimum was found to coincide with the phase 0.5 and equal durations for both the eclipses implying a circular orbit. We have analyzed these H_α light curves with the Wilson's program. The complete light curve comprising of 134 points is given in Table II of Edalati Khalesse & Riazi. The complete light curves were used for the analysis. The magnitudes were converted into light units and normalized with the

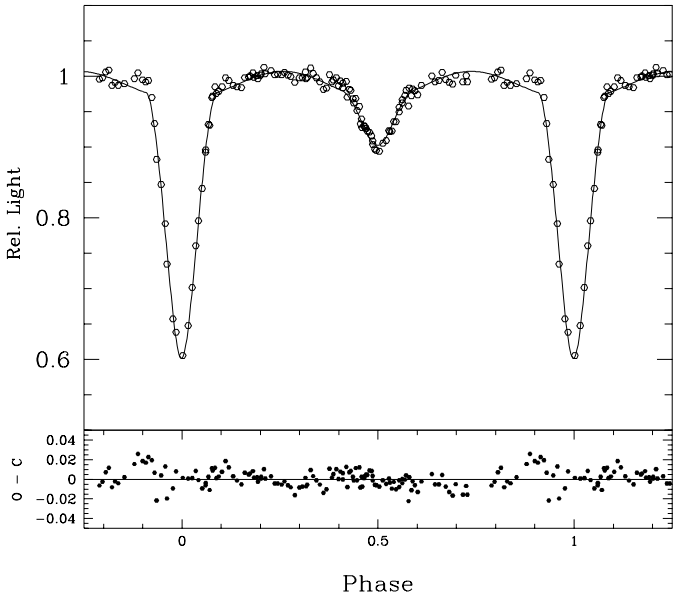

Figure 4.14: The $H_{\alpha w}$ band light curve. The top panel shows the light curve and the model fit with A_2 as free parameter and the bottom panel shows the residuals.

average light around phase 0.25 as mentioned above.

The light curves are fitted with the same set of free parameters as in the analysis of other light curves. The model fits along with the data points are shown in Fig. 4.14 and 4.15. The parameters are given in Table 4.11. The inclination agrees very well with the values of inclination derived from light curves at other wavelengths. The size of the primary star is also agreeing with that obtained from the analysis in the other wavelengths. But the values of the secondary temperature (T_2) derived from the H_α wave bands are much higher than that derived from the analysis of the light curves in the other neighboring wave bands. It is higher in the $H_{\alpha w}$ band by $\sim$ 450 K than what is derived from V and by $\sim$ 100 K than that from the J band. The value of T_2 derived from the $H_{\alpha n}$ light curve is higher than that derived form the $H_{\alpha w}$ light curve by $\sim 100K$.

Sarma, Rao & Abhyankar (1996) also analyzed the same $H_{\alpha w}$ & $H_{\alpha n}$ light curves of Edalati, Khalesse & Riazi (1989) with the Wilson's program (Wilson & Devinney 1971). They also obtained a T_2 in these H_α bands which are comparatively higher than the T_2 obtained from U, B and V band light curves. Further the T_2 derived from the $H_{\alpha n}$ light curve is higher than that derived from the $H_{\alpha w}$ light

Table 4.11: Elements derived from the analysis of $H_{\alpha w}$ and $H_{\alpha n}$ band data of R CMa. f: fixed parameter

Parameter	$H_{\alpha w}$		$H_{\alpha n}$	
	$A_2 = 0.5$	$A_2 = free$	$A_2 = 0.5$	$A_2 = free$
T_1^f	7310 K	7310 K	7310 K	7310 K
T_2	4695 ± 23 K	4695 ± 22 K	4756 ± 42	4756 ± 42 K
q^f	0.158	0.158	0.158	0.158
i	$79^o.47 \pm 0.09$	$79^o.64 \pm 0.098$	$79^o.448 \pm 0.14$	$79^o.68 \pm 0.17$
Ω_1	3.423 ± 0.030	3.384 ± 0.027	3.558 ± 0.061	3.482 ± 0.057
Ω_2	2.1234	2.1234	2.1234	2.1234
$r_{1\ pole}$	0.306 ± 0.003	0.309 ± 0.003	0.294 ± 0.006	0.300 ± 0.005
$r_{1\ point}$	0.314 ± 0.003	0.318 ± 0.003	0.298 ± 0.006	0.308 ± 0.006
$r_{1\ side}$	0.311 ± 0.003	0.315 ± 0.003	0.298 ± 0.006	0.305 ± 0.006
$r_{1\ back}$	0.313 ± 0.003	0.317 ± 0.003	0.300 ± 0.006	0.307 ± 0.006
$r_{2\ pole}$	0.2173	0.2173	0.2173	0.2173
$r_{2\ point}$	0.3202	0.3202	0.3202	0.3202
$r_{2\ side}$	0.2260	0.2260	0.2260	0.2260
$r_{2\ back}$	0.2579	0.2579	0.2579	0.2579
x_1^f	0.490	0.490	0.490	0.490
x_2^f	0.655	0.655	0.655	0.655
$x_{1\ bol}^f$	0.464	0.464	0.464	0.464
$x_{2\ bol}^f$	0.537	0.537	0.537	0.537
g_1^f	1.00	1.00	1.00	1.00
g_2^f	0.32	0.32	0.32	0.32
A_1^f	1.00	1.00	1.00	1.00
A_2	0.500^f	0.29 ± 0.05	0.500^f	0.22 ± 0.098
$L_1/(L_1+L_2)$	0.903 ± 0.003	0.905 ± 0.003	0.898 ± 0.006	0.895 ± 0.006
$L_2/(L_1+L_2)$	0.097 ± 0.005	0.095 ± 0.004	0.102 ± 0.009	0.105 ± 0.009
l_3	0.0000^f	0.0000^f	0.0000^f	0.0000^f
Phase shift	-0.0014 ± 0.0002	-0.0014 ± 0.0002	0.0000 ± 0.0004	0.0000 ± 0.0004

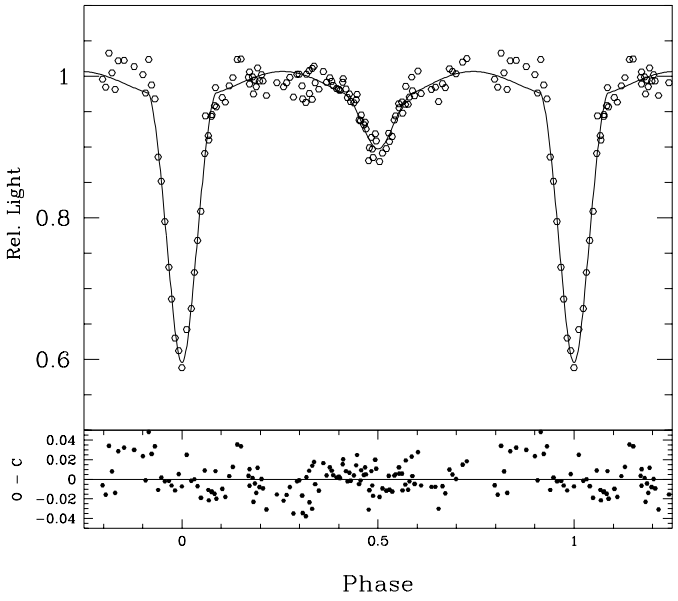

Figure 4.15: The $H_{\alpha n}$ band light curve. The top panel shows the light curve and the model fit and the bottom panel shows the residuals.

curve by $\sim 100K$ consistent with our results.

A similar rise in T_2 in the narrow and intermediate band light curves of Algol centered around the Hydrogen lines H_α and H_β was noticed by Richards, Mochnacki & Bolton (1988). Their analysis of the H_α and H_β light curves of β Per gave high T_2 compared to the T_2 derived from the neighboring wavelengths. As is noticed in the case of R CMa in the present analysis, their multi-wavelength study of β Per resulted in a secondary with the derived temperature increasing from the optical to the near IR wavelengths. The H_α and H_β light curves of β Per and the H_α light curves of R CMa yielded temperatures of the secondary higher than that derived from the photometry in the neighboring wavelengths by a few hundreds of degrees. The rise in T_2 in the bands containing the Hydrogen lines were interpreted by Richards, Mochnacki & Bolton (1988) as due to excess absorption in the hydrogen lines by circumstellar material between the primary and the secondary and the resulting apparent increase in the orbital inclination and the primary fill-out factor.

To verify the above mentioned interpretation by Richards, Mochnacki & Bolton (1988), we analyzed the $H_{\alpha w}$ and $H_{\alpha n}$ light curves of R CMa with i and Ω_1 fixed to the values derived from the analysis of the V light curve of Sato (1971)

(Table 4.7) in the present study. The light curves were also analyzed with the i from Table 4.7 and Ω_1 from Table 4.11. The differences that we found in the values of i and Ω_1 between the V and the H_α light curves are very little and are insufficient to produce such a rise in the T_2 in the H_α bands. It was seen on analysis that the change in the values of i and Ω_1 have reduced T_2 by only a few tens of degrees where as the T_2 derived from these hydrogen bands are higher than the neighboring wavelengths by a few hundreds of degrees. It should be remembered that an increase in i will increase the depths of both the primary and the secondary eclipses whereas an increase in T_2 will be manifested in a light curve by suppression of the depth of the primary eclipse and enhancement of the secondary eclipse depth.

The possibility of the photospheric absorption in the H_α to be the reason for the above increase in T_2 was considered. This line will be much more intense in the spectrum of the F type primary star than in the spectrum of the K type secondary star. The expected equivalent width of the line is greater than $10\mathring{A}$ in the primary whereas it is less than $2\mathring{A}$ in the secondary (Kurucz 1979). Because of this, during the primary eclipse, when a good portion of the primary's surface, that contributes maximum towards the H_α absorption, is masked by the secondary's disk, in which H_α absorption is very little, we can expect an apparent brightening. During the secondary eclipse, when the secondary is masked to a great extent by the primary with a strong H_α absorption, we see an eclipse which is deeper than what is expected. These phenomena combinedly are expected to give a light curve that will result in a higher temperature for the secondary than what we get from a photometric band free of strong spectral features. However, if this is case, we expect to see a similar rise in temperature in the H_β band light curves too, since the H_β equivalent width is expected to be slightly larger than the equivalent width of H_α line in the primary. But the rise in the T_2 derived from H_β light curves of R CMa is much less compared to that was seen in the H_α light curves. In the case of β Per, Richards, Mochnacki & Bolton (1988) saw a remarkable rise in T_2 in both H_α and H_β bands. Detailed modelling of the light curves needs to be done, taking

Table 4.12: Elements of R CMa derived in various studies. Column: 2,4, and 5 are adopted from Sarma, Rao and Abhyankar (1996).

Parameter	Sato (1971)	Guinan (1977)	Radhakrishnan *et al.*(1985)	Budding *et al.*(1994)	Sarma *et al.*(1996)	Present Study
i (deg.)	80.00	80.44	79.93	81.25	79.514	79.48
q	0.124	0.15	0.13	0.15	0.158	0.158
r_1	0.325	0.327	0.319	0.311	0.305	0.306
r_2	0.219	0.220	0.217	0.218	0.234	0.234
$R_1/R_\odot$	1.88	1.8	1.73		1.48	1.50
$R_2/R_\odot$	1.24	1.2	1.18		1.13	1.15
T_1 K	7060		7072	7060	7310	7310
T_2 K	5700		5148	5000	4260	4355
log $L_1/L_\odot$	0.8958		0.8222		0.7622	0.765
log $L_2/L_\odot$	0.1626		-0.0655		-0.405	-0.365
$M_1/M_\odot$	1.78	1.7	1.52		1.070	1.07
$M_2/M_\odot$	0.22	0.26	0.199		0.168	0.17
$M_{bol,1}$	+2.45		+2.69		+2.78	+2.88
$M_{bol,2}$	+4.29		+4.91		+5.70	+5.71
Spectral Type:						
Primary	F1 V	F0 V	F2 V		F1 $\pm$ 1 V	F1 V
Secondary	G4 III	K3 IV - V	G8 IV - V		G2 to K0-2 IV-V	K3-4 IV

Table 4.13: Elements of R CMa derived from different bands. Adopted parameters are $T_1 = 7310K$, q = 0.158, $\Omega_2 = 2.1234$.

Photometric Band	Wavelength Å	i^o	T_2 K	A_2	Ω_1	$\frac{L_1}{(L_1+L_2)}$	$\frac{L_2}{(L_1+L_2)}$
K	22000	79.47	5158	0.84	3.612	0.723	0.277
J	12500	79.37	4580	0.50	3.566	0.823	0.177
$H_{\alpha w}$	6583	79.67	4695	0.29	3.384	0.905	0.095
$H_{\alpha n}$	6569	79.68	4756	0.22	3.482	0.895	0.105
V_{Guinan}	5500	79.54	4192	0.92	3.470	0.963	0.037
$V_{n,Guinan}$	5055	79.50	4240	0.71	3.506	0.969	0.031
V_{Sato}	5500	79.35	4250	0.50	3.434	0.961	0.039
$H_{\beta w}$	4860	79.21	4300	0.83	3.536	0.969	0.031
$H_{\beta n}$	4861	79.36	4328	0.76	3.428	0.970	0.030
B	4400	79.63	4393	0.72	3.443	0.975	0.025
B_n	4250	79.55	4103	0.62	3.474	0.987	0.013
U	3500	79.44	4124	0.67	3.461	0.991	0.009
U_n	3580	79.47	4299	1.00	3.431	0.986	0.014

care of the band widths of the filters, and the spectral distribution of the stars in these bands, to understand whether the above said phenomenon can be the reason for the higher T_2 derived from these bands. At present, it can only be commented that light curves obtained with intermediate band and narrow band filters, covering strong spectral features are not well suited to determine the temperatures and luminosities of the components in a binary system. But they can be efficient tools to tell us about the nature of the circumstellar environments.

4.4 Colours and Spectral Types of Individual Components

Fringent (1956) classified the primary component as F1V. Kitamura and Takahashi (1962) calculated the B-V colours of the components from the luminosity ratio calculated by Koch (1960) to be 0.42 for the primary and 0.72 for the secondary components. Based on these colours, they classified the primary and the secondary as F4 and G8 respectively. Since the estimated distance to the system at that time, from parallaxes, was only 30 parsecs, they assumed that the primary is reddened from F1 to F4 due to the presence of circumstellar matter around the primary. Spectroscopic study by Koch, Olson & Yoss (1965) classified the primary component as A9. Kitamura (1967) derived the spectral type of the primary as A9 V from the U-B and B-V colours of 0.0 and 0.33 respectively. Mean value of H_β indices, outside the eclipse, derived by Sato (1971) also matched well with an F1V star for the primary component. The U-B and B-V colours of 0.34 and 0.04 respectivey, averaged over the region outside eclipse, derived by Guinan (1977) were very close to those published by Kitamura (1967). Since the cooler component is very faint, Guinan, considering that the colours essentially represent the primary component, assigned the primary a spectral type $F0\pm1$. In view of the good agreement in spectral type of the primary from almost all the previous photometric and spectroscopic studies, Guinan concluded that the system is free of interstellar reddening and classified the system as F0 V + K3$\pm$2 IV.

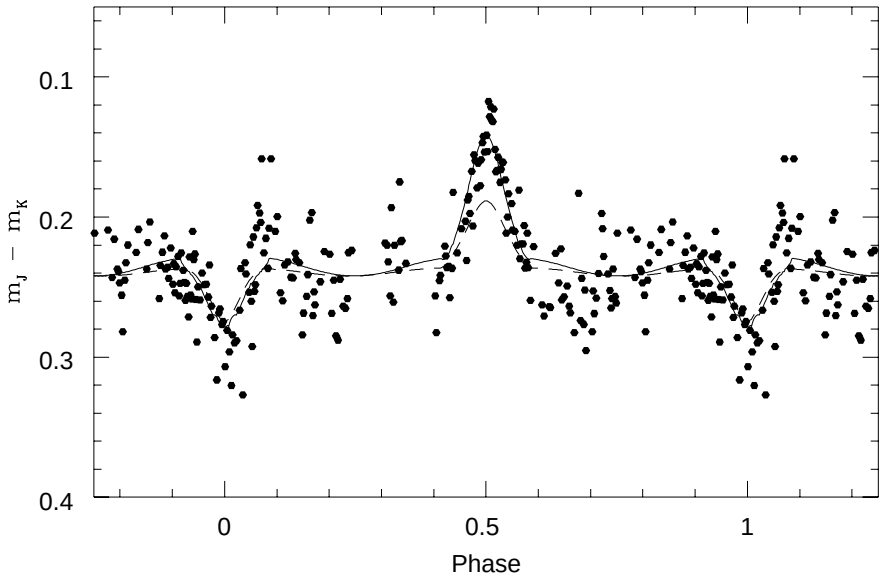

Figure 4.16: Colour curve of R CMa. The filled circles show the observed J - K colour curve. The continuous line shows the colour curve generated from the values of T_2 derived from the individual fits to the J and K light curves. The broken line is the colour curve generated by adopting a value 4250 K for T_2 derived from the analysis of the V band light curve.

In the present study, the magnitudes and colours of the components of R CMa are derived from the observed magnitudes outside eclipse and the derived light values at phase = 0.25 from the Wilson - Devinney fit as described in section 3.4. The derived magnitudes and colours of the components and the observed system magnitudes are given in Table 4.14. The (B-V), (U-V), (V-K) and (J-K) colours of the primary agree with an $F1 \pm 1$ V star. The (V-J) colour represents an A9 V star.

The (V-J), (V-K) and (J-K) colours of the secondary match well with K3-4 IV star. The adopted colours for subgiant star are given in Table 3.11. The (V-J), (V-K) and (J-K) colours of the secondary match well with a K3-4 IV star. But the derived values of T_2 vary from $\sim$ 4100 K in U & B_n to 5158 K in the K band which place the secondary in the range K0.5 - K6.5 V or G5 - K3.5 III. This difference in T_2 is large and it needs to be looked at carefully. This can be a probable indication of localized gas in the system. Looking at the derived colours of the secondary we can assign it a spectral type of K3-4 IV. The source of contamination of the light curve

Table 4.14: The magnitudes and colours of R CMa and its components

Photometric Band	System	Primary	Secondary
U	6.07	6.08	10.81
B	6.03	6.07	9.80
V	5.69	5.75	8.95
J	5.04	5.27	6.83
K	4.80	5.18	6.13
U-B	0.04	0.01	1.01
B-V	0.34	0.32	0.85
V-J	0.65	0.48	2.12
V-K	1.23	0.89	2.82
J-K	0.24	0.09	0.70

which causes the difference in the eclipse depths from the expected values towards longer wavelengths has to be determined and has to be taken care of in the model or light curve has to be corrected before analysis to make a reliable estimate of the spectral type of this star. As the contribution of the secondary star is a significant fraction of the total system light in the near IR wavelengths, the spectral type K3-4 IV, derived in the present study should be used in understanding the evolutionary status of this interesting Algol binary.

4.5 Period Variations

Being a well observed system, the period variation of R CMa has caught the interest of many investigators from the early days. From the photoelectric observations, Dugan (1924), Dugan & Wright (1939), Koch (1960) and Guinan (1977) concluded that there was an abrupt shortening in the period during 1914. Guinan analyzed all the observed times of primary minima before 1970. He obtained two periods

$1^d.1359499$ for (17) points before 1914 and $1^d.13593872$ for 54 points from 1914 to 1970. The period was found to have shortened by $0^s.96$ abruptly at around 1914.[2] He concluded that the abrupt shortening of the orbital period around 1914 may be the result of ejection of a large quantity of mass from the secondary into the system. He also didn't find any displacement of the phase of secondary minimum from 0.50 in his light curve. Though he couldn't find the exact location of the moment of secondary minimum, due to the shallowness of the secondary eclipse, he found that the secondary minimum occurred within 0.005 phase units of phase 0.5. The spectroscopic orbital elements of Struve & Smith (1950) gave an orbital eccentricity e = 0.0 indicating a circular orbit.

Koch (1960) felt that the O - C curve could be represented by a sine curve of semi-amplitude $0^d.032$. Radhakrishan, Sarma & Abhyankar (1984) derived an ephemeris

$$HJD\ MinI = 2430436.5832 + 1.13594197E \tag{4.2}$$

which gave sinusoidal O - C curve with a semi-amplitude $K = 0^d.029$. Since the secondary eclipse was always observed to be at $0^p.5$ apsidal motion was not considered. They interpreted this periodic variations of the values of O - C of the moments of primary minima as due to light time effect[3] happening in a triple system. By analysis of the O - C curve by Irwin's (1952) method, they concluded that R CMa is a triple system with a third body of $\sim 0.5 M_\odot$ M dwarf or white dwarf in a highly eccentric orbit $e = 0.45$ with a period of 91.44 years. In view of the observation of IR excess by Needham *et al.* (1980) they concluded that the third component may be an M Dwarf. Budding *et al.* (1994) have observed light curves of R CMa in B and V bands. They have also raised the possibility of a third body in R CMa and proposed that the period changes are the outcome of three body dynamical interaction and the resulting exchange of binding energy between the

[2]From the inspection of the O - C curve, Guinan (1977) has expressed doubts about how fast this change of period has happened. He concludes that if the 'visual estimates from 1914 - 1936 do not have systematic errors, more than one period variation seem to have occurred'.

[3]arising from the late or early arrival of the light from the system due to the periodic orbiting of R CMa around the common centre of mass in a triple system.

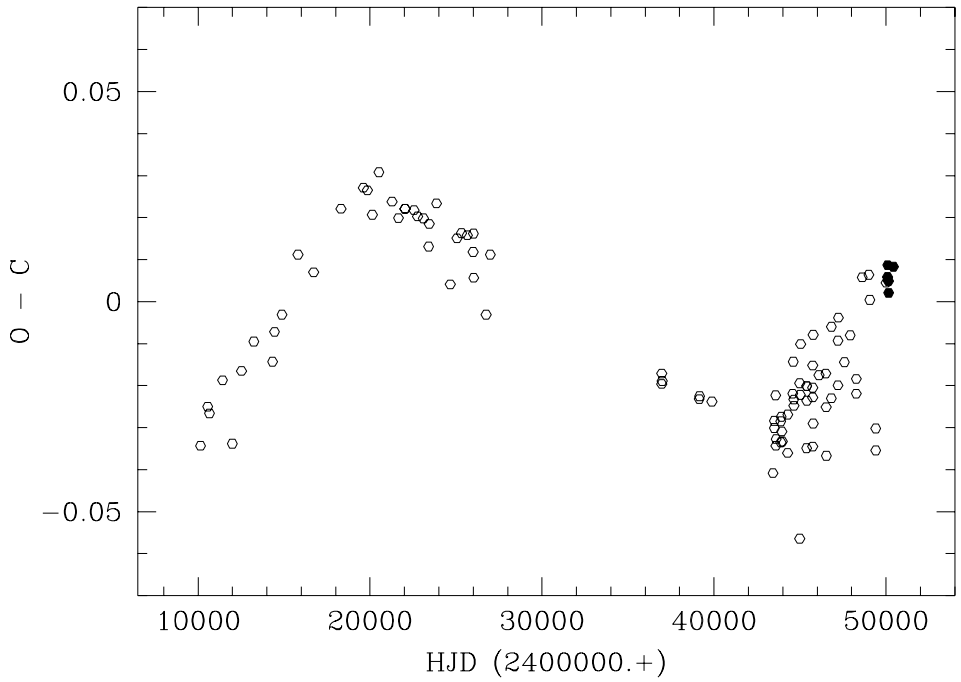

Figure 4.17: O - C curve of R CMa generated with the ephemeris of Radhakrishnan, Sarma & Abhyankar (1984). Filled circles show the moments of minima observed in the present study.

orbit of the binary system and that of the third body.

The values of O - C calculated from our epochs of minima are matching well with the periodic ephemeris given by Radhakrishan, Sarma & Abhyankar, thus confirming the periodic nature of the apparent variation of period proposed by them (Fig. 4.17). It is also interesting to note that the abrupt period change, noticed in 1914 is matching well with the point of inflection of the periodic O - C curve predicted by Radhakrishan, Sarma & Abhyankar. But the present excess depths in the secondary minima described above, makes the search for a third light tricky. The effect of a third light will be to suppress both the eclipse depths whereas in the present J and K light curves, suppression of the primary eclipse depths and enhancement of the secondary eclipse depths are observed. So if we have to look for a third component in the IR light curves, in which a third component was expected to make its presence felt if it is an M dwarf as predicted by Radhakrishan, Sarma & Abhyankar, we have to first look for the factor which increases the T_2, which is the disparity in the eclipse depths described before and take care of that

Table 4.15: Absolute dimensions of R CMa

Parameter	Primary	Secondary
Mass ($M_{\odot}$)	1.07 ± 0.19	0.17 ± 0.03
Mean Radius ($R_{\odot}$)	1.50 ± 0.03	1.15 ± 0.03
Mean Temperature (K)	7310 ± 100	4355 ± 240
$(L/L_{\odot})$	5.78 ± 0.38	0.43 ± 0.095
Mean log(g)	4.33 ± 0.02	3.72 ± 0.01
M_{bol}	$+2.88 \pm 0.03$	$+5.71 \pm 0.4$

in the model.

4.6 Absolute Dimensions

Sato (1971) derived the absolute elements of R CMa assuming that the secondary star is in contact with its Roche lobe and adopting the mass ratio corresponding to the fractional radius of the secondary star obtained from the light curve analysis. He derived the absolute elements, also, considering the primary's mass to be normal for its observed spectral type. Guinan (1977) calculated the mass of the secondary to be 0.26 $M_{\odot}$, assuming M_1 to be 1.70 $M_{\odot}$ corresponding to an F0V dwarf star and using the value of q derived from $f(m)$, M_1 and i. The secondary star was found to be deviating very much from the Main Sequence Mass-Luminosity relation and its mass was too small for a K3 IV-V star by a factor of 2. Using the spectroscopic elements of Struve & Smith (1950), he calculated the radii to be 1.8 and 1.2 $R_{\odot}$ for the primary and the secondary respectively. He observed that the primary's size is normal for an F0V star, but the secondary is much bigger for a dwarf star of the same spectral type. The masses of the components derived by Guinan & Ianna (1983) were similar to those derived by Guinan (1977). From the derived values of the luminosities and temperatures they calculated the radii of

the components to be 1.7 $R_\odot$ and 1.0 $R_\odot$ for the primary and the secondary. Absolute elements of R CMa derived in some of the other major studies are given in Table 4.12 along with those derived in the present study.

Table 4.15 shows the absolute dimensions of R CMa derived in the present study. The masses are calculated assuming a circular orbit and adopting the mass ratio and separation between components from Tomkin (1985). The radii are calculated using Wilson's program for the derived potentials for the Roche equipotential surfaces representing the surfaces of the components. The size of the secondary is determined by the size of the Roche Lobe bounding it. We can see fron Table 4.13 that the analysis of the K band light curve gave results different from that from the other bands. So when calculating the average values of parameters, K band results are excluded. The radius of the primary is derived from the average value of Ω_1 from Table 4.13. Similarly L_2 is calculated from the average value of T_2 from Table 4.13. The absolute dimensions derived in this study are in good agreement with the values derived by Sarma, Rao & Abhyankar (1996), which is one of the latest major studies on this system, except that our average temperature and luminosity of the secondary are slightly higher. The significance of these derived values in the context of the evolution of the system are given in the next section.

4.7 Evolutionary Status

Guinan (1977) from his study of the light curves in the optical wavelengths concluded that the system is evolved, undergone large scale mass exchange and continuing at present with low rate of mass transfer. From astrometric measurements of the parallax, Guinan & Ianna (1983) estimated the space motions of R CMa and concluded that it is a member of the old disk population and estimated its age to be $2 - 6 \times 10^9$ years. Sarma, Rao & Abhyankar (1996) from their photometric study, observed the primary and the secondary to be overluminous for their masses. The secondary was found to be an evolved star, which has become a giant and lost a

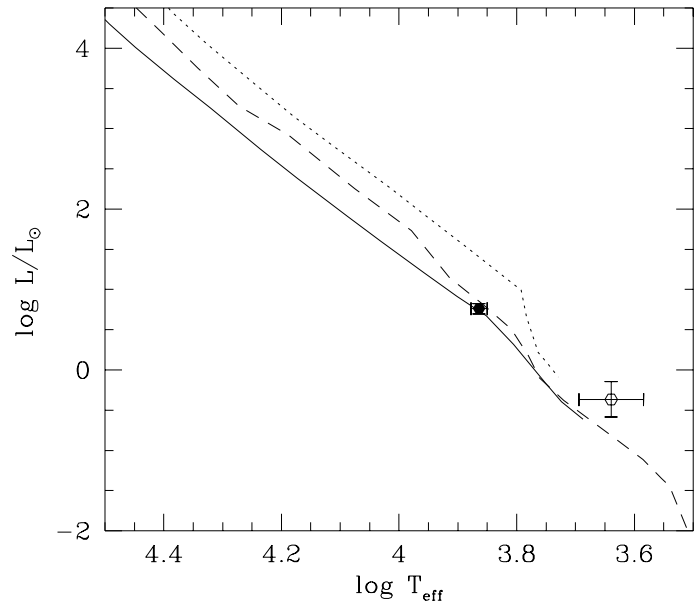

Figure 4.18: The H - R diagram. The filled circle represent the primary component of R CMa and the open circle the secondary component.

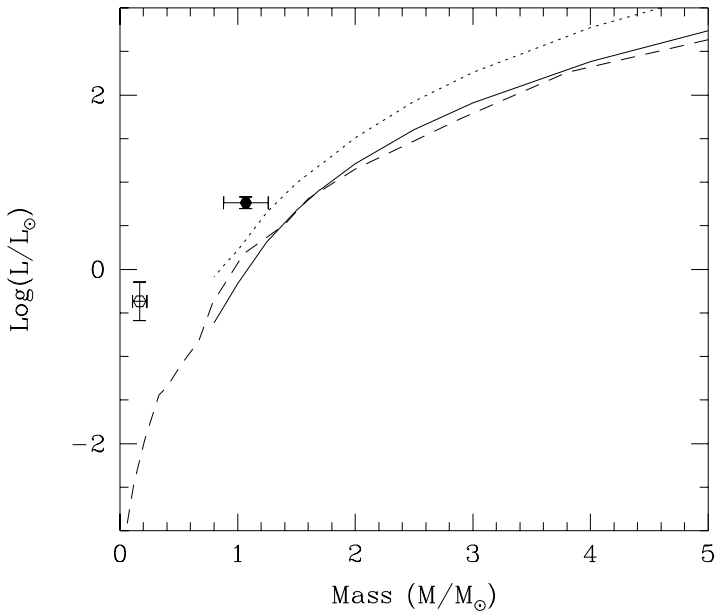

Figure 4.19: Mass - Luminosity diagram for the main sequence stars. The filled circle represents the primary component of R CMa and the open circle represents the secondary component.

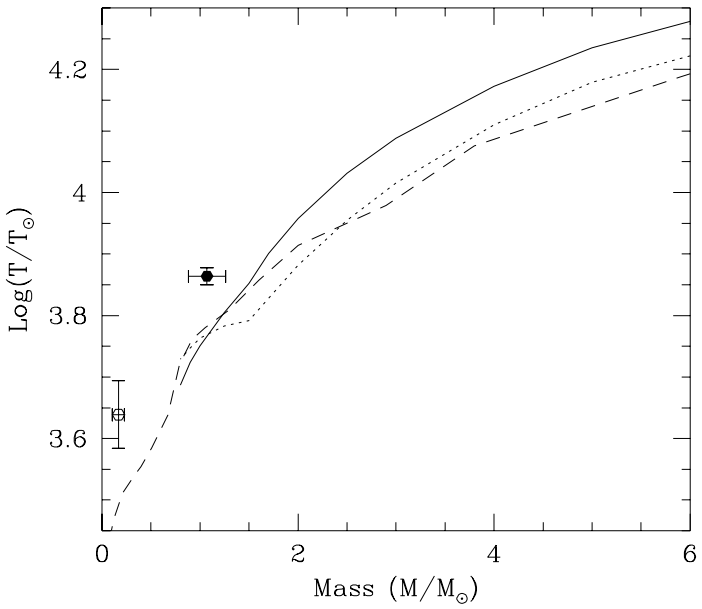

Figure 4.20: The Mass - Temperature diagram for the main sequence stars. The primary is represented by the filled circle and the secondary by the open circle.

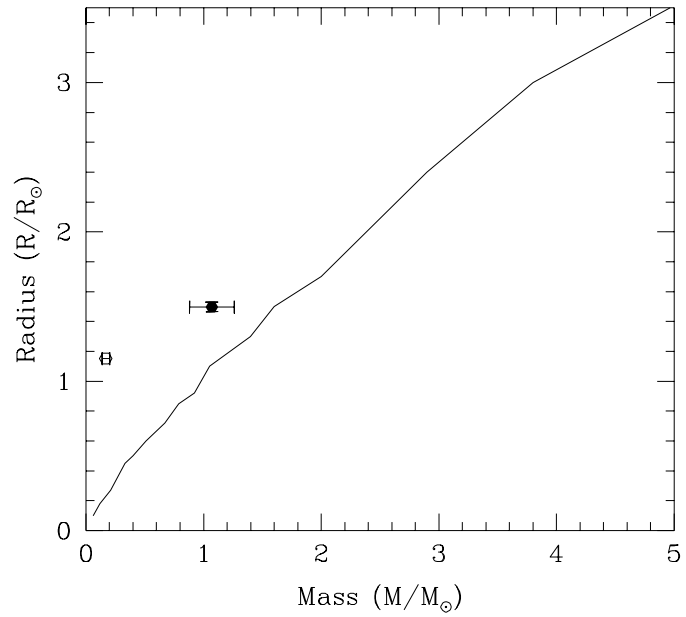

Figure 4.21: The position of the components of R CMa in the main sequence Mass - Radius diagram. The primary is denoted by the filled circle and the secondary by the open circle.

large fraction of its original mass due to Roche lobe overflow, following evolutionary expansion. The overluminosity of the primary was attributed to He enrichment resulting from the accretion of He rich material from the Roche lobe overflowing secondary in its expanding phase. They estimated the He content of the primary to be 52%. From the estimated masses of the components, they observed that the mass transfer in this system would have been non-conservative with the system losing $\sim 0.9 M_{\odot}$ from its initial total mass.

Fig. 4.18 shows the components of R CMa in the HR diagram. The continuous line shows the ZAMS and the dotted line shows TAMS relations taken from the model of Schaller *et al*. (1992). The broken line is the HR diagram taken from Lang (1992). The primary lies well on the main sequence relation where as the secondary is overluminous. Fig. 4.20 and 4.21 whow the Mass - Temperature and Mass - Luminosity diagrams for the main sequence stars. Fig. 4.19 shows the Mass - Radius relation for main sequence stars taken from Lang (1992) and the positions of the components of R CMa. We cab see that both the components of R CMa are overluminous, larger and hotter for main sequence stars of corresponding masses. The secondary is overluminous by more than 5 magnitudes. We can understand the deviations of the secondary from the main sequence relations in the context of a star which has already evolved out of the main sequence phase to become a giant. The overluminosity of the primary can be understood in terms of its increased helium content resulting from helium enriched material gained from the secondary.

4.8 Conclusions

- There is a steady and systematic variation in the temperature of the secondary component, varying from $\sim 4100K$ in the U band to $\sim 5100K$ in the K band. A more careful look into the nature of the components and their environments and the model is needed.

- Secondary is overluminous for its mass by more than 5 magnitudes and is larger and hotter for a main sequence star. It is an evolved star undergone large scale mass loss and constrained in size by its Roche lobe.

- There is an asymmetry in the light curve around the secondary eclipse with the observed points showing positive residuals before the secondary eclipse and negative residuals after the secondary eclipse. The asymmetry of the secondary eclipse is noticed by many observers before. This can be due to the presence of gas streams as explained in the context of RZ Cas.

- The light curve in the K band has a deeper secondary minimum than what can be expected from the observations in the V bands and this is severely affecting the determination of the secondary temperature from the K band. This can point to phase dependent emission or absorption by extra matter present in the system.

- The periodicity of the O-C as calculated by Radhakrishan, Sarma & Abhyankar (1984) is confirmed with our values of the O-C of the epochs of the primary minima following the periodic curve calculated by them. The probable presence of a third body in the system has to be seriously considered. Due to the disparity between the observed depths of eclipses and the depths expected from the model, J & K light curves yielded higher T_2 than light curves in the optical bands. This problem has to be sorted out to do a search for third light in the J & K light curves.

- The secondary minima appear at phase 0.5. The O - C values of the moments of secondary and primary minima show similar values ruling out the possibility of apsidal motion in an elliptical orbit.

- Temperatures derived from light curves obtained with intermediate or narrow band filters with strong spectral features like H_α cannot be taken as authentic. In these bands, the eclipse depths can be affected by these spectral

lines, which will lead us to wrong temperatures. In the case of Algol like systems, where the component stars are of different spectral types, the amount of the relative contribution from the line towards the system light will be varying throughout the eclipse.

Chapter 5

Conclusion and Scope for future work

Algols are an interesting class of binaries which come under the subgroup 'semi-detached' among the eclipsing binaries. The light curves of these stars are characterized by a deep primary eclipse and a shallow secondary eclipse in the optical bands. Except for two (β Per and UX Her) out of a total of nearly 400 (Budding 1989), no other Algols have been observed for their near IR light curves and almost all the available information about this class are derived from the observations in the optical wavelengths. This thesis reports extensive observations of two short-period Algol systems, RZ Cas and R CMa, done in the near IR photometric bands J and K; and complete light curves with good coverage of phases are obtained for these systems in these bands for the first time.

The main factor which attracted us towards the near IR light curve study of these stars was the expected enhanced depth of the secondary minima in these bands compared to those in the optical photometric bands. In these systems the secondary is much cooler than the primary and so the secondary minima are very shallow in the optical bands. A sufficiently deep secondary minimum is needed to resolve the features on the secondary star, especially the hemisphere facing the primary. Numerical simulations are done to demonstrate the increased depth of the secondary minimum in the IR bands compared to the optical bands and the result is shown in Fig. 1.2. Simulations are also done to demonstrate how a cool spot on the secondary star can go undetected in the the optical photometric bands,

UBV, but make itself noticeable in the IR bands (Section 2.3.4). Also it is demonstrated that in Algol type systems, the parameter A_2, the bolometric albedo of the secondary star, cannot be fixed to the theoretical value and ignored. It could be seen that in the regions of the light curves outside the eclipse, the effect of a cool spot on the back side of the secondary and a high value of A_2 can mimic each other.

5.1 RZ Casiopeiae

The first J and K light curves of RZ Cas are obtained. The light curves are analyzed using the Wilson's program. 7 epochs of primary minima and 3 epochs of secondary minima are observed and an ephemeris is derived for the epochs of primary minima. The values of the O - C of the epochs of primary minima show that no major period change has happened in the system since HJD 2448581. But the O - C residuals after this epoch have not been increasing in a perfect linear way after this epoch.

The J and K light curves were analyzed individually as well as simultaneously. We have also analyzed the UBV light curves of Chambliss (1976) using the Wilson's program. The value of the inclination i derived from the J & K light curves is less than that derived from the UBV bands by $\sim 1^o$. The relative size of the primary star derived from the J & K and UBV bands are matching. The light curves are analyzed with $A_2 = 0.5$ and with A_2 as a free parameter and the resulting values of the system parameters are derived.

The J & K light curves showed a high A_2 (> 0.7) compared to the theoretical value of 0.5 for a low mass star with a convective envelope. All the UBV light curves fitted well with an A_2 around 0.5. It is understood by the present study that the high value of A_2 that we found in the case of our IR light curves need not be of photospheric origin. A high A_2 can mimic a cool spot located on the back side of the secondary star in the J & K bands. These spots can go un-noticed in the UBV bands since the secondary is already much fainter in those bands. A gas stream,

directed from the inner Lagrangian point towards the pole of the primary, directed by its polar magnetic field can also mimic a high A_2.

The value of T_2 derived from the J & K light curves is less than that derived from our analysis of the UBV light curves by ~ 25 K. The problem of lack of consistent models in all wavelengths with a unique set of temperatures for the components (T_1, T_2) is a major problem seen in many Algols. We have proposed a cool spot on the secondary to explain this difference in T_2 in RZ Cas and as an alternate explanation for the high A_2 described above.

The modeling of a cool spot on the secondary is done for the J & K light curves using the Wilson's program. A cool spot (lat. $= 80^o$, long. $\sim 180^o$, rad. $\sim 20^o$ & Temp. factor ~ 0.75) is fixed on the secondary and the system parameters are adjusted. The residuals are found to be less than that for the model without spot in the J band. At present we forward the spot model as one of the strong possibilities. Additional observations of the IR light curves of this system with improved accuracy will help verifying the possible presence of a cool spot and detecting the motion of the spot if it is migrating.

Another strong possibility is the presence of a gas stream in the system which can mimic a high A_2 as described before. Modeling of the stream is not attempted in this thesis. The distortions of the light curves due to gas streams will not be symmetrical with respect to the minima due to the diversion of the gas stream from a radial fall to the primary towards the direction of rotation due to the Coriolis force. It is notable that RZ Cas is showing asymmetry especially with respect to the secondary minimum clearly seen in Figs. 3.3 and 3.4 and Table 3.8. There is a rise of flux before the secondary eclipse and a fall of flux when the system emerges out of the secondary eclipse especially in the J band. In optical bands also the eclipses are found to be slightly asymmetric and the residuals (observed - model) are either systematically positive or negative in fixed regions of all the three light curves which are clear from the residuals given in Figs. 3.5, 3.6 and 3.7. The nature of the distribution of residuals around the minima is indicative of

circumstellar gas around the primary star.

From the observed magnitudes and the relative contribution from each component outside the eclipse, colours of individual components are calculated in different wavelengths and spectral types are derived. It is concluded that the primary is an A3 V star as was found by other investigators. From the colours, the secondary is classified as K0 - K4 IV star. The temperature T_2 of the secondary, derived from the light curve analysis in the different wave bands are not compatible with the derived colours. A systematic deviation of the T_2 derived from the light curve analysis is found from that represented by the observed colours and a single temperature does not fit the light curves in different wave-bands. Dark spots on the secondary star, gas streams, or circumstellar matter are likely to be the cause for these changes in T_2.

Absolute dimensions of RZ Cas are calculated, combining the results from the spectroscopic studies (Maxted, Hill & Hilditch 1994) and our photometric investigation. The primary was found to be close to ZAMS branch and in the HR diagram and the secondary is over-luminous for its temperature. The primary is slightly under-luminous and undersized for a ZAMS star of the same mass and the secondary is over-luminous and oversized. The secondary's deviations from the main sequence relations are large and is found to be an evolved star. The primary, though a main sequence star, shows mild deviations from the main sequence relations. We have to look at these deviations in terms of a star of 'unnatural' history. The primary star started hydrogen burning at a much lower mass and then gained mass from the secondary which overflowed its Roche lobe due to evolutionary expansion after the exhaustion of the core hydrogen.

5.2 R Canis Majoris

R CMa is a well noticed member among the Algols, being the one with the lowest mass ratio in the class and a star bright enough to be observed with small telescopes. Though Kopal (1955) proposed a subclass of Algols, with R CMa as the prototype, having extremely small mass function, later studies argued that R CMa is a normal Algol with a low mass secondary. Radhakrishnan, Sarma & Abhyankar (1984) have derived a periodic O - C curve of R CMa with nearly sinusoidal variations in period and an amplitude of $0^d.0029$. They have interpreted this to be caused by light time effect due to a tertiary component of $\sim 0.5 M_\odot$ M type dwarf or white dwarf in a highly eccentric orbit.

The J & K bands light curves with good coverage of phases are observed as a part of this study. These are the first light curves of this system in these near IR photometric bands. Totally 5 epochs of primary minima and 4 epochs of secondary minima are observed. A new ephemeris is calculated for the epochs of primary minima. The values of O - C of primary minima for all the 4 primary minima observed by us fall close to the theoretical curve derived by Radhakrishnan, Sarma and Abhyankar (1984).

The J and K light curves are analyzed separately with the Wilson's program. The U, U_n, B, B_n, V, V_n, $H_{\beta w}$ and $H_{\beta n}$ light curves of Guinan (1977) and $H_{\alpha w}$ and $H_{\alpha n}$ light curves of of Riazi, Bagheri & Gafhihi (1994) were also analyzed using the same model. The T_2 derived from the J and K band light curves are ~ 300 K and ~ 1000 K higher than that obtained from the V band. In the J and K bands, the secondary minima were found deeper by 0.03 and 0.07 magnitudes and the primary minima were found to be shallower by 0.01 and 0.02 magnitudes respectively than what was expected for a secondary of temperature 4250 K obtained from the analysis of the V band light curve. Due to this disparity, we have not attempted a simultaneous fit of the J & K band light curves. Also third light was not searched for in the present analysis since the third light suppresses the depths of

both the primary and the secondary eclipses whereas we are finding an enhancement of the depth of the secondary eclipse and suppression of the primary eclipse depth towards the near IR wavelengths. So the third body proposed by Radhakrishnan, Sarma and Abhyankar (1984) by Radhakrishnan, Sarma and Abhyankar (1984) is photometrically undetected in the present study also. Before attempting a solution for third body with our J and K light curves, the reason for the above mentioned disparity in the eclipse depths needs to be found out and incorporated in the model or filtered out of the light curve before attempting a solution. This is not done in the present study. A possible reason for the enhanced depths of secondary eclipse in the K band is the presence of absorbing gas at the back side of the primary star resulting from mass loss. The role of H^- bound - free absorption in the stellar atmosphere and its influence on the near IR light curves also needs to be seriously considered.

The value of i derived from the near IR and and all the optical light curves are in excellent agreement. The J band light curve showed a remarkable asymmetry in the case of R CMa. The normal points are just above the model just before the secondary eclipse and are lying below the theoretical line when the system emerges outside the secondary eclipse. This type of an asymmetry of the light curve is not observed in the K band, but in both the bands, the second quadrature is slightly lower than the first.

All the light curves are analyzed in two modes, with A_2 fixed to the theoretical value of 0.5 and with A_2 as free parameter. The J band didn't show any abnormal A_2 and it converged well with an A_2 of 0.5. But the K band, converged with $A_2 \sim 0.8$. In the optical bands also most of the light curves of Guinan (1977) showed a high A_2. Since R CMa is reported to have a variable amount of circumstellar gas, by previous investigators, we analyzed one more well observed V light curve obtained at a different epoch. The V light curve of Sato (1971) was analyzed with the Wilson's program and the results are compared with the results of our analysis of the V and V_n of Guinan (1977). The inclination and the relative sizes of

the primary are in very good agreement among the two sets of light curves. The derived values of T_2 also are in excellent agreement. But A_2 was found to have high values for the V band light curves of Guinan (1977) where as Sato's V light curve converged well with the theoretical value of 0.5. From this change of A_2 from epoch to epoch, and in different light curves it is concluded that the high value of A_2 is not of photospheric origin. The most probable candidate, which can cause this can be a stream of gas from the lobe filling secondary to the primary. This can produce an absorption of the primary's observed light, when the system moves towards the primary eclipse, which will mimic a high A_2. In all the bands, except in U which is highly scattered, the broad band curves yielded a higher value of A_2 than the narrow band curves. This can also give us some clues about the reason for this observed high A_2.

Since R CMa was showing higher temperatures in the IR bands, compared to that in optical bands, we took up the analysis of the H_α light curves of this system observed by Edalati, Khalesse, & Riazi (1989). The idea was to look at the behavior of the system at a wavelength between V and J. The T_2 from the analysis of the H_α light curves is higher than that obtained from the J band and all the other optical bands. $H_{\alpha n}$ light curve, upon analysis, gave a T_2, $\sim 100^o$ higher than that from the analysis of $H_{\alpha w}$. The solution of $H_{\alpha w}$ light curve yielded a T_2, which is higher than that derived from V band by $\sim 450^o$ K and by $\sim 100^o$ K from that derived from J band. We have attempted to explain this higher T_2 seen in the H_α bands as due to the photospheric absorption of H_α line which is strong in the primary and weak in the secondary and the resulting expected changes in the depths of eclipses. However, in that case, one would also expect to see higher T_2 in H_β band since H_β absorption also is strong in the primary, but weak in the secondary. But such a strong rise in T_2 is not seen in the H_β bands, though there T_2 derived from $H_\beta n$ is higher than that derived from $H_\beta w$ by a few tens of degrees. However it will be interesting to do light curve simulations with the filter profiles and model atmospheres for the primary and the secondary properly taken care of and verifying the amount of changes in the depth of eclipses and resulting changes in T_2,

and compare it with the eclipse depths and resulting T_2, without any photospheric absorption in these wavelengths.

The primary of R CMa is close to the ZAMS on the HR diagram and the position of the secondary implies an evolved component. Both the primary and the secondary are over-luminous, larger and hotter for main sequence stars of their respective masses. The secondary is over-luminous by more than 5 magnitudes. The deviations of the secondary from the main sequence relations can be understood in terms of a star which has evolved to become a giant and lost large part of its mass through mass transfer and loss. The deviations of the primary can be due to its increased helium content.

5.3 Scope for Future work

The present work is an attempt to understand the Algol systems RZ Cas and R CMa in the near IR wavelengths, where the secondary components were expected to give more relative contribution to the total light output from the binary system than in the optical wavelengths. It was expected that we would be able to learn more about the secondary stars and about the circumstellar environments in in these systems, which have got a history of active mass transfer, and the possibility of the secondaries being chromospherically active due to their fast rotation and possessing convective atmospheres. Like any other similar investigations, our explorations of the phenomena in the near IR bands has certainly answered some questions, but have also raised some interesting new questions. These can be pursued further both through modeling and appropriate experimentation to gain a deeper understanding of these otherwise well studied systems.

As seen in the case of optical study of many Algols, the derived temperatures of the secondary component in different wavelengths were found to vary. In the case of RZ Cas, the T_2 derived from the J & K light curves was found to be less than that was derived from the optical bands. There is a possibility of a cool

spot on the secondary star as observed from our model fit. This needs to be verified through additional, more accurate, observations of light curves in the near IR bands. This will also help us to look for chromospheric activity, of which spot is another manifestation and spot migration if any as observed in RS CVns binaries. Observation of high resolution spectra of RZ Cas in the Ca II H and K wavelengths centered around primary minimum and subtraction of the contribution from the primary from the observed composite spectra may help to look for the core emission from the secondary in these lines which is an indication of the chromospheric activity.

In the case of R CMa, a large increase in T_2 was observed towards the infrared wavelengths. This type of rise in temperature was also noticed in the analysis of β Per (Richard, Mochnacki & Bolton (1988)). In many Algols, it was found difficult to fit light curves in all observed wavelengths with a unique set of temperatures (T_1, T_2) by many investigators. This type of differences in T_2 is a major problem since it will influence the estimated luminosity in a severe way. Spectroscopy in the near IR wavelengths can help us to get some clues about the reason for this differences in T_2. In addition to giving information about the spectral features, the resulting continuum will help to detect the free - free emission from the circumstellar plasma (including gas streams or discs if present) which are expected in Algols and to know about their role in the estimation of parameters.

Modeling the gas streams will be helpful to know about their influence on the observed light curves. The rise in flux seen before the secondary eclipse and the fall in the flux near the end of the secondary eclipse seen in many Algols has to be carefully handled. The inclusion of stream in the light curve model will also help us to know whether the high A_2 seen in many Algol light curves is a result of gas streams.

Appendix : 1

J band observations of RZ Cas (RZ Cas - HR 791)

Hel. JD. -2400000.	Phase	Rel. mag.	Hel. JD. -2400000.	Phase	Rel. mag.	Hel. JD. -2400000.	Phase	Rel. mag.
50031.38444	.1842	.108	50033.35167	.8300	.017	50035.38295	.5295	.224
50031.38980	.1887	.107	50033.35662	.8342	.122	50035.38432	.5306	.226
50031.39144	.1900	.087	50033.35706	.8345	.107	50035.38874	.5343	.183
50031.39613	.1940	.064	50033.35813	.8354	.074	50035.39004	.5354	.152
50031.41166	.2070	.092	50033.36377	.8402	.054	50035.39479	.5394	.156
50031.41289	.2080	.086	50033.36495	.8412	.077	50035.39509	.5396	.124
50031.41801	.2123	.062	50035.22989	.4014	.074	50035.39608	.5405	.153
50031.41910	.2132	.059	50035.23110	.4024	.056	50035.40103	.5446	.126
50031.43287	.2247	.036	50035.23693	.4073	.047	50035.40262	.5459	.128
50031.43325	.2250	.069	50035.23758	.4079	.067	50035.40691	.5495	.108
50031.43922	.2300	.070	50035.23868	.4088	.047	50035.41408	.5555	.115
50033.13632	.6499	.059	50035.24410	.4133	.072	50035.41512	.5564	.124
50033.13780	.6511	.069	50035.24525	.4143	.035	50035.41542	.5566	.139
50033.14282	.6553	.047	50035.25649	.4237	.078	50035.41996	.5604	.100
50033.14416	.6564	.089	50035.25745	.4245	.076	50035.42090	.5612	.115
50033.14486	.6570	.098	50035.25867	.4255	.069	50035.42234	.5624	.117
50033.15058	.6618	.034	50035.26279	.4290	.071	50035.42763	.5669	.122
50033.15165	.6627	.024	50035.26388	.4299	.084	50035.42793	.5671	.110
50033.20953	.7111	.019	50035.26419	.4301	.093	50035.42905	.5681	.127
50033.21067	.7121	.043	50035.26877	.4340	.113	50037.09534	.9621	.515
50033.21568	.7163	.038	50035.27016	.4351	.122	50037.09653	.9631	.595
50033.21682	.7172	.099	50035.27440	.4387	.091	50037.10219	.9679	.672
50033.22360	.7229	.082	50035.27559	.4397	.097	50037.10330	.9688	.719
50033.22403	.7232	.053	50035.28114	.4443	.134	50037.10774	.9725	.734
50033.22449	.7236	.052	50035.28220	.4452	.119	50037.10903	.9736	.723
50033.22570	.7246	.036	50035.28773	.4498	.146	50037.11461	.9783	.826
50033.23730	.7344	.046	50035.28833	.4503	.156	50037.11569	.9792	.808
50033.23852	.7354	.095	50035.28937	.4512	.160	50037.11985	.9826	.917
50033.24373	.7397	.054	50035.29495	.4559	.168	50037.12092	.9835	.953
50033.24498	.7408	.067	50035.29609	.4568	.164	50037.12653	.9882	1.023
50033.24976	.7448	.045	50035.30120	.4611	.191	50037.12687	.9885	1.061
50033.25110	.7459	.016	50035.30220	.4619	.181	50037.13307	.9937	1.075
50033.25662	.7505	.018	50035.30632	.4654	.130	50037.13408	.9945	1.109
50033.25692	.7508	.049	50035.30741	.4663	.168	50037.13470	.9951	1.111
50033.26300	.7558	.055	50035.31155	.4697	.197	50037.14036	.9998	1.114
50033.26426	.7569	.044	50035.31252	.4706	.212	50037.14086	.0002	1.152
50033.26469	.7573	.044	50035.31632	.4737	.216	50037.14240	.0015	1.155
50033.26970	.7615	.024	50035.31740	.4746	.219	50037.14843	.0066	1.105
50033.27084	.7624	.029	50035.32248	.4789	.222	50037.14981	.0077	1.046
50033.27642	.7671	.062	50035.32818	.4837	.258	50037.15528	.0123	.990
50033.27802	.7684	.055	50035.32932	.4846	.278	50037.15650	.0133	.965
50033.28415	.7735	.059	50035.33464	.4891	.266	50037.16175	.0177	.932
50033.28525	.7745	.035	50035.33571	.4900	.246	50037.16298	.0187	.876
50033.29014	.7786	.028	50035.34006	.4936	.259	50037.16790	.0228	.838
50033.29138	.7796	.071	50035.34110	.4945	.260	50037.16966	.0243	.860
50033.29684	.7842	.107	50035.34493	.4977	.252	50037.17491	.0287	.771
50033.29811	.7852	.044	50035.34648	.4990	.279	50037.17542	.0291	.778
50033.30403	.7902	.032	50035.35122	.5029	.274	50037.17658	.0301	.742
50033.30540	.7913	.071	50035.35232	.5039	.278	50037.18113	.0339	.649
50033.31007	.7952	.087	50035.35625	.5071	.281	50037.18176	.0344	.632
50033.31113	.7961	.069	50035.35733	.5080	.222	50037.18298	.0355	.635
50033.31517	.7995	.023	50035.36207	.5120	.273	50037.18968	.0411	.523
50033.31620	.8004	.039	50035.36306	.5128	.250	50037.19051	.0418	.504
50033.32079	.8042	.049	50035.36707	.5162	.253	50037.19158	.0427	.461
50033.32196	.8052	.030	50035.36853	.5174	.245	50037.20005	.0497	.464
50033.32691	.8093	.050	50035.37285	.5210	.236	50037.20128	.0508	.438
50033.32810	.8103	.052	50035.37381	.5218	.263	50037.20796	.0564	.324
50033.34453	.8241	.056	50035.37418	.5221	.235	50037.20915	.0574	.310
50033.34574	.8251	.081	50035.37838	.5257	.200	50037.21380	.0612	.284
50033.35044	.8290	.093	50035.37946	.5266	.206	50037.21491	.0622	.291

J band observations of RZ Cas (Continued)

Hel. JD. -2400000.	Phase	Rel. mag.	Hel. JD. -2400000.	Phase	Rel. mag.	Hel. JD. -2400000.	Phase	Rel. mag.
50037.21996	.0664	.234	50057.32739	.8890	.147	50062.23011	.9909	1.092
50037.22106	.0673	.193	50057.33137	.8924	.125	50062.23359	.9938	1.086
50037.22629	.0717	.152	50057.33225	.8931	.130	50062.23458	.9946	1.130
50037.22740	.0726	.188	50057.33705	.8971	.127	50062.25134	.0086	1.088
50037.23165	.0762	.197	50057.33810	.8980	.166	50062.25511	.0118	1.060
50037.23285	.0772	.191	50057.34177	.9011	.122	50062.25616	.0127	1.095
50037.23682	.0805	.145	50057.34643	.9050	.150	50062.25939	.0154	.973
50037.23800	.0815	.138	50057.34839	.9066	.136	50062.26066	.0164	.994
50037.24262	.0854	.130	50057.35508	.9122	.173	50062.26426	.0194	.905
50037.24377	.0863	.119	50057.35644	.9134	.124	50062.28801	.0393	.555
50037.24778	.0897	.134	50057.36361	.9194	.156	50062.28917	.0403	.533
50037.24885	.0906	.120	50057.36467	.9202	.144	50062.29343	.0438	.509
50051.24416	.7996	.079	50057.37139	.9259	.137	50062.29452	.0447	.491
50051.24533	.8006	.090	50057.37232	.9266	.141	50062.29865	.0482	.402
50051.24572	.8009	.085	50057.37666	.9303	.204	50062.29974	.0491	.446
50051.25843	.8115	.058	50057.38197	.9347	.258	50062.30331	.0521	.348
50051.25957	.8125	.100	50057.38601	.9381	.266	50062.30432	.0529	.377
50051.26852	.8200	.088	50061.12070	.0627	.267	50062.30836	.0563	.326
50051.26989	.8211	.064	50061.12170	.0635	.278	50062.30948	.0573	.289
50051.27832	.8282	.073	50061.12273	.0644	.262	50062.31364	.0607	.270
50051.28005	.8296	.124	50061.12700	.0679	.221	50062.31476	.0617	.314
50051.29651	.8434	.107	50061.12821	.0690	.244	50062.31838	.0647	.241
50051.29792	.8446	.119	50061.13187	.0720	.257	50062.31871	.0650	.272
50051.30337	.8491	.151	50061.13287	.0729	.228	50062.31944	.0656	.190
50051.31094	.8555	.102	50061.13752	.0768	.180	50062.32094	.0668	.214
50051.31230	.8566	.083	50061.13861	.0777	.140	50062.33361	.0774	.139
50051.32142	.8642	.106	50061.14236	.0808	.140	50062.33463	.0783	.131
50051.32243	.8651	.135	50061.14357	.0818	.154	50062.33793	.0811	.116
50051.33185	.8730	.096	50061.14784	.0854	.159	50062.33897	.0819	.127
50051.33368	.8745	.083	50061.14908	.0864	.120	50065.18517	.4632	.178
50051.34026	.8800	.095	50061.15323	.0899	.133	50065.18576	.4637	.161
50051.34166	.8812	.113	50061.15369	.0903	.134	50065.19075	.4678	.158
50051.35023	.8883	.122	50061.15485	.0912	.119	50065.19209	.4690	.156
50051.35174	.8896	.066	50061.15801	.0939	.133	50065.19314	.4698	.204
50053.33032	.5449	.147	50061.15864	.0944	.165	50065.19423	.4708	.229
50053.33165	.5461	.179	50061.16280	.0979	.145	50065.19903	.4748	.231
50053.33683	.5504	.159	50061.16692	.1013	.128	50065.20121	.4766	.180
50053.33785	.5512	.125	50061.16812	.1024	.145	50065.20183	.4771	.199
50053.34736	.5592	.120	50061.17232	.1059	.123	50065.20604	.4806	.194
50053.34854	.5602	.121	50061.17329	.1067	.116	50065.20707	.4815	.229
50053.35345	.5643	.094	50062.14273	.9177	.093	50065.21035	.4842	.211
50053.35464	.5653	.102	50062.14399	.9188	.073	50065.21134	.4851	.196
50053.36449	.5735	.094	50062.14975	.9236	.191	50065.21539	.4885	.225
50053.38114	.5875	.063	50062.15082	.9245	.193	50065.21634	.4892	.229
50053.38224	.5884	.077	50062.15371	.9269	.171	50065.22017	.4925	.227
50053.38257	.5887	.088	50062.15495	.9280	.179	50065.22119	.4933	.262
50053.38768	.5929	.076	50062.19102	.9582	.513	50065.22461	.4962	.280
50053.38895	.5940	.066	50062.19214	.9591	.536	50065.22674	.4980	.283
50053.38954	.5945	.078	50062.19915	.9650	.676	50065.23056	.5011	.252
50053.40564	.6080	.108	50062.20032	.9659	.725	50065.23153	.5020	.278
50053.40691	.6090	.099	50062.20384	.9689	.717	50065.23497	.5048	.246
50053.40800	.6099	.099	50062.20519	.9700	.759	50065.23593	.5056	.227
50057.30597	.8711	.157	50062.20911	.9733	.877	50065.23945	.5086	.241
50057.30736	.8723	.089	50062.21010	.9741	.848	50065.24044	.5094	.212
50057.31266	.8767	.091	50062.21458	.9779	.945	50065.24533	.5135	.242
50057.31399	.8778	.127	50062.21554	.9787	.929	50065.25105	.5183	.232
50057.32009	.8829	.138	50062.21950	.9820	.987	50065.25227	.5193	.213
50057.32078	.8835	.134	50062.22063	.9829	.981	50065.25656	.5229	.217
50057.32191	.8845	.134	50062.22569	.9872	1.029	50065.25757	.5237	.199
50057.32643	.8882	.108	50062.22902	.9899	.973	50065.26168	.5272	.186

J band observations of RZ Cas (Continued)

Hel. JD. -2400000.	Phase	Rel. mag.	Hel. JD. -2400000.	Phase	Rel. mag.	Hel. JD. -2400000.	Phase	Rel. mag.
50065.26569	.5305	.150	50087.29575	.9617	.647	50092.15310	.0256	.847
50065.28535	.5470	.121	50087.29664	.9625	.694	50092.15341	.0258	.817
50065.29168	.5523	.093	50087.29762	.9633	.698	50092.15434	.0266	.831
50065.29285	.5533	.057	50087.30275	.9676	.736	50092.15464	.0269	.799
50065.29860	.5581	.090	50087.30372	.9684	.733	50092.15894	.0305	.788
50065.29959	.5589	.068	50087.30476	.9693	.743	50092.15983	.0312	.780
50086.10021	.9615	.534	50087.31052	.9741	.904	50092.16074	.0320	.763
50086.10118	.9623	.632	50087.31147	.9749	.868	50092.16674	.0370	.703
50086.18484	.0323	.731	50087.31297	.9761	.919	50092.16775	.0378	.621
50086.18583	.0331	.667	50090.15163	.3511	.053	50092.16880	.0387	.627
50086.19127	.0377	.609	50090.15287	.3521	.010	50093.22457	.9220	.154
50086.19214	.0384	.605	50090.18936	.3826	-.009	50093.22558	.9229	.150
50086.19909	.0442	.511	50090.19028	.3834	.004	50093.23039	.9269	.169
50086.20002	.0450	.534	50090.19837	.3902	.054	50093.23131	.9277	.203
50086.20472	.0489	.503	50090.19938	.3910	.070	50093.23572	.9313	.209
50086.20566	.0497	.495	50090.20378	.3947	.026	50093.23671	.9322	.192
50086.21004	.0534	.439	50090.20425	.3951	.010	50093.24082	.9356	.274
50086.21104	.0542	.391	50090.20517	.3959	.026	50093.24180	.9364	.282
50086.21603	.0584	.326	50090.21014	.4000	.021	50093.24625	.9402	.306
50086.21698	.0592	.316	50090.21097	.4007	.050	50093.24723	.9410	.301
50086.22097	.0625	.247	50090.22025	.4085	.011	50093.25065	.9438	.329
50086.22258	.0639	.273	50090.23784	.4232	.064	50093.25166	.9447	.332
50086.22696	.0675	.241	50090.23897	.4241	.072	50093.25661	.9488	.409
50086.22797	.0684	.236	50090.24770	.4315	.047	50093.25771	.9497	.390
50086.23296	.0726	.174	50090.25894	.4409	.102	50093.26198	.9533	.439
50086.23404	.0735	.178	50090.25988	.4416	.094	50093.26304	.9542	.472
50086.23812	.0769	.161	50090.26609	.4468	.108	50093.27324	.9627	.637
50086.23910	.0777	.166	50090.26644	.4471	.103	50093.27418	.9635	.604
50086.24317	.0811	.130	50090.29411	.4703	.152	50093.27447	.9638	.606
50086.24408	.0819	.159	50090.29503	.4710	.180	50093.28146	.9696	.708
50086.24916	.0861	.147	50090.29540	.4714	.165	50093.28239	.9704	.736
50086.25031	.0871	.181	50090.30002	.4752	.208	50093.28749	.9747	.780
50086.25064	.0874	.177	50090.30099	.4760	.229	50093.28850	.9755	.804
50086.25505	.0910	.182	50090.30547	.4798	.218	50093.29254	.9789	.884
50086.25607	.0919	.157	50090.30650	.4806	.193	50093.29358	.9798	.918
50086.25637	.0922	.141	50090.30757	.4815	.194	50093.29835	.9837	.892
50086.26111	.0961	.158	50092.08426	.9680	.684	50093.29867	.9840	.979
50086.26221	.0970	.174	50092.08522	.9688	.665	50093.29963	.9848	1.035
50086.26727	.1013	.146	50092.08940	.9723	.850	50093.30419	.9886	1.033
50086.26832	.1021	.118	50092.09041	.9731	.801	50093.30515	.9894	1.031
50086.27203	.1053	.138	50092.09200	.9745	.853	50093.30611	.9902	1.027
50086.27293	.1060	.127	50092.09558	.9775	.928	50093.31204	.9952	1.100
50086.27881	.1109	.140	50092.09655	.9783	.888	50093.31299	.9960	1.072
50086.27987	.1118	.129	50092.10208	.9829	.929	50093.31408	.9969	1.109
50086.28501	.1161	.149	50092.10240	.9832	.970	50093.31953	.0015	1.113
50086.28620	.1171	.115	50092.10338	.9840	.982	50093.31991	.0018	1.116
50086.29124	.1213	.120	50092.10940	.9890	1.033	50093.32085	.0026	1.140
50086.29218	.1221	.098	50092.11039	.9899	1.038	50093.32492	.0060	1.094
50086.29693	.1261	.099	50092.11541	.9941	1.191	50093.32598	.0069	1.078
50086.29790	.1269	.134	50092.11643	.9949	1.121	50093.32695	.0077	1.087
50086.30316	.1313	.116	50092.12107	.9988	1.186	50093.33288	.0126	.955
50086.30433	.1323	.148	50092.12309	.0005	1.140	50093.33391	.0135	.975
50086.30473	.1326	.134	50092.12862	.0051	1.163	50093.33498	.0144	1.012
50086.30910	.1363	.132	50092.13429	.0098	1.139	50093.33918	.0179	.953
50086.31502	.1412	.111	50092.13585	.0112	1.113	50093.34015	.0187	.917
50086.31600	.1420	.120	50092.14059	.0151	1.072	50093.34574	.0234	.836
50086.32084	.1461	.121	50092.14151	.0159	.994	50093.34681	.0243	.830
50086.32182	.1469	.125	50092.14678	.0203	.950	50093.35098	.0278	.749
50087.28932	.9564	.490	50092.14773	.0211	.866	50093.35192	.0286	.726
50087.29038	.9572	.511	50092.14804	.0213	.879	50093.35549	.0315	.662

J band observations of RZ Cas (Continued)

Hel. JD. -2400000.	Phase	Rel. mag.	Hel. JD. -2400000.	Phase	Rel. mag.	Hel. JD. -2400000.	Phase	Rel. mag.
50093.35648	.0324	.611	50096.09803	.3264	.040	50115.16931	.2818	.023
50093.36073	.0359	.581	50096.10335	.3309	.062	50115.20216	.3093	.094
50093.36165	.0367	.635	50096.10433	.3317	.072	50115.20316	.3102	.075
50093.36588	.0402	.547	50096.10468	.3320	.084	50115.20765	.3139	.082
50093.36692	.0411	.500	50096.10934	.3359	.069	50115.20862	.3147	.020
50093.36789	.0419	.532	50096.11033	.3367	.043	50115.21240	.3179	.077
50095.08971	.4825	.274	50096.11517	.3408	.045	50115.21336	.3187	.068
50095.09065	.4833	.268	50096.11615	.3416	.035	50115.22079	.3249	.080
50095.09378	.4859	.279	50096.12023	.3450	.038	50115.22171	.3257	.033
50095.09468	.4866	.260	50096.12119	.3458	.063	50115.22573	.3290	.032
50095.09798	.4894	.261	50096.12589	.3497	.055	50115.22669	.3298	.020
50095.09830	.4897	.284	50096.12712	.3508	.052	50115.23266	.3348	.036
50095.09934	.4905	.288	50096.13287	.3556	.079	50115.23353	.3356	.023
50095.10268	.4933	.286	50096.13317	.3558	.078	50115.23759	.3390	.025
50095.10366	.4941	.257	50096.13743	.3594	.066	50115.23849	.3397	.034
50095.10402	.4944	.245	50096.13845	.3602	.043	50115.24259	.3431	.034
50095.10732	.4972	.262	50096.13876	.3605	.045	50115.24363	.3440	.053
50095.10828	.4980	.245	50096.14289	.3640	.051	50115.24794	.3476	.081
50095.11193	.5011	.245	50096.14388	.3648	.052	50115.24900	.3485	.080
50095.11286	.5018	.233	50096.14763	.3679	.047	50115.25333	.3521	.050
50095.11729	.5055	.260	50096.14792	.3682	.070	50115.25426	.3529	.050
50095.11832	.5064	.289	50115.07788	.2053	.063	50117.11771	.9119	.122
50095.12195	.5094	.294	50115.07893	.2062	.096	50117.11812	.9123	.112
50095.12287	.5102	.270	50115.08303	.2096	.101	50117.12097	.9147	.133
50095.12723	.5139	.282	50115.08410	.2105	.065	50117.12197	.9155	.151
50095.12826	.5147	.226	50115.08760	.2135	.043	50117.12509	.9181	.126
50095.13253	.5183	.248	50115.08851	.2142	.008	50117.12610	.9190	.084
50095.13287	.5186	.220	50115.09191	.2171	.042	50117.12978	.9220	.144
50095.13388	.5194	.253	50115.09283	.2178	.090	50117.13073	.9228	.140
50095.13811	.5230	.239	50115.09626	.2207	.053	50117.13168	.9236	.180
50095.13845	.5232	.222	50115.09731	.2216	.067	50117.13501	.9264	.150
50095.13949	.5241	.224	50115.10298	.2263	.081	50117.13596	.9272	.195
50095.13980	.5244	.220	50115.10391	.2271	.110	50117.13972	.9304	.206
50095.14373	.5277	.211	50115.10723	.2299	.087	50117.14072	.9312	.176
50095.14402	.5279	.204	50115.10813	.2306	.074	50117.14168	.9320	.166
50095.14496	.5287	.189	50115.11145	.2334	.053	50117.14465	.9345	.223
50095.14920	.5322	.227	50115.11236	.2342	.036	50117.14565	.9353	.238
50095.15027	.5331	.219	50115.11575	.2370	.025	50117.14869	.9379	.276
50095.15057	.5334	.208	50115.11667	.2378	.000	50117.14967	.9387	.262
50095.15485	.5370	.213	50115.12239	.2426	.048	50117.15265	.9412	.296
50095.15517	.5372	.220	50115.12341	.2434	.057	50117.15363	.9420	.291
50095.15612	.5380	.182	50115.12749	.2468	.065	50117.15457	.9428	.313
50095.15645	.5383	.181	50115.12870	.2479	.061	50117.15764	.9453	.401
50095.16202	.5430	.185	50115.13209	.2507	.073	50117.15860	.9461	.421
50095.16305	.5438	.159	50115.13308	.2515	.042	50117.16308	.9499	.435
50095.16337	.5441	.164	50115.13652	.2544	.070	50117.16417	.9508	.417
50095.16709	.5472	.137	50115.13753	.2552	.065	50117.16782	.9539	.483
50095.16744	.5475	.128	50115.14087	.2580	.059	50117.16907	.9549	.449
50095.16840	.5483	.169	50115.14193	.2589	.036	50117.17014	.9558	.460
50095.17403	.5530	.175	50115.14286	.2597	.017	50117.17317	.9583	.483
50095.17436	.5533	.159	50115.14865	.2645	.041	50117.17426	.9593	.489
50095.17536	.5541	.115	50115.14986	.2656	.049	50117.17523	.9601	.515
50095.17966	.5577	.103	50115.15085	.2664	.039	50117.17864	.9629	.581
50095.18069	.5586	.128	50115.15429	.2693	.062	50117.17956	.9637	.601
50095.18477	.5620	.126	50115.15527	.2701	.055	50117.18333	.9668	.632
50095.18508	.5623	.144	50115.15964	.2737	.030	50117.18433	.9677	.664
50095.19018	.5665	.133	50115.16341	.2769	.032	50117.18757	.9704	.694
50095.19050	.5668	.109	50115.16433	.2777	.032	50117.18853	.9712	.728
50095.19146	.5676	.106	50115.16471	.2780	.024	50117.18884	.9715	.720
50096.09704	.3256	.014	50115.16837	.2810	.010	50117.19226	.9743	.832

J band observations of RZ Cas (Continued)

Hel. JD. -2400000.	Phase	Rel. mag.	Hel. JD. -2400000.	Phase	Rel. mag.	Hel. JD. -2400000.	Phase	Rel. mag.
50117.19260	.9746	.811	50117.26623	.0362	.562	50416.31761	.2340	.060
50117.19361	.9754	.803	50117.26657	.0365	.581	50416.33360	.2474	.004
50117.19710	.9784	.897	50416.15321	.0965	.108	50416.33539	.2489	.065
50117.19802	.9791	.830	50416.15353	.0967	.115	50416.33571	.2491	.053
50117.19833	.9794	.859	50416.15504	.0980	.108	50416.34088	.2535	.035
50117.20166	.9822	.914	50416.16273	.1044	.083	50416.34119	.2537	.048
50117.20272	.9831	.842	50416.16324	.1048	.072	50416.34422	.2563	.060
50117.20303	.9833	.858	50416.16451	.1059	.083	50416.34906	.2603	-.007
50117.20714	.9868	1.047	50416.16484	.1062	.071	50416.34944	.2606	.003
50117.20753	.9871	1.023	50416.20799	.1423	.074	50416.35074	.2617	.010
50117.20856	.9879	1.088	50416.21047	.1444	.082	50416.35111	.2620	-.002
50117.21200	.9908	1.170	50416.22752	.1586	.082	50416.36268	.2717	.079
50117.21289	.9916	1.124	50416.22972	.1605	.073	50416.36369	.2725	.077
50117.21321	.9918	1.099	50416.23002	.1607	.057	50416.36502	.2737	.069
50117.21644	.9945	1.074	50416.23963	.1687	.046	50416.37342	.2807	.002
50117.21755	.9955	1.117	50416.23994	.1690	.057	50416.37374	.2809	.001
50117.22121	.9985	1.087	50416.24111	.1700	.071	50416.37494	.2820	.030
50117.22216	.9993	1.160	50416.24142	.1702	.089	50416.37532	.2823	.047
50117.22326	.0002	1.183	50416.24709	.1750	.039	50416.37584	.2827	.032
50117.22637	.0029	1.121	50416.24740	.1753	.041	50416.38115	.2872	.061
50117.22670	.0031	1.147	50416.24883	.1764	.104	50416.38147	.2874	.034
50117.22770	.0040	1.128	50416.24929	.1768	.119	50416.38259	.2884	.014
50117.23301	.0084	1.112	50416.25477	.1814	.104	50416.38296	.2887	.023
50117.23407	.0093	1.059	50416.25672	.1830	.113	50416.39023	.2947	.052
50117.23436	.0095	1.059	50416.25740	.1836	.087	50416.39054	.2950	.052
50117.23784	.0124	1.027	50416.29187	.2125	.023	50416.39179	.2961	.036
50117.23916	.0136	.986	50416.29222	.2127	.031	50416.39215	.2964	.033
50117.24256	.0164	1.011	50416.29339	.2137	.053	50416.39754	.3009	.034
50117.24416	.0177	.977	50416.29446	.2146	.046	50416.39787	.3011	.027
50117.24453	.0180	.952	50416.30114	.2202	.065	50416.41195	.3129	.040
50117.24891	.0217	.855	50416.30146	.2205	.064	50416.41229	.3132	.032
50117.24995	.0226	.797	50416.30275	.2216	.058	50416.41385	.3145	.049
50117.25025	.0228	.820	50416.30308	.2218	.052	50416.42125	.3207	.065
50117.25445	.0263	.800	50416.30883	.2266	.060	50416.42156	.3210	.069
50117.25477	.0266	.796	50416.30915	.2269	.064	50416.42305	.3222	.073
50117.25578	.0275	.828	50416.31055	.2281	.068	50416.42986	.3279	.054
50117.26011	.0311	.642	50416.31085	.2283	.044	50416.43055	.3285	.056
50117.26107	.0319	.641	50416.31573	.2324	.064	50416.43220	.3299	.060
50117.26496	.0351	.629	50416.31605	.2327	.066	50416.43259	.3302	.064
50117.26590	.0359	.614	50416.31731	.2337	.066		.	

Appendix : 2

K band observations of RZ Cas (RZ Cas - HR 791)

Hel. JD. -2400000.	Phase	Rel. mag.	Hel. JD. -2400000.	Phase	Rel. mag.	Hel. JD. -2400000.	Phase	Rel. mag.
49997.27583	.6476	-.153	49997.45396	.7966	-.098	50000.48153	.3296	-.130
49997.27616	.6479	-.137	49997.45499	.7975	-.105	50000.48265	.3305	-.158
49997.27737	.6489	-.158	49997.45607	.7984	-.123	50000.48309	.3309	-.166
49997.27774	.6492	-.136	49997.46031	.8019	-.159	50000.48783	.3349	-.156
49997.28606	.6562	-.122	49997.46150	.8029	-.151	50000.48991	.3366	-.167
49997.28721	.6571	-.099	49997.46776	.8082	-.159	50000.49027	.3369	-.153
49997.28843	.6581	-.109	49997.46885	.8091	-.153	50000.49617	.3419	-.116
49997.29345	.6623	-.089	49997.46991	.8100	-.146	50000.49747	.3429	-.103
49997.29467	.6634	-.151	49997.47380	.8132	-.157	50000.49784	.3433	-.097
49997.29584	.6643	-.109	49997.47492	.8142	-.149	50015.40338	.8138	-.128
49997.29620	.6646	-.138	49997.47592	.8150	-.131	50015.40463	.8148	-.137
49997.30196	.6695	-.115	49997.48658	.8239	-.071	50015.41010	.8194	-.115
49997.30524	.6722	-.139	49997.48766	.8248	-.161	50015.41132	.8204	-.142
49997.31124	.6772	-.113	49997.48880	.8258	-.170	50015.41755	.8257	-.117
49997.31227	.6781	-.101	49997.49296	.8293	-.136	50015.41939	.8272	-.068
49997.32372	.6877	-.094	49997.49408	.8302	-.131	50015.42490	.8318	-.095
49997.32532	.6890	-.134	49997.49940	.8346	-.151	50015.42637	.8330	-.092
49997.33286	.6953	-.137	49997.50090	.8359	-.133	50015.42668	.8333	-.048
49997.33389	.6962	-.099	49997.50695	.8410	-.133	50015.43222	.8379	-.113
49997.33520	.6973	-.108	49997.50858	.8423	-.076	50015.43336	.8389	-.084
49997.34368	.7044	-.088	50000.33809	.2096	-.127	50015.43999	.8444	-.100
49997.34408	.7047	-.109	50000.33923	.2106	-.119	50015.44108	.8453	-.098
49997.34689	.7070	-.109	50000.34044	.2116	-.124	50015.44139	.8456	-.095
49997.34721	.7073	-.107	50000.34078	.2119	-.105	50015.44629	.8497	-.165
49997.35650	.7151	-.169	50000.34656	.2167	-.086	50015.44761	.8508	-.163
49997.35768	.7161	-.167	50000.34823	.2181	-.117	50015.44798	.8511	-.149
49997.35882	.7170	-.168	50000.36070	.2285	-.121	50015.45382	.8560	-.116
49997.36498	.7222	-.144	50000.36119	.2289	-.114	50015.45496	.8570	-.143
49997.36623	.7232	-.133	50000.36256	.2301	-.109	50015.46082	.8619	-.124
49997.36736	.7242	-.148	50000.37244	.2383	-.111	50015.46203	.8629	-.076
49997.37248	.7285	-.118	50000.37377	.2395	-.121	50015.46869	.8684	-.124
49997.37352	.7293	-.101	50000.37486	.2404	-.136	50015.47615	.8747	-.056
49997.37828	.7333	-.115	50000.38405	.2481	-.166	50016.29311	.5582	-.008
49997.37958	.7344	-.151	50000.38520	.2490	-.083	50016.30625	.5692	-.078
49997.38066	.7353	-.159	50000.39040	.2534	-.081	50016.32493	.5848	-.076
49997.38460	.7386	-.165	50000.39160	.2544	-.107	50016.33217	.5909	-.063
49997.38587	.7397	-.164	50000.39265	.2552	-.117	50016.33406	.5924	-.056
49997.38699	.7406	-.159	50000.39728	.2591	-.133	50016.33478	.5930	-.086
49997.39168	.7445	-.152	50000.39932	.2608	-.157	50016.33927	.5968	-.123
49997.39401	.7465	-.149	50000.40476	.2654	-.098	50016.34035	.5977	-.121
49997.39521	.7475	-.090	50000.40698	.2672	-.156	50016.34067	.5980	-.134
49997.40082	.7522	-.060	50000.41138	.2709	-.123	50016.34551	.6020	-.125
49997.40197	.7531	-.100	50000.41249	.2718	-.130	50016.34664	.6030	-.143
49997.40306	.7540	-.074	50000.41370	.2729	-.115	50016.34708	.6033	-.125
49997.41005	.7599	-.121	50000.41782	.2763	-.104	50016.35139	.6069	-.121
49997.41121	.7609	-.153	50000.41918	.2774	-.097	50016.35245	.6078	-.137
49997.41242	.7619	-.133	50000.42059	.2786	-.115	50016.36561	.6188	-.066
49997.42181	.7697	-.102	50000.42463	.2820	-.174	50016.37159	.6238	-.066
49997.42292	.7707	-.072	50000.42590	.2831	-.164	50016.37271	.6248	-.088
49997.43021	.7768	-.146	50000.43300	.2890	-.142	50016.37934	.6303	-.124
49997.43158	.7779	-.130	50000.43450	.2903	-.132	50016.38021	.6311	-.134
49997.43271	.7788	-.131	50000.43576	.2913	-.145	50016.38142	.6321	-.114
49997.44008	.7850	-.105	50000.45147	.3045	-.151	50016.40386	.6508	-.120
49997.44054	.7854	-.102	50000.46308	.3142	-.121	50016.40491	.6517	-.144
49997.44166	.7863	-.114	50000.46445	.3153	-.147	50016.40880	.6550	-.129
49997.44280	.7873	-.137	50000.46967	.3197	-.184	50016.41004	.6560	-.083
49997.44719	.7910	-.150	50000.46997	.3199	-.127	50016.41588	.6609	-.118
49997.44752	.7912	-.102	50000.47119	.3210	-.152	50016.41737	.6621	-.175
49997.44852	.7921	-.074	50000.47624	.3252	-.149	50016.42265	.6666	-.163
49997.44960	.7930	-.080	50000.47753	.3263	-.183	50016.42372	.6675	-.124

K band observations of RZ Cas (Continued)

Hel. JD. -2400000.	Phase	Rel. mag.	Hel. JD. -2400000.	Phase	Rel. mag.	Hel. JD. -2400000.	Phase	Rel. mag.
50016.42787	.6709	-.121	50017.30565	.4053	-.147	50017.46975	.5426	.009
50016.42909	.6719	-.094	50017.31055	.4094	-.138	50017.47084	.5435	-.010
50016.43295	.6752	-.136	50017.31155	.4103	-.143	50017.47670	.5484	.005
50016.43427	.6763	-.151	50017.31257	.4111	-.113	50017.47795	.5495	-.041
50016.43890	.6802	-.138	50017.31646	.4144	-.144	50017.48261	.5534	-.059
50016.44014	.6812	-.080	50017.31769	.4154	-.127	50017.48322	.5539	-.060
50016.44651	.6865	-.104	50017.31903	.4165	-.117	50017.48440	.5549	-.047
50016.44763	.6875	-.105	50017.32816	.4241	-.133	50017.48985	.5594	-.014
50016.45195	.6911	-.135	50017.32933	.4251	-.114	50017.49074	.5602	-.019
50016.45316	.6921	-.153	50017.33052	.4261	-.139	50017.49208	.5613	-.016
50016.45346	.6923	-.145	50017.33469	.4296	-.102	50017.49928	.5673	-.027
50016.45816	.6963	-.131	50017.33583	.4306	-.102	50017.50080	.5686	-.064
50016.45937	.6973	-.100	50017.34007	.4341	-.086	50017.50601	.5729	-.127
50016.46478	.7018	-.123	50017.34736	.4402	-.081	50017.50652	.5734	-.110
50016.46587	.7027	-.149	50017.35192	.4440	-.091	50017.50761	.5743	-.142
50016.46624	.7030	-.149	50017.35300	.4449	-.052	50017.51279	.5786	-.091
50016.47106	.7071	-.150	50017.35694	.4482	-.067	50017.51325	.5790	-.088
50016.47273	.7085	-.120	50017.35809	.4492	-.021	50017.51425	.5798	-.121
50016.47946	.7141	-.143	50017.35927	.4502	-.049	50017.51455	.5801	-.100
50016.48681	.7202	-.117	50017.36375	.4539	-.005	50017.52142	.5858	-.091
50016.48804	.7213	-.133	50017.36505	.4550	-.017	50032.15681	.8304	-.073
50016.48921	.7222	-.160	50017.36558	.4555	-.027	50032.16882	.8404	-.054
50016.49650	.7283	-.134	50017.36969	.4589	-.016	50032.17145	.8426	-.093
50016.49757	.7292	-.108	50017.37147	.4604	-.022	50032.17264	.8436	-.071
50016.49881	.7303	-.083	50017.37260	.4613	-.003	50032.17827	.8483	-.093
50016.50411	.7347	-.152	50017.37668	.4647	.065	50032.17941	.8493	-.085
50016.50583	.7362	-.137	50017.37832	.4661	-.004	50032.23854	.8987	-.070
50016.51204	.7414	-.113	50017.38185	.4691	.046	50032.24008	.9000	-.054
50016.51375	.7428	-.116	50017.38378	.4707	.086	50032.24565	.9047	-.017
50016.51863	.7469	-.120	50017.38765	.4739	.090	50032.24668	.9056	-.064
50016.51976	.7478	-.105	50017.38883	.4749	.083	50032.25572	.9131	-.094
50016.52628	.7533	-.085	50017.39274	.4782	.080	50032.25680	.9140	-.090
50016.52760	.7544	-.109	50017.39381	.4791	.109	50032.26200	.9184	-.096
50016.53266	.7586	-.118	50017.39421	.4794	.108	50032.26301	.9192	-.048
50016.53367	.7595	-.084	50017.39947	.4838	.183	50032.26334	.9195	-.018
50017.23670	.3476	-.113	50017.40009	.4843	.170	50032.26861	.9239	.034
50017.23802	.3487	-.119	50017.40116	.4852	.164	50032.26969	.9248	-.039
50017.23924	.3498	-.135	50017.40631	.4895	.181	50032.27051	.9255	-.043
50017.24405	.3538	-.186	50017.40741	.4905	.163	50032.27782	.9316	-.054
50017.24523	.3548	-.148	50017.41136	.4938	.182	50032.27900	.9326	.020
50017.25226	.3607	-.177	50017.41605	.4977	.194	50032.28411	.9369	-.026
50017.25353	.3617	-.141	50017.41703	.4985	.210	50032.29133	.9429	.117
50017.25855	.3659	-.148	50017.42134	.5021	.187	50032.29300	.9443	.128
50017.25970	.3669	-.131	50017.42235	.5030	.168	50032.29367	.9449	.117
50017.26076	.3678	-.115	50017.42755	.5073	.187	50032.29995	.9501	.204
50017.26485	.3712	-.125	50017.43265	.5116	.116	50032.30134	.9513	.217
50017.26603	.3722	-.122	50017.43379	.5125	.096	50032.30164	.9515	.217
50017.27027	.3757	-.130	50017.43854	.5165	.116	50032.30848	.9573	.231
50017.27258	.3776	-.108	50017.43997	.5177	.121	50032.31646	.9639	.296
50017.27695	.3813	-.150	50017.44052	.5182	.053	50032.32265	.9691	.359
50017.27931	.3833	-.147	50017.44507	.5220	.060	50032.32764	.9733	.484
50017.28812	.3907	-.108	50017.44560	.5224	.078	50032.32862	.9741	.453
50017.28913	.3915	-.107	50017.44750	.5240	.074	50032.33300	.9778	.477
50017.29018	.3924	-.097	50017.45573	.5309	.062	50032.33397	.9786	.518
50017.29627	.3975	-.152	50017.45617	.5312	.022	50032.33893	.9827	.569
50017.29668	.3978	-.098	50017.45735	.5322	.061	50032.34503	.9878	.571
50017.29772	.3987	-.082	50017.46320	.5371	.064	50032.34606	.9887	.592
50017.29875	.3995	-.101	50017.46435	.5381	.066	50032.35059	.9925	.615
50017.30360	.4036	-.131	50017.46470	.5384	.021	50032.35168	.9934	.655
50017.30466	.4045	-.122	50017.46930	.5422	-.017	50032.35561	.9967	.744

K band observations of RZ Cas (Continued)

Hel. JD. -2400000.	Phase	Rel. mag.	Hel. JD. -2400000.	Phase	Rel. mag.	Hel. JD. -2400000.	Phase	Rel. mag.
50032.35661	.9975	.757	50055.18770	.0989	-.016	50064.27600	.7025	-.155
50032.36062	.0009	.693	50055.18827	.0994	-.093	50064.28043	.7062	-.104
50032.36097	.0012	.674	50055.19344	.1037	-.015	50064.28179	.7074	-.128
50032.36200	.0020	.744	50055.19410	.1043	-.059	50064.28700	.7117	-.167
50032.36584	.0053	.615	50055.19526	.1052	-.051	50064.28813	.7127	-.132
50032.36811	.0072	.623	50055.19578	.1057	-.073	50064.29197	.7159	-.127
50032.36918	.0080	.635	50055.19626	.1061	-.023	50064.29294	.7167	-.076
50032.37403	.0121	.654	50055.20244	.1112	-.079	50064.29339	.7171	-.075
50032.37451	.0125	.615	50055.20388	.1124	-.057	50064.30868	.7299	-.123
50032.37557	.0134	.683	50055.20858	.1164	-.086	50064.31405	.7344	-.086
50032.37591	.0137	.673	50055.20955	.1172	-.064	50064.31529	.7354	-.078
50032.38006	.0171	.598	50055.20997	.1175	-.086	50064.32010	.7394	-.096
50032.38044	.0175	.605	50056.25389	.9909	.667	50064.32112	.7403	-.134
50032.38182	.0186	.501	50056.26356	.9990	.719	50114.19592	.4675	.037
50032.38580	.0220	.502	50056.26462	.9999	.772	50114.19754	.4688	.064
50032.38677	.0228	.495	50056.26807	.0028	.696	50114.19784	.4691	.087
50032.39107	.0264	.481	50056.26901	.0036	.696	50114.19899	.4700	.079
50032.39221	.0273	.427	50056.27237	.0064	.725	50114.20747	.4771	.105
50032.39634	.0308	.349	50056.27342	.0073	.721	50114.20859	.4781	.092
50032.39742	.0317	.340	50056.27403	.0078	.696	50114.21397	.4826	.100
50032.39863	.0327	.380	50056.27752	.0107	.678	50114.21484	.4833	.140
50032.40428	.0374	.312	50056.27866	.0116	.673	50114.21597	.4842	.122
50032.40538	.0383	.332	50056.28222	.0146	.605	50114.22500	.4918	.156
50032.40568	.0386	.332	50056.28356	.0157	.584	50114.22612	.4927	.159
50032.41045	.0426	.208	50056.28769	.0192	.541	50114.23116	.4969	.166
50032.41183	.0437	.164	50056.28869	.0200	.593	50114.23220	.4978	.148
50032.41607	.0473	.165	50056.29374	.0243	.567	50114.23613	.5011	.153
50032.41720	.0482	.141	50056.29463	.0250	.516	50114.23727	.5020	.163
50032.41749	.0485	.141	50056.29911	.0287	.449	50114.24171	.5058	.134
50032.42193	.0522	.114	50056.30011	.0296	.468	50114.24281	.5067	.107
50032.42289	.0530	.123	50056.30467	.0334	.402	50114.24907	.5119	.082
50032.42757	.0569	.088	50056.30562	.0342	.438	50114.25022	.5129	.096
50032.42873	.0579	.081	50056.30982	.0377	.306	50114.25585	.5176	.064
50032.42902	.0581	.085	50056.31089	.0386	.268	50114.25694	.5185	.078
50032.43506	.0632	.040	50056.31735	.0440	.341	50114.26530	.5255	.062
50032.43618	.0641	.071	50056.31831	.0448	.298	50114.26559	.5257	.048
50032.43681	.0646	.055	50056.32219	.0481	.204	50114.26659	.5266	.072
50032.44200	.0690	.027	50056.32316	.0489	.232	50114.27118	.5304	.076
50032.44307	.0699	-.018	50056.32713	.0522	.153	50114.27218	.5313	.044
50032.44899	.0748	-.001	50056.32811	.0530	.131	50114.27733	.5356	.037
50032.44934	.0751	-.014	50056.33228	.0565	.055	50114.28873	.5451	.018
50032.45430	.0793	-.034	50056.33344	.0575	.085	50114.28981	.5460	.027
50032.45463	.0795	-.015	50056.33757	.0609	.075	50114.29376	.5493	.016
50032.45558	.0803	-.021	50056.33861	.0618	.089	50114.29484	.5502	-.019
50032.46023	.0842	-.010	50056.34337	.0658	.094	50386.13517	.9823	.612
50032.46126	.0851	-.047	50056.34448	.0667	-.005	50386.13547	.9826	.607
50032.46545	.0886	-.085	50056.34944	.0709	-.006	50386.13657	.9835	.620
50032.46645	.0894	-.069	50056.35044	.0717	-.013	50386.13686	.9838	.630
50055.15381	.0706	.050	50056.35495	.0755	-.008	50386.14686	.9921	.698
50055.15587	.0723	-.010	50056.35665	.0769	.005	50386.14720	.9924	.691
50055.15988	.0756	-.062	50056.36187	.0813	-.027	50386.14856	.9935	.761
50055.16127	.0768	-.031	50056.36298	.0822	-.002	50386.14920	.9941	.751
50055.17262	.0863	.005	50056.36745	.0859	-.081	50386.15689	.0005	.746
50055.17307	.0867	-.008	50056.36841	.0867	-.087	50386.15719	.0008	.756
50055.17430	.0877	-.047	50056.37238	.0901	-.056	50386.15821	.0016	.769
50055.17492	.0882	-.057	50056.37781	.0946	.000	50386.15852	.0019	.761
50055.17953	.0921	-.054	50056.37935	.0959	-.026	50386.17101	.0123	.713
50055.18086	.0932	-.097	50056.38327	.0992	-.038	50386.17132	.0126	.729
50055.18550	.0971	-.060	50064.27335	.7003	-.153	50386.17226	.0134	.701
50055.18703	.0983	.003	50064.27455	.7013	-.129	50386.17307	.0140	.711

K band observations of RZ Cas (Continued)

Hel. JD. -2400000.	Phase	Rel. mag.	Hel. JD. -2400000.	Phase	Rel. mag.	Hel. JD. -2400000.	Phase	Rel. mag.
50386.18323	.0225	.566	50386.43430	.2326	-.141	50387.36424	.0106	.710
50386.18361	.0229	.573	50386.43575	.2338	-.141	50387.36455	.0109	.716
50386.18516	.0242	.552	50386.43610	.2341	-.119	50387.36582	.0119	.676
50386.18554	.0245	.548	50386.44563	.2421	-.140	50387.37277	.0178	.649
50386.18633	.0251	.547	50386.44593	.2423	-.129	50387.37314	.0181	.639
50386.18664	.0254	.584	50386.44710	.2433	-.133	50387.37469	.0194	.575
50386.20416	.0401	.273	50386.44743	.2436	-.131	50387.37499	.0196	.582
50386.20445	.0403	.263	50386.45717	.2517	-.117	50387.38314	.0264	.496
50386.20551	.0412	.259	50386.45824	.2526	-.123	50387.38347	.0267	.475
50386.20582	.0414	.254	50386.45868	.2530	-.137	50387.38470	.0277	.478
50386.21439	.0486	.234	50386.46693	.2599	-.139	50387.38509	.0281	.472
50386.21477	.0489	.211	50386.46724	.2602	-.151	50387.39175	.0336	.432
50386.21589	.0499	.180	50386.46845	.2612	-.163	50387.39212	.0339	.443
50386.21619	.0501	.178	50386.46876	.2614	-.169	50387.39269	.0344	.414
50386.22428	.0569	.118	50386.47859	.2696	-.164	50387.39440	.0359	.337
50386.22464	.0572	.101	50386.47890	.2699	-.165	50387.39472	.0361	.333
50386.22570	.0581	.106	50386.48018	.2710	-.141	50387.40082	.0412	.281
50386.22603	.0584	.099	50386.48125	.2719	-.144	50387.40148	.0418	.270
50386.25710	.0843	-.031	50386.49517	.2835	-.144	50387.40292	.0430	.294
50386.25741	.0846	-.027	50386.49589	.2841	-.148	50387.41014	.0490	.214
50386.25849	.0855	-.052	50386.49723	.2852	-.122	50387.41042	.0493	.208
50386.25881	.0858	-.056	50386.49756	.2855	-.124	50387.41179	.0504	.175
50386.26618	.0919	-.043	50387.26036	.9237	-.010	50387.41249	.0510	.156
50386.26672	.0924	-.056	50387.26066	.9240	-.004	50387.42011	.0574	.110
50386.26802	.0935	-.053	50387.26176	.9249	-.004	50387.42045	.0577	.102
50386.26836	.0938	-.050	50387.26206	.9251	-.007	50387.42176	.0587	.083
50386.28023	.1037	-.068	50387.27095	.9326	.043	50387.42777	.0638	.042
50386.28089	.1043	-.073	50387.27126	.9328	.039	50387.42809	.0640	.039
50386.28201	.1052	-.067	50387.27245	.9338	.027	50387.42941	.0651	.045
50386.28233	.1055	-.057	50387.27278	.9341	.031	50387.42997	.0656	.038
50386.30934	.1281	-.095	50387.27849	.9389	.068	50387.43617	.0708	.005
50386.30967	.1283	-.098	50387.27882	.9392	.066	50387.43672	.0713	-.001
50386.31078	.1293	-.089	50387.28043	.9405	.082	50387.43798	.0723	.008
50386.31116	.1296	-.090	50387.28506	.9444	.127	50387.43842	.0727	.026
50386.32930	.1447	-.098	50387.28538	.9446	.131	50387.43874	.0730	.019
50386.32959	.1450	-.102	50387.28648	.9456	.144	50387.44541	.0785	.003
50386.33075	.1460	-.090	50387.29346	.9514	.227	50387.44574	.0788	-.001
50386.33108	.1462	-.086	50387.29373	.9516	.230	50387.44690	.0798	-.029
50386.37727	.1849	-.116	50387.29535	.9530	.226	50387.44720	.0800	-.039
50386.37759	.1851	-.108	50387.30182	.9584	.285	50387.45600	.0874	-.006
50386.37950	.1867	-.115	50387.30215	.9587	.320	50387.45646	.0878	-.035
50386.37981	.1870	-.117	50387.30353	.9598	.338	50387.45776	.0889	-.042
50386.38792	.1938	-.106	50387.31731	.9714	.480	50387.45857	.0895	-.041
50386.38863	.1944	-.102	50387.31760	.9716	.468	50387.46690	.0965	-.062
50386.39069	.1961	-.109	50387.31780	.9718	.483	50387.46767	.0972	-.079
50386.39114	.1965	-.107	50387.31838	.9723	.447	50387.46906	.0983	-.077
50386.39949	.2035	-.117	50387.32061	.9741	.481	50387.46938	.0986	-.063
50386.39983	.2038	-.113	50387.32714	.9796	.575	50387.48087	.1082	-.063
50386.40120	.2049	-.120	50387.32801	.9803	.569	50387.48119	.1085	-.075
50386.40159	.2052	-.122	50387.33000	.9820	.601	50387.48230	.1094	-.057
50386.41062	.2128	-.143	50387.33732	.9881	.681	50387.48269	.1097	-.041
50386.41094	.2131	-.141	50387.33765	.9884	.718	50387.49386	.1191	-.076
50386.41211	.2140	-.105	50387.33880	.9893	.716	50387.49424	.1194	-.044
50386.41246	.2143	-.113	50387.34469	.9943	.772	50387.49494	.1200	-.074
50386.42135	.2218	-.138	50387.34595	.9953	.734	50387.49606	.1209	-.073
50386.42169	.2220	-.134	50387.34701	.9962	.720	50387.49634	.1211	-.058
50386.42345	.2235	-.156	50387.35586	.0036	.736	50388.25838	.7587	-.114
50386.42378	.2238	-.153	50387.35617	.0039	.755	50388.25870	.7590	-.114
50386.43230	.2309	-.126	50387.35749	.0050	.752	50388.26019	.7602	-.117
50386.43297	.2315	-.143	50387.35791	.0053	.741	50388.26050	.7605	-.123

K band observations of RZ Cas (Continued)

Hel. JD. -2400000.	Phase	Rel. mag.	Hel. JD. -2400000.	Phase	Rel. mag.	Hel. JD. -2400000.	Phase	Rel. mag.
50388.26948	.7680	-.097	50388.49956	.9605	.289	50417.18839	.9625	.354
50388.26981	.7683	-.068	50388.50019	.9610	.330	50417.18870	.9628	.377
50388.27151	.7697	-.072	50388.50873	.9681	.471	50417.19442	.9676	.411
50388.27404	.7718	-.079	50388.50997	.9692	.459	50417.19473	.9678	.372
50388.28198	.7784	-.109	50388.51032	.9695	.461	50417.19585	.9688	.420
50388.28356	.7798	-.109	50415.28163	.3672	-.120	50417.19616	.9690	.398
50388.28391	.7800	-.127	50415.28267	.3681	-.115	50417.20204	.9739	.424
50388.28935	.7846	-.113	50415.28311	.3685	-.104	50417.20236	.9742	.457
50388.28975	.7849	-.122	50415.30697	.3884	-.108	50417.20356	.9752	.454
50388.29100	.7860	-.105	50415.30744	.3888	-.125	50417.20388	.9755	.416
50388.29763	.7915	-.099	50415.30929	.3904	-.152	50417.20560	.9769	.447
50388.29796	.7918	-.098	50415.31088	.3917	-.107	50417.20591	.9772	.465
50388.29935	.7930	-.119	50415.31736	.3971	-.160	50417.20692	.9780	.509
50388.29966	.7932	-.119	50415.31768	.3974	-.141	50417.21127	.9817	.586
50388.31212	.8037	-.127	50415.31899	.3985	-.091	50417.21281	.9829	.655
50388.31244	.8039	-.107	50415.31953	.3990	-.111	50417.21335	.9834	.644
50388.31366	.8049	-.103	50415.32657	.4049	-.112	50417.22224	.9908	.623
50388.32087	.8110	-.098	50415.32690	.4051	-.103	50417.22356	.9919	.605
50388.32153	.8115	-.098	50415.32794	.4060	-.128	50417.22387	.9922	.620
50388.32187	.8118	-.095	50415.32898	.4069	-.109	50417.22691	.9947	.665
50388.32340	.8131	-.099	50415.33815	.4145	-.120	50417.23723	.0034	.692
50388.32377	.8134	-.104	50415.33846	.4148	-.100	50417.23788	.0039	.683
50388.32981	.8185	-.086	50415.35778	.4310	-.074	50417.24265	.0079	.662
50388.33015	.8187	-.079	50415.35841	.4315	-.132	50417.24296	.0082	.683
50388.33136	.8198	-.101	50415.35957	.4325	-.123	50417.24419	.0092	.647
50388.33820	.8255	-.087	50415.36059	.4333	-.125	50417.24453	.0095	.637
50388.33916	.8263	-.099	50415.36151	.4341	-.115	50417.24619	.0109	.658
50388.34037	.8273	-.092	50415.37974	.4493	-.024	50417.24684	.0114	.674
50388.34071	.8276	-.082	50415.38059	.4500	-.032	50417.25108	.0150	.605
50388.34820	.8338	-.064	50415.38915	.4572	-.016	50417.25138	.0152	.614
50388.34920	.8347	-.077	50415.39043	.4583	.017	50417.25256	.0162	.619
50388.35088	.8361	-.103	50415.39980	.4661	-.014	50417.25302	.0166	.544
50388.35121	.8364	-.112	50415.40171	.4677	.062	50417.25840	.0211	.459
50388.36012	.8438	-.100	50415.40216	.4681	.077	50417.25876	.0214	.468
50388.36044	.8441	-.101	50415.40288	.4687	.046	50417.25982	.0223	.458
50388.36170	.8451	-.088	50415.41171	.4761	.136	50417.26022	.0226	.456
50388.37115	.8530	-.084	50415.41254	.4768	.138	50417.26156	.0237	.457
50388.38016	.8606	-.086	50415.41416	.4781	.117	50417.26186	.0240	.454
50388.38096	.8612	-.072	50415.41465	.4785	.141	50417.26669	.0280	.373
50388.38252	.8626	-.066	50415.42110	.4839	.172	50417.26700	.0283	.379
50388.39356	.8718	-.106	50415.42198	.4847	.146	50417.26816	.0293	.375
50388.39389	.8721	-.064	50415.42318	.4857	.126	50417.26848	.0295	.321
50388.39536	.8733	-.061	50415.42350	.4859	.181	50417.27552	.0354	.269
50388.40297	.8797	-.056	50415.43444	.4951	.172	50417.27584	.0357	.273
50388.41756	.8919	-.083	50415.43633	.4967	.200	50417.27702	.0367	.278
50388.41928	.8933	-.100	50415.44477	.5037	.168	50417.27741	.0370	.344
50388.43266	.9045	-.036	50415.44552	.5044	.144	50417.27927	.0385	.313
50388.44298	.9131	-.040	50415.44720	.5058	.179	50417.27966	.0389	.313
50388.44330	.9134	-.049	50415.44776	.5062	.160	50417.28653	.0446	.249
50388.45483	.9230	-.035	50417.16228	.9407	.101	50417.28688	.0449	.246
50388.45514	.9233	-.025	50417.16258	.9409	.075	50417.28800	.0459	.150
50388.45650	.9245	-.011	50417.16364	.9418	.080	50417.28833	.0461	.156
50388.46664	.9329	.047	50417.16979	.9470	.099	50417.29359	.0505	.127
50388.46739	.9336	.048	50417.17015	.9473	.087	50417.29392	.0508	.120
50388.46906	.9350	.056	50417.18005	.9555	.225	50417.29516	.0518	.159
50388.47687	.9415	.085	50417.18038	.9558	.246	50417.29563	.0522	.121
50388.47720	.9418	.082	50417.18156	.9568	.240	50417.29593	.0525	.148
50388.47925	.9435	.135	50417.18196	.9571	.231	50417.29986	.0558	.116
50388.48804	.9508	.199	50417.18703	.9614	.332	50417.30022	.0561	.129
50388.48836	.9511	.195	50417.18735	.9616	.326	50417.30174	.0574	.089

K band observations of RZ Cas (Continued)

Hel. JD. -2400000.	Phase	Rel. mag.	Hel. JD. -2400000.	Phase	Rel. mag.	Hel. JD. -2400000.	Phase	Rel. mag.
50417.30211	.0577	.079	50417.33804	.0877	-.063	50417.38528	.1272	-.099
50417.30245	.0579	.094	50417.34836	.0964	-.102	50417.39101	.1320	-.075
50417.30682	.0616	.090	50417.34946	.0973	-.088	50417.39133	.1323	-.071
50417.30715	.0619	.093	50417.34979	.0975	-.087	50417.39262	.1334	-.092
50417.30827	.0628	.098	50417.35539	.1022	-.109	50417.39295	.1337	-.083
50417.30858	.0631	.082	50417.36268	.1083	-.076	50417.39833	.1382	-.110
50417.31314	.0669	.063	50417.36376	.1092	-.077	50417.39871	.1385	-.097
50417.31348	.0672	.086	50417.37105	.1153	-.079	50417.39931	.1390	-.082
50417.31453	.0681	.016	50417.37136	.1156	-.085	50417.40064	.1401	-.077
50417.31490	.0684	-.001	50417.37659	.1200	-.097	50417.40103	.1404	-.104
50417.32621	.0778	-.049	50417.37700	.1203	-.093	50417.40141	.1407	-.100
50417.32651	.0781	-.038	50417.37811	.1212	-.101	50417.40748	.1458	-.084
50417.32806	.0794	-.031	50417.37843	.1215	-.117	50417.40783	.1461	-.100
50417.33504	.0852	-.023	50417.38339	.1257	-.118	50417.40887	.1470	-.094
50417.33541	.0855	-.026	50417.38372	.1259	-.114	50417.40921	.1473	-.084
50417.33755	.0873	-.067	50417.38489	.1269	-.099			

Appendix : 3

J band observations of R CMa (R CMa - BD-15^{o} 1734)

Hel. JD. -2400000.	Phase	Rel. mag.	Hel. JD. -2400000.	Phase	Rel. mag.	Hel. JD. -2400000.	Phase	Rel. mag.
50031.48158	.9064	-.330	50034.41687	.4904	-.188	50051.42318	.4614	-.251
50031.48277	.9075	-.331	50034.41816	.4915	-.174	50051.44046	.4766	-.185
50031.48343	.9080	-.309	50034.42287	.4957	-.185	50051.44158	.4776	-.185
50031.48900	.9129	-.311	50034.43104	.5029	-.154	50051.44219	.4781	-.202
50031.48959	.9135	-.298	50034.43153	.5033	-.159	50051.45284	.4875	-.168
50031.49164	.9153	-.304	50034.43273	.5044	-.149	50051.45390	.4885	-.185
50031.49626	.9193	-.296	50034.43823	.5092	-.166	50051.45988	.4937	-.159
50031.49728	.9202	-.262	50034.43898	.5099	-.178	50051.46156	.4952	-.174
50031.50184	.9242	-.283	50034.43998	.5107	-.167	50051.46809	.5009	-.174
50031.50313	.9254	-.269	50034.44907	.5188	-.180	50051.46911	.5018	-.185
50031.50849	.9301	-.256	50034.45028	.5198	-.176	50051.47663	.5085	-.201
50031.50958	.9311	-.242	50034.45604	.5249	-.194	50051.47774	.5094	-.174
50031.51369	.9347	-.242	50034.45710	.5258	-.211	50051.48402	.5150	-.180
50031.51479	.9356	-.258	50034.46359	.5315	-.212	50051.48502	.5159	-.174
50031.51900	.9394	-.236	50034.46543	.5332	-.228	50051.49403	.5238	-.186
50031.52066	.9408	-.264	50034.46594	.5336	-.240	50051.50228	.5310	-.229
50031.52160	.9416	-.260	50034.47427	.5409	-.251	50054.42117	.1006	-.333
50033.46163	.6495	-.346	50034.47537	.5419	-.244	50054.42223	.1015	-.329
50033.46282	.6505	-.335	50034.48290	.5485	-.278	50054.47738	.1501	-.301
50033.46756	.6547	-.368	50034.48417	.5497	-.261	50054.47853	.1511	-.299
50033.46865	.6557	-.334	50034.49210	.5566	-.249	50054.48346	.1554	-.308
50033.46925	.6562	-.342	50034.49248	.5570	-.256	50054.48450	.1564	-.328
50033.47354	.6600	-.342	50034.49360	.5580	-.279	50054.48872	.1601	-.331
50033.47451	.6608	-.303	50034.49389	.5582	-.278	50054.48972	.1609	-.354
50033.47492	.6612	-.305	50034.49982	.5634	-.287	50054.50283	.1725	-.337
50033.47945	.6652	-.312	50034.50091	.5644	-.301	50054.50390	.1734	-.334
50033.48075	.6663	-.320	50034.50125	.5647	-.292	50054.51040	.1792	-.343
50033.48110	.6666	-.320	50034.50774	.5704	-.302	50054.51144	.1801	-.369
50033.48845	.6731	-.315	50034.50847	.5710	-.303	50054.51666	.1847	-.330
50033.48960	.6741	-.317	50034.50978	.5722	-.311	50054.51775	.1856	-.384
50033.49051	.6749	-.312	50034.51509	.5769	-.316	50054.52404	.1912	-.355
50033.49720	.6808	-.330	50034.51616	.5778	-.313	50057.41753	.7384	-.317
50033.49816	.6816	-.339	50035.45797	.4069	-.341	50057.41846	.7392	-.324
50033.49851	.6820	-.346	50035.45893	.4077	-.316	50057.42488	.7448	-.347
50033.50342	.6863	-.336	50035.45926	.4080	-.309	50057.42604	.7459	-.346
50033.51025	.6923	-.348	50035.47041	.4179	-.325	50057.43138	.7506	-.343
50033.51125	.6932	-.329	50035.47155	.4189	-.317	50057.43187	.7510	-.368
50033.51579	.6972	-.333	50035.47551	.4224	-.313	50057.43606	.7547	-.367
50033.51671	.6980	-.330	50035.47643	.4232	-.306	50057.43699	.7555	-.341
50033.51708	.6983	-.348	50035.47673	.4234	-.349	50057.44240	.7603	-.351
50033.52206	.7027	-.339	50035.48099	.4272	-.346	50057.44630	.7637	-.359
50033.52304	.7035	-.340	50035.48197	.4280	-.347	50057.44743	.7647	-.354
50033.52333	.7038	-.353	50035.48800	.4333	-.327	50057.45177	.7685	-.369
50034.36682	.4463	-.262	50035.48895	.4342	-.315	50057.45291	.7695	-.345
50034.36857	.4479	-.269	50035.49326	.4380	-.328	50057.45660	.7728	-.357
50034.37450	.4531	-.272	50035.49647	.4408	-.262	50057.45755	.7736	-.348
50034.37570	.4542	-.260	50035.49759	.4418	-.272	50057.46351	.7788	-.346
50034.37613	.4545	-.260	50035.50466	.4480	-.265	50057.46474	.7799	-.341
50034.38101	.4588	-.248	50035.50595	.4491	-.274	50057.47016	.7847	-.341
50034.38142	.4592	-.247	50035.50988	.4526	-.278	50057.47602	.7899	-.335
50034.38259	.4602	-.252	50035.51076	.4534	-.251	50057.47698	.7907	-.331
50034.38746	.4645	-.237	50035.51109	.4537	-.241	50057.48192	.7950	-.334
50034.38790	.4649	-.242	50035.51511	.4572	-.217	50057.48301	.7960	-.333
50034.38912	.4660	-.232	50035.51604	.4580	-.212	50057.48719	.7997	-.328
50034.39422	.4705	-.217	50035.52090	.4623	-.249	50057.48821	.8006	-.318
50034.39569	.4718	-.221	50035.52489	.4658	-.209	50057.49193	.8039	-.315
50034.40305	.4782	-.189	50051.41207	.4516	-.275	50057.49298	.8048	-.310
50034.40418	.4792	-.202	50051.41418	.4535	-.272	50057.50094	.8118	-.340
50034.41029	.4846	-.183	50051.41531	.4545	-.266	50057.50218	.8129	-.331
50034.41149	.4857	-.183	50051.41570	.4548	-.261	50057.50659	.8168	-.346

J band observations of R CMa (Continued)

Hel. JD. -2400000.	Phase	Rel. mag.	Hel. JD. -2400000.	Phase	Rel. mag.	Hel. JD. -2400000.	Phase	Rel. mag.
50057.50761	.8177	-.331	50058.50395	.6948	-.360	50085.36813	.3438	-.317
50057.50793	.8179	-.330	50058.50518	.6958	-.341	50085.36847	.3441	-.321
50057.51296	.8224	-.332	50058.50977	.6999	-.337	50085.37180	.3471	-.330
50057.51400	.8233	-.340	50058.51095	.7009	-.339	50085.37277	.3479	-.344
50057.51865	.8274	-.327	50058.51704	.7063	-.335	50085.37813	.3526	-.362
50057.51957	.8282	-.336	50058.51741	.7066	-.352	50085.37936	.3537	-.336
50057.52376	.8319	-.308	50058.51845	.7075	-.342	50085.38325	.3572	-.340
50057.52882	.8363	-.317	50059.39496	.4791	-.168	50085.38419	.3580	-.331
50057.53008	.8374	-.309	50059.40053	.4840	-.154	50085.38845	.3617	-.347
50058.29610	.5118	-.172	50059.40728	.4900	-.140	50085.38952	.3627	-.349
50058.29794	.5134	-.172	50059.41167	.4938	-.184	50085.38994	.3630	-.336
50058.30198	.5170	-.193	50059.41579	.4975	-.157	50085.39373	.3664	-.344
50058.30318	.5180	-.188	50059.42032	.5015	-.169	50085.39476	.3673	-.330
50058.30623	.5207	-.188	50059.42480	.5054	-.172	50085.39864	.3707	-.334
50058.30722	.5216	-.181	50059.42821	.5084	-.183	50085.39960	.3715	-.316
50058.31051	.5245	-.199	50059.42858	.5087	-.182	50085.40296	.3745	-.321
50058.31141	.5253	-.184	50059.43402	.5135	-.183	50085.40409	.3755	-.334
50058.31507	.5285	-.189	50059.43448	.5139	-.186	50085.40797	.3789	-.343
50058.31621	.5295	-.203	50059.43818	.5172	-.192	50085.40898	.3798	-.333
50058.31999	.5328	-.211	50059.44265	.5211	-.212	50085.41313	.3835	-.335
50058.32096	.5337	-.205	50059.44307	.5215	-.200	50085.41418	.3844	-.347
50058.32130	.5340	-.203	50059.44736	.5253	-.196	50085.41749	.3873	-.342
50058.32778	.5397	-.200	50059.44791	.5257	-.200	50085.41847	.3882	-.336
50058.33139	.5428	-.228	50059.45213	.5295	-.230	50085.42376	.3928	-.338
50058.33178	.5432	-.237	50059.45671	.5335	-.223	50085.42470	.3936	-.321
50058.33293	.5442	-.228	50059.45715	.5339	-.213	50085.42886	.3973	-.339
50058.33718	.5479	-.263	50059.46148	.5377	-.238	50085.42988	.3982	-.313
50058.33814	.5488	-.250	50059.47765	.5519	-.257	50085.43392	.4018	-.338
50058.34243	.5526	-.250	50059.48185	.5556	-.257	50085.43517	.4029	-.325
50058.40319	.6061	-.320	50059.48249	.5562	-.275	50085.43915	.4064	-.322
50058.40440	.6071	-.323	50059.48373	.5573	-.305	50085.44012	.4072	-.309
50058.40476	.6074	-.333	50059.49049	.5632	-.307	50085.44388	.4105	-.330
50058.40979	.6119	-.331	50059.49107	.5637	-.323	50085.44494	.4115	-.342
50058.41026	.6123	-.321	50059.49630	.5683	-.306	50085.44844	.4145	-.356
50058.41118	.6131	-.330	50059.50013	.5717	-.313	50085.44937	.4154	-.338
50058.41537	.6168	-.331	50059.50059	.5721	-.278	50085.45435	.4197	-.353
50058.41634	.6176	-.298	50059.50419	.5753	-.316	50085.45533	.4206	-.324
50058.41664	.6179	-.303	50059.50780	.5785	-.296	50085.45862	.4235	-.281
50058.42089	.6216	-.314	50059.51195	.5821	-.309	50085.46289	.4273	-.304
50058.42209	.6227	-.314	50059.51544	.5852	-.322	50085.46390	.4281	-.325
50058.42923	.6290	-.319	50059.51877	.5881	-.302	50085.46766	.4315	-.311
50058.43544	.6344	-.350	50059.51922	.5885	-.325	50085.46862	.4323	-.292
50058.44121	.6395	-.304	50059.52254	.5914	-.326	50086.34168	.2009	-.372
50058.44246	.6406	-.309	50085.32342	.3045	-.350	50086.34269	.2018	-.354
50058.44676	.6444	-.326	50085.32452	.3055	-.363	50086.34662	.2052	-.327
50058.44799	.6455	-.305	50085.32815	.3087	-.353	50086.35081	.2089	-.336
50058.45282	.6497	-.312	50085.32918	.3096	-.351	50086.35535	.2129	-.319
50058.45331	.6502	-.324	50085.33389	.3137	-.369	50086.35694	.2143	-.300
50058.45442	.6512	-.303	50085.33505	.3147	-.336	50086.36015	.2171	-.317
50058.46040	.6564	-.339	50085.33961	.3187	-.345	50086.36111	.2180	-.302
50058.46444	.6600	-.344	50085.34068	.3197	-.344	50086.36539	.2218	-.365
50058.46555	.6610	-.339	50085.34418	.3228	-.354	50086.37192	.2275	-.327
50058.47408	.6685	-.340	50085.34521	.3237	-.347	50086.37295	.2284	-.363
50058.48037	.6740	-.325	50085.34955	.3275	-.353	50086.37613	.2312	-.361
50058.48422	.6774	-.343	50085.35055	.3284	-.346	50086.37708	.2320	-.314
50058.48521	.6783	-.367	50085.35639	.3335	-.351	50086.38060	.2351	-.335
50058.49402	.6860	-.350	50085.35738	.3344	-.335	50086.38415	.2383	-.356
50058.49520	.6870	-.341	50085.36245	.3388	-.339	50086.38511	.2391	-.370
50058.49619	.6879	-.310	50085.36344	.3397	-.355	50086.38958	.2430	-.357
50058.49992	.6912	-.321	50085.36710	.3429	-.355	50086.39054	.2439	-.346

J band observations of R CMa (Continued)

Hel. JD. -2400000.	Phase	Rel. mag.	Hel. JD. -2400000.	Phase	Rel. mag.	Hel. JD. -2400000.	Phase	Rel. mag.
50086.39385	.2468	-.347	50088.26800	.8967	-.326	50088.40157	.0142	.152
50086.39481	.2477	-.343	50088.26896	.8975	-.332	50088.40293	.0154	.118
50086.39927	.2516	-.350	50088.27010	.8985	-.325	50088.40382	.0162	.122
50086.40385	.2556	-.338	50088.27453	.9024	-.327	50088.40712	.0191	.113
50086.40952	.2606	-.336	50088.27551	.9033	-.322	50088.40810	.0200	.109
50086.41623	.2665	-.381	50088.27915	.9065	-.306	50088.41291	.0242	.077
50086.41731	.2675	-.384	50088.28011	.9073	-.319	50088.41952	.0300	.004
50086.42174	.2714	-.372	50088.28115	.9082	-.315	50088.42051	.0309	-.015
50086.42315	.2726	-.383	50088.28521	.9118	-.329	50088.42543	.0353	-.051
50086.42765	.2766	-.366	50088.28613	.9126	-.325	50088.42636	.0361	-.060
50086.42860	.2774	-.344	50088.28718	.9135	-.307	50088.43066	.0399	-.089
50086.43300	.2813	-.344	50088.29225	.9180	-.319	50088.43178	.0408	-.092
50086.43395	.2821	-.366	50088.29315	.9188	-.312	50088.43279	.0417	-.102
50086.43836	.2860	-.333	50088.29714	.9223	-.299	50088.43372	.0425	-.104
50086.44305	.2901	-.322	50088.29802	.9231	-.279	50088.43930	.0475	-.156
50086.44397	.2909	-.329	50088.30276	.9273	-.271	50088.44040	.0484	-.132
50086.44789	.2944	-.338	50088.30374	.9281	-.275	50088.44488	.0524	-.161
50086.44880	.2952	-.346	50088.30889	.9327	-.260	50088.44586	.0532	-.165
50086.45384	.2996	-.339	50088.30980	.9335	-.246	50088.44999	.0569	-.212
50086.45492	.3006	-.325	50088.31271	.9360	-.239	50088.45154	.0582	-.221
50086.45900	.3042	-.330	50088.31363	.9368	-.223	50088.45262	.0592	-.210
50086.45996	.3050	-.337	50088.31394	.9371	-.220	50090.34031	.7210	-.360
50087.37093	.1069	-.312	50088.31807	.9407	-.193	50090.34066	.7213	-.337
50087.37200	.1079	-.310	50088.31899	.9415	-.204	50090.34320	.7235	-.373
50087.37630	.1117	-.329	50088.32287	.9450	-.208	50090.35904	.7374	-.343
50087.37725	.1125	-.324	50088.32381	.9458	-.193	50090.35936	.7377	-.349
50087.38087	.1157	-.305	50088.32804	.9495	-.172	50090.36323	.7411	-.340
50087.38246	.1171	-.344	50088.32895	.9503	-.184	50090.36359	.7415	-.347
50087.38710	.1212	-.340	50088.33224	.9532	-.135	50090.36854	.7458	-.336
50087.38813	.1221	-.320	50088.33314	.9540	-.099	50090.36963	.7468	-.358
50087.39395	.1272	-.338	50088.33718	.9576	-.109	50090.37605	.7524	-.345
50087.39490	.1281	-.305	50088.33815	.9584	-.102	50090.38251	.7581	-.356
50087.39900	.1317	-.322	50088.34211	.9619	-.071	50090.38488	.7602	-.388
50087.39997	.1325	-.323	50088.34657	.9658	-.054	50090.40296	.7761	-.349
50087.40449	.1365	-.327	50088.34747	.9666	-.044	50090.40389	.7769	-.364
50087.40548	.1374	-.344	50088.35121	.9699	-.001	50090.41215	.7842	-.363
50087.40585	.1377	-.322	50088.35213	.9707	.000	50090.41317	.7851	-.333
50087.41060	.1419	-.317	50088.35351	.9719	.031	50090.42068	.7917	-.326
50087.41162	.1428	-.333	50088.35436	.9727	.041	50090.42165	.7926	-.323
50087.41691	.1474	-.349	50088.35819	.9761	.060	50090.42711	.7974	-.328
50087.41788	.1483	-.343	50088.35914	.9769	.067	50090.42812	.7983	-.329
50087.42290	.1527	-.309	50088.35954	.9772	.069	50090.43388	.8033	-.332
50087.42394	.1536	-.318	50088.36434	.9815	.091	50090.44215	.8106	-.328
50087.42820	.1574	-.329	50088.36531	.9823	.090	50090.44313	.8115	-.348
50087.42911	.1582	-.317	50088.36878	.9854	.149	50090.44782	.8156	-.340
50087.43456	.1630	-.362	50088.36983	.9863	.150	50090.44815	.8159	-.353
50087.43564	.1639	-.350	50088.37341	.9895	.132	50090.44915	.8168	-.324
50087.44026	.1680	-.378	50088.37429	.9902	.151	50090.45466	.8216	-.326
50087.44125	.1689	-.294	50088.37580	.9916	.120	50090.45565	.8225	-.311
50087.44589	.1729	-.314	50088.37675	.9924	.126	50090.45951	.8259	-.338
50088.24445	.8759	-.322	50088.38112	.9962	.151	50090.45982	.8262	-.351
50088.24533	.8767	-.329	50088.38217	.9972	.142	50090.46408	.8299	-.348
50088.24674	.8779	-.327	50088.38314	.9980	.158	50090.46508	.8308	-.314
50088.25107	.8818	-.330	50088.38686	.0013	.162	50092.22714	.3820	-.364
50088.25592	.8860	-.326	50088.38779	.0021	.163	50092.22818	.3829	-.363
50088.25684	.8868	-.319	50088.39120	.0051	.151	50092.23756	.3911	-.342
50088.25801	.8879	-.312	50088.39215	.0059	.179	50092.23892	.3923	-.345
50088.26212	.8915	-.322	50088.39580	.0092	.152	50092.24494	.3976	-.347
50088.26307	.8923	-.324	50088.39679	.0100	.153	50092.25049	.4025	-.342
50088.26411	.8932	-.324	50088.40065	.0134	.137	50092.25146	.4034	-.322

J band observations of R CMa (Continued)

Hel. JD. -2400000.	Phase	Rel. mag.	Hel. JD. -2400000.	Phase	Rel. mag.	Hel. JD. -2400000.	Phase	Rel. mag.
50092.25641	.4077	-.312	50092.41560	.5479	-.228	50095.26532	.0565	-.231
50092.25736	.4086	-.310	50092.41656	.5487	-.225	50095.26969	.0604	-.239
50092.26248	.4131	-.335	50092.41704	.5491	-.274	50095.27001	.0607	-.240
50092.26345	.4139	-.347	50092.41820	.5502	-.289	50095.27085	.0614	-.229
50092.26870	.4186	-.343	50092.42287	.5543	-.279	50095.27565	.0656	-.227
50092.26984	.4196	-.319	50092.42398	.5553	-.280	50095.27600	.0659	-.247
50092.27486	.4240	-.325	50092.42490	.5561	-.292	50095.27710	.0669	-.289
50092.27583	.4248	-.296	50092.42881	.5595	-.298	50096.25718	.9297	-.249
50092.28009	.4286	-.304	50092.42999	.5605	-.281	50096.25840	.9308	-.275
50092.28135	.4297	-.282	50092.43403	.5641	-.293	50096.26474	.9364	-.225
50092.28669	.4344	-.307	50092.43505	.5650	-.309	50096.27249	.9432	-.207
50092.28786	.4354	-.322	50092.43975	.5691	-.339	50096.27284	.9435	-.207
50092.29355	.4404	-.294	50092.44066	.5699	-.335	50096.27834	.9483	-.129
50092.29449	.4413	-.280	50092.44464	.5734	-.335	50096.30372	.9707	-.054
50092.30006	.4462	-.271	50092.44559	.5743	-.318	50096.30409	.9710	-.017
50092.30124	.4472	-.273	50092.44970	.5779	-.327	50096.30440	.9713	-.009
50092.30212	.4480	-.234	50092.45068	.5788	-.322	50096.31031	.9765	.021
50092.30668	.4520	-.259	50092.45480	.5824	-.335	50096.31062	.9767	.054
50092.30700	.4523	-.257	50092.45570	.5832	-.309	50096.31165	.9777	.063
50092.30802	.4532	-.231	50093.39164	.4071	-.331	50096.31593	.9814	.111
50092.31243	.4571	-.223	50093.39282	.4081	-.310	50096.31717	.9825	.117
50092.31348	.4580	-.214	50093.39885	.4135	-.302	50096.32523	.9896	.135
50092.31897	.4628	-.233	50093.39989	.4144	-.319	50096.32621	.9905	.167
50092.32000	.4637	-.221	50093.40534	.4192	-.324	50096.32658	.9908	.182
50092.32369	.4670	-.211	50093.40630	.4200	-.304	50096.33218	.9957	.186
50092.32472	.4679	-.199	50093.41115	.4243	-.315	50096.33325	.9967	.189
50092.32997	.4725	-.208	50093.41216	.4252	-.303	50096.33356	.9969	.160
50092.33100	.4734	-.199	50093.41252	.4255	-.337	50096.33834	.0011	.170
50092.33130	.4737	-.201	50093.41768	.4300	-.338	50096.33934	.0020	.177
50092.33602	.4778	-.211	50093.41802	.4303	-.322	50096.33965	.0023	.199
50092.33703	.4787	-.179	50093.41923	.4314	-.311	50096.39561	.0516	-.159
50092.33736	.4790	-.176	50093.42350	.4352	-.290	50096.39655	.0524	-.174
50092.34197	.4831	-.171	50093.42444	.4360	-.299	50096.40069	.0560	-.192
50092.34311	.4841	-.164	50093.42875	.4398	-.283	50096.40162	.0569	-.208
50092.34868	.4890	-.173	50093.42976	.4407	-.275	50096.40195	.0571	-.209
50092.34966	.4898	-.166	50093.43011	.4410	-.274	50096.40592	.0606	-.233
50092.35396	.4936	-.172	50093.43746	.4474	-.269	50096.40685	.0615	-.262
50092.35558	.4950	-.179	50093.43849	.4484	-.252	50096.41034	.0645	-.268
50092.35591	.4953	-.163	50093.44438	.4535	-.248	50096.41069	.0648	-.251
50092.35704	.4963	-.152	50093.44542	.4545	-.235	50096.41104	.0651	-.283
50092.36112	.4999	-.146	50093.44912	.4577	-.237	50096.41229	.0662	-.276
50092.36214	.5008	-.137	50093.45000	.4585	-.246	50096.41621	.0697	-.290
50092.36645	.5046	-.169	50093.45413	.4621	-.251	50096.41866	.0718	-.321
50092.36738	.5054	-.187	50093.45512	.4630	-.226	50096.42262	.0753	-.309
50092.37247	.5099	-.196	50093.45934	.4667	-.236	50096.42359	.0762	-.303
50092.37358	.5109	-.166	50093.45965	.4670	-.218	50096.42721	.0794	-.324
50092.37888	.5156	-.183	50093.46385	.4707	-.211	50096.42812	.0802	-.305
50092.37990	.5164	-.191	50093.46485	.4716	-.219	50096.43238	.0839	-.314
50092.38539	.5213	-.199	50093.46515	.4718	-.213	50096.43333	.0848	-.325
50092.38629	.5221	-.175	50095.24138	.0355	-.044	50096.43804	.0889	-.336
50092.39173	.5269	-.182	50095.24237	.0363	-.057	50096.43839	.0892	-.400
50092.39208	.5272	-.211	50095.24756	.0409	-.086	50096.44259	.0929	-.317
50092.39322	.5282	-.194	50095.24867	.0419	-.078	50096.44359	.0938	-.320
50092.39351	.5284	-.187	50095.24953	.0426	-.100	50096.44804	.0977	-.325
50092.39850	.5328	-.221	50095.25519	.0476	-.102	50096.44905	.0986	-.322
50092.39955	.5337	-.224	50095.25551	.0479	-.115	50096.45334	.1024	-.319
50092.39987	.5340	-.223	50095.25656	.0488	-.145	50096.45422	.1032	-.333
50092.40463	.5382	-.225	50095.26365	.0551	-.207	50115.27225	.6691	-.322
50092.40559	.5391	-.232	50095.26401	.0554	-.207	50115.27353	.6702	-.334
50092.40946	.5425	-.241	50095.26495	.0562	-.201	50115.27927	.6752	-.328

J band observations of R CMa (Continued)

Hel. JD. -2400000.	Phase	Rel. mag.	Hel. JD. -2400000.	Phase	Rel. mag.	Hel. JD. -2400000.	Phase	Rel. mag.
50115.28027	.6761	-.346	50115.37895	.7630	-.348	50118.33926	.3690	-.331
50115.28062	.6764	-.354	50115.37992	.7638	-.343	50118.33958	.3693	-.332
50115.28413	.6795	-.335	50115.38405	.7675	-.364	50118.34055	.3701	-.365
50115.28533	.6806	-.327	50115.38509	.7684	-.361	50118.34491	.3740	-.342
50115.28565	.6809	-.330	50115.38551	.7688	-.355	50118.34524	.3743	-.335
50115.28904	.6838	-.336	50115.39287	.7752	-.359	50118.34613	.3751	-.332
50115.29013	.6848	-.344	50115.39385	.7761	-.354	50118.35071	.3791	-.356
50115.29390	.6881	-.356	50115.39955	.7811	-.378	50118.35101	.3794	-.363
50115.29485	.6890	-.349	50115.40084	.7823	-.356	50118.35195	.3802	-.339
50115.30036	.6938	-.340	50118.23080	.2735	-.338	50118.35725	.3848	-.360
50115.30136	.6947	-.343	50118.23169	.2743	-.345	50118.35816	.3856	-.345
50115.30503	.6979	-.358	50118.23671	.2787	-.387	50118.35901	.3864	-.339
50115.30600	.6988	-.334	50118.23762	.2795	-.379	50118.35932	.3867	-.335
50115.30933	.7017	-.326	50118.23792	.2798	-.375	50118.36409	.3909	-.322
50115.31030	.7026	-.334	50118.24326	.2845	-.371	50118.36439	.3911	-.343
50115.31465	.7064	-.338	50118.24415	.2853	-.347	50118.36544	.3921	-.366
50115.31564	.7073	-.333	50118.24978	.2902	-.331	50118.36573	.3923	-.366
50115.31965	.7108	-.335	50118.25232	.2925	-.368	50118.36941	.3956	-.342
50115.32062	.7116	-.352	50118.25262	.2927	-.344	50118.36974	.3958	-.356
50115.32462	.7152	-.350	50118.25672	.2963	-.384	50118.37098	.3969	-.353
50115.32567	.7161	-.350	50118.25761	.2971	-.404	50118.37550	.4009	-.343
50115.33118	.7209	-.338	50118.25791	.2974	-.410	50118.37585	.4012	-.336
50115.33224	.7219	-.340	50118.26531	.3039	-.346	50118.37680	.4021	-.357
50115.33592	.7251	-.345	50118.27535	.3127	-.380	50118.38246	.4070	-.328
50115.33702	.7261	-.333	50118.27625	.3135	-.423	50118.38277	.4073	-.333
50115.34087	.7295	-.350	50118.27656	.3138	-.413	50118.38372	.4081	-.349
50115.34189	.7304	-.363	50118.28031	.3171	-.355	50118.38828	.4122	-.333
50115.34527	.7333	-.364	50118.28180	.3184	-.366	50118.38923	.4130	-.366
50115.34629	.7342	-.344	50118.28281	.3193	-.382	50118.38953	.4133	-.378
50115.34977	.7373	-.344	50118.29037	.3260	-.349	50118.39372	.4169	-.368
50115.35080	.7382	-.331	50118.29148	.3269	-.361	50118.39403	.4172	-.390
50115.35720	.7438	-.341	50118.30121	.3355	-.396	50118.39433	.4175	-.388
50115.35821	.7447	-.345	50118.30314	.3372	-.352	50416.50685	.8521	-.334
50115.36168	.7478	-.352	50118.30497	.3388	-.376	50416.50735	.8525	-.329
50115.36258	.7486	-.354	50118.32700	.3582	-.363	50416.50873	.8537	-.335
50115.36295	.7489	-.346	50118.32739	.3586	-.372	50416.51293	.8574	-.340
50115.36762	.7530	-.343	50118.32833	.3594	-.364	50416.51404	.8584	-.328
50115.36862	.7539	-.335	50118.33421	.3646	-.358			
50115.37300	.7577	-.335	50118.33514	.3654	-.324			
50115.37406	.7587	-.342	50118.33896	.3687	-.327			

Appendix : 4

K band observations of R CMa (R CMa - BD-15^o 1734)

Hel. JD. -2400000.	Phase	Rel. mag.	Hel. JD. -2400000.	Phase	Rel. mag.	Hel. JD. -2400000.	Phase	Rel. mag.
49763.14819	.6870	-.585	49764.21957	.6302	-.552	49764.33707	.7336	-.588
49763.14856	.6874	-.594	49764.22035	.6309	-.560	49764.34238	.7383	-.567
49763.14942	.6881	-.577	49764.22058	.6311	-.559	49764.34378	.7395	-.568
49763.14976	.6884	-.583	49764.22132	.6317	-.556	49764.34453	.7402	-.566
49763.15062	.6892	-.593	49764.22688	.6366	-.554	49764.34514	.7407	-.596
49763.15103	.6895	-.604	49764.22753	.6372	-.562	49764.34538	.7409	-.596
49763.15130	.6898	-.611	49764.22847	.6380	-.530	49766.23259	.4023	-.549
49763.15169	.6901	-.614	49764.22882	.6383	-.531	49766.23282	.4025	-.569
49763.18837	.7224	-.531	49764.22963	.6390	-.521	49766.23376	.4033	-.561
49763.18878	.7228	-.557	49764.22986	.6392	-.537	49766.23464	.4041	-.575
49763.18908	.7230	-.580	49764.23490	.6437	-.557	49766.23509	.4045	-.587
49763.19030	.7241	-.566	49764.23512	.6439	-.539	49766.23532	.4047	-.592
49763.19082	.7245	-.548	49764.23611	.6447	-.553	49766.24165	.4103	-.545
49763.19221	.7258	-.519	49764.23736	.6458	-.557	49766.24267	.4112	-.575
49763.20219	.7346	-.558	49764.23757	.6460	-.563	49766.24287	.4113	-.570
49763.20269	.7350	-.553	49764.24477	.6524	-.558	49766.24374	.4121	-.548
49763.20346	.7357	-.552	49764.24500	.6526	-.536	49766.24406	.4124	-.573
49763.20480	.7369	-.549	49764.24523	.6528	-.545	49766.24428	.4126	-.574
49763.20574	.7377	-.575	49764.24656	.6539	-.563	49766.25445	.4215	-.514
49763.20621	.7381	-.571	49764.24776	.6550	-.582	49766.25585	.4228	-.511
49763.20650	.7384	-.561	49764.24798	.6552	-.581	49766.25665	.4235	-.534
49763.25039	.7770	-.561	49764.25276	.6594	-.586	49766.25686	.4236	-.528
49763.25062	.7772	-.566	49764.25349	.6600	-.587	49766.26176	.4280	-.523
49763.25091	.7774	-.533	49764.25370	.6602	-.562	49766.26302	.4291	-.536
49763.25981	.7853	-.560	49764.25460	.6610	-.542	49766.26409	.4300	-.543
49763.26059	.7860	-.530	49764.25524	.6616	-.548	49766.26431	.4302	-.542
49763.26151	.7868	-.533	49764.26284	.6683	-.585	49766.26998	.4352	-.520
49763.26310	.7882	-.526	49764.26384	.6692	-.597	49766.27074	.4359	-.502
49763.26331	.7884	-.532	49764.26473	.6699	-.583	49766.27229	.4372	-.489
49763.26350	.7885	-.528	49764.26494	.6701	-.571	49766.27248	.4374	-.480
49763.26371	.7887	-.535	49764.27110	.6755	-.525	49766.27725	.4416	-.503
49763.27039	.7946	-.574	49764.27176	.6761	-.515	49766.27870	.4429	-.534
49763.27084	.7950	-.561	49764.27263	.6769	-.515	49766.27890	.4430	-.524
49763.27194	.7960	-.558	49764.27558	.6795	-.606	49766.27970	.4438	-.472
49763.27223	.7962	-.560	49764.27597	.6798	-.575	49766.28858	.4516	-.449
49763.27324	.7971	-.566	49764.27823	.6818	-.560	49766.29003	.4528	-.435
49763.27348	.7973	-.537	49764.28363	.6866	-.590	49766.29840	.4602	-.438
49763.27435	.7981	-.538	49764.28448	.6873	-.599	49766.29980	.4614	-.451
49763.27520	.7988	-.559	49764.28469	.6875	-.581	49766.30048	.4620	-.448
49763.27541	.7990	-.553	49764.28611	.6888	-.550	49766.30072	.4623	-.432
49763.28202	.8048	-.572	49764.28656	.6892	-.597	49766.30106	.4626	-.441
49763.28335	.8060	-.566	49764.28682	.6894	-.589	49766.30609	.4670	-.386
49763.28356	.8062	-.552	49764.30171	.7025	-.600	49766.30706	.4678	-.345
49763.28558	.8080	-.546	49764.30260	.7033	-.612	49766.30731	.4681	-.409
49763.28646	.8087	-.561	49764.30330	.7039	-.566	49766.30753	.4683	-.419
49763.31082	.8302	-.537	49764.30399	.7045	-.554	50032.49119	.7952	-.517
49763.31171	.8310	-.513	49764.30506	.7054	-.592	50032.49189	.7958	-.516
49763.31194	.8312	-.500	49764.30557	.7059	-.581	50032.49641	.7998	-.560
49763.31272	.8319	-.508	49764.30594	.7062	-.591	50032.49984	.8028	-.571
49763.31307	.8322	-.500	49764.31142	.7110	-.550	50032.50049	.8034	-.548
49763.31988	.8382	-.501	49764.31214	.7117	-.545	50032.50880	.8107	-.548
49763.32085	.8390	-.504	49764.31283	.7123	-.525	50032.50953	.8113	-.566
49764.20579	.6180	-.585	49764.31322	.7126	-.545	50032.51286	.8143	-.543
49764.20602	.6183	-.595	49764.31435	.7136	-.546	50032.51355	.8149	-.550
49764.20688	.6190	-.597	49764.32385	.7220	-.613	50036.49450	.3194	-.539
49764.20828	.6202	-.596	49764.32481	.7228	-.510	50036.49526	.3201	-.545
49764.20985	.6216	-.555	49764.32768	.7254	-.527	50036.49959	.3239	-.543
49764.21074	.6224	-.558	49764.32790	.7255	-.511	50036.50038	.3246	-.554
49764.21099	.6226	-.563	49764.33662	.7332	-.583	50036.50513	.3287	-.604
49764.21924	.6299	-.559	49764.33685	.7334	-.567	50036.50609	.3296	-.551

K band observations of R CMa (Continued)

Hel. JD. -2400000.	Phase	Rel. mag.	Hel. JD. -2400000.	Phase	Rel. mag.	Hel. JD. -2400000.	Phase	Rel. mag.
50036.50638	.3298	-.564	50061.35307	.2029	-.581	50116.17723	.4657	-.363
50036.51069	.3336	-.565	50061.35458	.2042	-.581	50116.18496	.4725	-.341
50036.51136	.3342	-.551	50061.35846	.2076	-.566	50116.18590	.4734	-.353
50036.51467	.3371	-.543	50061.35866	.2078	-.570	50116.19059	.4775	-.343
50036.52327	.3447	-.556	50061.35935	.2084	-.544	50116.19155	.4783	-.316
50036.52402	.3454	-.555	50061.35960	.2086	-.563	50116.19774	.4838	-.307
50055.47889	.0317	-.319	50061.36335	.2119	-.584	50116.19866	.4846	-.320
50055.47960	.0324	-.314	50061.36706	.2152	-.555	50116.20508	.4902	-.303
50055.48276	.0351	-.376	50061.36788	.2159	-.553	50116.20608	.4911	-.323
50055.48345	.0358	-.250	50061.37182	.2194	-.598	50116.21657	.5004	-.264
50055.48687	.0388	-.339	50061.37252	.2200	-.586	50116.22115	.5044	-.272
50055.49018	.0417	-.358	50061.37269	.2202	-.597	50116.22585	.5085	-.280
50055.49097	.0424	-.334	50061.37619	.2233	-.602	50116.22677	.5093	-.274
50055.50029	.0506	-.405	50061.37680	.2238	-.564	50116.23099	.5131	-.268
50055.50159	.0517	-.423	50061.38542	.2314	-.582	50116.23201	.5139	-.274
50056.41110	.8524	-.531	50061.38949	.2350	-.570	50116.23867	.5198	-.340
50056.41192	.8531	-.496	50061.39034	.2357	-.561	50116.24309	.5237	-.332
50056.42398	.8637	-.535	50061.39722	.2418	-.558	50116.24408	.5246	-.355
50056.42465	.8643	-.519	50061.39793	.2424	-.553	50116.24827	.5283	-.362
50056.42836	.8676	-.515	50061.47107	.3068	-.551	50116.25367	.5330	-.360
50056.43315	.8718	-.530	50061.47194	.3075	-.551	50116.25460	.5338	-.363
50056.43384	.8724	-.515	50061.47637	.3114	-.581	50116.25786	.5367	-.398
50056.43727	.8754	-.555	50061.47708	.3121	-.597	50116.25882	.5376	-.407
50056.43816	.8762	-.543	50061.48113	.3156	-.592	50116.26246	.5408	-.425
50056.44154	.8792	-.553	50061.48528	.3193	-.533	50116.26352	.5417	-.419
50056.44230	.8798	-.537	50061.48625	.3201	-.598	50116.26746	.5452	-.421
50056.45021	.8868	-.533	50061.48997	.3234	-.591	50116.27215	.5493	-.430
50056.45404	.8902	-.544	50061.49791	.3304	-.554	50116.27249	.5496	-.442
50056.46042	.8958	-.522	50061.50158	.3336	-.550	50116.27347	.5505	-.444
50056.46106	.8964	-.529	50061.50200	.3340	-.536	50116.27890	.5552	-.456
50056.46459	.8995	-.535	50061.50539	.3370	-.555	50116.28328	.5591	-.489
50056.47434	.9080	-.485	50061.50846	.3397	-.529	50116.28892	.5641	-.495
50056.47905	.9122	-.502	50114.32854	.8383	-.533	50116.29004	.5650	-.525
50056.48314	.9158	-.500	50114.33493	.8439	-.515	50116.29619	.5705	-.516
50056.48395	.9165	-.489	50114.33607	.8449	-.532	50116.29998	.5738	-.539
50056.48729	.9195	-.488	50114.34124	.8495	-.544	50116.30094	.5746	-.525
50056.48794	.9200	-.488	50114.34233	.8504	-.521	50116.30730	.5802	-.528
50056.49144	.9231	-.516	50114.34660	.8542	-.540	50116.30824	.5811	-.547
50056.49221	.9238	-.494	50114.34758	.8551	-.529	50116.31195	.5843	-.562
50056.52270	.9506	-.403	50114.35423	.8609	-.546	50116.31678	.5886	-.551
50056.52351	.9513	-.391	50114.35524	.8618	-.536	50116.31786	.5895	-.528
50056.52666	.9541	-.370	50114.36164	.8674	-.561	50116.32141	.5927	-.540
50056.52729	.9547	-.387	50114.36274	.8684	-.527	50116.32236	.5935	-.533
50056.53109	.9580	-.258	50114.36831	.8733	-.530	50116.33134	.6014	-.574
50061.29958	.1558	-.573	50114.37436	.8786	-.515	50116.33618	.6057	-.579
50061.29995	.1561	-.578	50114.37558	.8797	-.508	50116.33721	.6066	-.562
50061.30119	.1572	-.550	50114.38116	.8846	-.519	50116.34110	.6100	-.582
50061.30143	.1574	-.545	50114.38593	.8888	-.519	50116.34213	.6109	-.572
50061.32224	.1758	-.562	50114.38700	.8898	-.542	50116.35304	.6205	-.520
50061.32360	.1770	-.560	50114.39255	.8946	-.541	50116.35782	.6247	-.514
50061.32845	.1812	-.554	50114.39369	.8956	-.542	50116.36804	.6337	-.557
50061.33091	.1834	-.564	50114.39890	.9002	-.564	50116.36902	.6346	-.540
50061.33547	.1874	-.525	50114.39987	.9011	-.581	50116.37380	.6388	-.547
50061.33652	.1883	-.561	50114.40470	.9053	-.565	50116.37491	.6397	-.541
50061.33670	.1885	-.576	50114.40572	.9062	-.531	50116.37530	.6401	-.539
50061.34031	.1917	-.578	50114.40976	.9098	-.548	50116.37864	.6430	-.529
50061.34424	.1951	-.580	50114.41071	.9106	-.518	50116.37969	.6440	-.529
50061.34499	.1958	-.581	50116.17092	.4602	-.422	50116.38403	.6478	-.566
50061.35223	.2022	-.546	50116.17181	.4610	-.422	50117.32273	.4741	-.382
50061.35247	.2024	-.574	50116.17636	.4650	-.398	50117.32364	.4749	-.361

K band observations of R CMa (Continued)

Hel. JD. -2400000.	Phase	Rel. mag.	Hel. JD. -2400000.	Phase	Rel. mag.	Hel. JD. -2400000.	Phase	Rel. mag.
50117.32796	.4787	-.336	50141.18782	.4831	-.330	50145.13728	.9599	-.271
50117.33283	.4830	-.340	50141.18814	.4833	-.312	50145.13824	.9607	-.338
50117.33413	.4842	-.333	50141.18908	.4842	-.323	50145.14256	.9645	-.285
50117.33451	.4845	-.340	50141.19329	.4879	-.337	50145.14326	.9651	-.270
50117.33923	.4887	-.303	50141.19360	.4881	-.331	50145.14422	.9660	-.259
50117.34458	.4934	-.292	50141.19401	.4885	-.325	50145.14453	.9662	-.228
50117.34543	.4941	-.287	50141.19901	.4929	-.304	50145.14912	.9703	-.256
50117.34898	.4972	-.270	50141.19992	.4937	-.299	50145.14957	.9707	-.231
50117.35339	.5011	-.293	50141.20316	.4966	-.296	50145.15148	.9724	-.235
50117.35428	.5019	-.278	50141.20347	.4968	-.305	50145.15180	.9726	-.204
50117.35775	.5050	-.281	50141.20870	.5014	-.306	50145.15282	.9735	-.191
50117.36016	.5071	-.291	50141.21006	.5026	-.305	50145.15780	.9779	-.235
50117.36348	.5100	-.280	50141.21437	.5064	-.295	50145.15816	.9782	-.176
50117.36905	.5149	-.296	50141.21536	.5073	-.305	50145.15914	.9791	-.129
50117.36999	.5157	-.323	50141.22030	.5117	-.291	50145.16316	.9826	-.145
50117.37317	.5185	-.334	50141.22066	.5120	-.301	50145.16346	.9829	-.129
50117.37406	.5193	-.324	50141.22169	.5129	-.309	50145.16442	.9837	-.132
50117.37845	.5232	-.330	50141.24097	.5299	-.360	50145.16801	.9869	-.144
50117.38195	.5263	-.348	50141.24128	.5301	-.348	50145.16831	.9872	-.117
50117.38606	.5299	-.378	50141.24215	.5309	-.346	50145.16916	.9879	-.101
50117.38695	.5307	-.375	50141.24725	.5354	-.382	50145.16946	.9882	-.060
50119.12454	.0603	-.407	50141.24797	.5360	-.387	50145.17370	.9919	-.053
50119.12554	.0612	-.435	50141.24886	.5368	-.369	50145.17464	.9927	-.054
50119.12586	.0615	-.425	50141.25638	.5434	-.370	50145.17864	.9963	-.080
50119.12621	.0618	-.435	50141.25724	.5442	-.380	50145.17894	.9965	-.091
50119.13094	.0659	-.459	50141.25813	.5450	-.390	50145.17991	.9974	-.158
50119.13210	.0670	-.480	50141.25841	.5452	-.371	50145.18022	.9977	-.101
50119.13869	.0728	-.470	50141.26931	.5548	-.465	50145.18414	.0011	-.133
50119.13901	.0730	-.508	50141.27550	.5603	-.485	50145.18444	.0014	-.127
50119.14013	.0740	-.516	50141.27584	.5605	-.470	50145.18976	.0061	-.145
50119.14046	.0743	-.502	50141.27690	.5615	-.463	50145.19008	.0063	-.111
50119.14415	.0776	-.493	50141.28151	.5655	-.515	50145.19101	.0072	-.110
50119.14446	.0778	-.496	50141.28272	.5666	-.495	50145.19479	.0105	-.084
50119.14545	.0787	-.472	50141.28730	.5706	-.495	50145.19511	.0108	-.068
50119.14969	.0824	-.523	50141.28762	.5709	-.490	50145.19611	.0116	-.156
50119.15003	.0827	-.515	50141.28864	.5718	-.512	50145.20263	.0174	-.103
50119.15104	.0836	-.505	50141.29341	.5760	-.533	50145.20122	.0161	-.153
50119.15138	.0839	-.496	50141.29371	.5763	-.536	50145.20292	.0176	-.095
50119.15499	.0871	-.508	50141.29473	.5772	-.508	50145.20377	.0184	-.136
50119.15532	.0874	-.503	50141.29509	.5775	-.513	50145.20407	.0186	-.134
50119.15633	.0883	-.507	50145.10587	.9322	-.421	50145.20891	.0229	-.131
50119.16488	.0958	-.513	50145.10617	.9325	-.417	50145.20922	.0232	-.149
50119.17034	.1006	-.495	50145.10721	.9334	-.462	50145.21013	.0240	-.230
50119.17069	.1009	-.512	50145.10753	.9337	-.466	50145.21043	.0243	-.199
50119.17458	.1044	-.539	50145.11167	.9373	-.424	50145.21431	.0277	-.250
50119.17489	.1046	-.529	50145.11268	.9382	-.421	50145.21463	.0280	-.254
50119.17583	.1055	-.558	50145.11300	.9385	-.431	50145.21565	.0288	-.222
50119.17619	.1058	-.563	50145.11692	.9419	-.419	50145.21991	.0326	-.309
50119.17977	.1089	-.570	50145.11722	.9422	-.414	50145.22024	.0329	-.315
50119.18009	.1092	-.569	50145.11816	.9430	-.408	50145.22123	.0338	-.344
50119.18102	.1100	-.569	50145.12180	.9462	-.380	50145.22518	.0372	-.325
50119.18134	.1103	-.563	50145.12275	.9471	-.410	50145.22548	.0375	-.317
50119.18563	.1141	-.520	50145.12307	.9473	-.404	50145.22735	.0391	-.311
50119.18598	.1144	-.522	50145.12717	.9510	-.397	50145.22776	.0395	-.314
50119.18691	.1152	-.516	50145.12750	.9512	-.371	50145.23121	.0425	-.314
50119.19078	.1186	-.506	50145.12841	.9520	-.358	50145.23152	.0428	-.317
50119.19114	.1189	-.494	50145.13208	.9553	-.349	50145.23249	.0437	-.330
50141.18113	.4772	-.312	50145.13238	.9555	-.299	50145.23279	.0439	-.336
50141.18143	.4774	-.332	50145.13342	.9565	-.329	50145.23624	.0470	-.368
50141.18237	.4783	-.312	50145.13680	.9594	-.314	50145.23657	.0473	-.363

K band observations of R CMa (Continued)

Hel. JD. -2400000.	Phase	Rel. mag.	Hel. JD. -2400000.	Phase	Rel. mag.	Hel. JD. -2400000.	Phase	Rel. mag.
50145.23746	.0480	-.345	50154.10095	.8508	-.561	50154.23127	.9655	-.233
50145.24152	.0516	-.434	50154.10191	.8516	-.561	50154.23156	.9657	-.253
50145.24186	.0519	-.423	50154.10221	.8519	-.543	50154.23247	.9665	-.240
50145.24286	.0528	-.457	50154.10777	.8568	-.517	50154.23580	.9695	-.248
50145.24316	.0531	-.496	50154.10868	.8576	-.520	50154.23609	.9697	-.196
50145.24794	.0573	-.446	50154.10898	.8578	-.511	50154.23706	.9706	-.211
50145.24827	.0576	-.459	50154.11352	.8618	-.510	50154.24090	.9740	-.176
50145.25203	.0609	-.424	50154.11385	.8621	-.534	50154.24118	.9742	-.188
50145.25321	.0619	-.444	50154.11491	.8630	-.528	50154.24209	.9750	-.182
50145.25798	.0661	-.418	50154.11927	.8669	-.565	50154.24589	.9784	-.207
50145.26207	.0697	-.486	50154.11957	.8671	-.541	50154.24830	.9805	-.176
50145.26240	.0700	-.433	50154.12052	.8680	-.550	50154.24858	.9807	-.162
50145.26777	.0747	-.528	50154.12116	.8685	-.546	50154.24960	.9816	-.147
50145.26810	.0750	-.500	50154.12652	.8733	-.550	50154.25334	.9849	-.157
50145.27237	.0788	-.539	50154.12684	.8735	-.544	50154.25364	.9852	-.154
50145.27705	.0829	-.549	50154.12772	.8743	-.556	50154.25459	.9860	-.104
50145.27734	.0832	-.537	50154.13472	.8805	-.503	50154.25910	.9900	-.120
50145.27832	.0840	-.539	50154.13508	.8808	-.511	50154.25949	.9903	-.110
50148.25864	.7077	-.617	50154.13612	.8817	-.539	50154.26042	.9911	-.079
50148.25950	.7084	-.581	50154.13641	.8820	-.509	50154.26460	.9948	-.071
50148.26042	.7092	-.575	50154.14567	.8901	-.534	50154.26492	.9951	-.082
50148.26626	.7144	-.565	50154.14603	.8904	-.526	50154.26601	.9961	-.069
50148.26657	.7146	-.555	50154.14689	.8912	-.551	50154.27621	.0050	-.058
50148.26862	.7164	-.516	50154.14720	.8915	-.548	50154.27718	.0059	-.075
50148.27396	.7211	-.521	50154.15177	.8955	-.549	50154.27747	.0061	-.089
50148.27426	.7214	-.522	50154.15294	.8965	-.520	50154.28273	.0108	-.172
50148.27514	.7222	-.575	50154.15325	.8968	-.516	50154.29051	.0176	-.190
50148.28913	.7345	-.565	50154.15913	.9020	-.548	50154.29081	.0179	-.239
50148.28942	.7347	-.536	50154.16295	.9053	-.563	50154.29699	.0233	-.276
50148.29041	.7356	-.607	50154.16409	.9063	-.517	50154.29810	.0243	-.292
50148.29715	.7416	-.572	50154.16960	.9112	-.539	50412.50775	.3316	-.565
50148.29863	.7429	-.544	50154.16996	.9115	-.536	50412.50938	.3330	-.557
50148.30382	.7474	-.591	50154.17086	.9123	-.554	50412.51567	.3385	-.554
50148.30410	.7477	-.591	50154.17514	.9161	-.551	50412.51582	.3387	-.553
50148.30607	.7494	-.580	50154.17635	.9171	-.546	50412.51687	.3396	-.542
50148.30637	.7497	-.548	50154.18099	.9212	-.495	50412.51705	.3398	-.532
50153.25657	.1074	-.513	50154.18132	.9215	-.493	50412.52245	.3445	-.547
50153.25761	.1084	-.527	50154.18233	.9224	-.497	50412.52261	.3446	-.553
50153.25795	.1086	-.574	50154.18695	.9265	-.472	50412.52423	.3461	-.553
50153.26139	.1117	-.582	50154.18729	.9268	-.474	50412.52440	.3462	-.547
50153.26173	.1120	-.524	50154.18820	.9276	-.454	50413.45828	.1683	-.529
50153.26921	.1186	-.517	50154.19675	.9351	-.478	50413.45850	.1685	-.530
50153.26981	.1191	-.516	50154.19707	.9354	-.461	50413.45948	.1694	-.574
50153.27068	.1199	-.563	50154.19789	.9361	-.455	50413.45964	.1695	-.574
50153.27511	.1238	-.572	50154.20181	.9395	-.445	50413.46484	.1741	-.535
50153.27613	.1247	-.531	50154.20210	.9398	-.428	50413.48586	.1926	-.562
50153.28114	.1291	-.516	50154.20299	.9406	-.450	50413.48604	.1928	-.573
50153.28247	.1302	-.533	50154.20719	.9443	-.463	50413.48680	.1934	-.567
50153.28280	.1305	-.560	50154.20747	.9445	-.444	50413.48696	.1936	-.576
50154.08173	.8338	-.503	50154.20843	.9454	-.412	50413.49350	.1993	-.563
50154.08218	.8342	-.496	50154.21386	.9502	-.400	50413.49445	.2002	-.569
50154.08312	.8351	-.521	50154.21709	.9530	-.369	50413.49567	.2012	-.587
50154.08341	.8353	-.504	50154.21739	.9533	-.342	50413.49585	.2014	-.578
50154.08819	.8395	-.525	50154.21818	.9540	-.362	50413.50155	.2064	-.571
50154.08996	.8411	-.527	50154.22151	.9569	-.315	50413.50185	.2067	-.596
50154.09030	.8414	-.576	50154.22185	.9572	-.299	50413.50297	.2077	-.567
50154.09481	.8453	-.558	50154.22276	.9580	-.309	50413.50320	.2079	-.564
50154.09512	.8456	-.561	50154.22619	.9610	-.277	50413.50867	.2127	-.576
50154.09607	.8465	-.543	50154.22647	.9613	-.287	50413.50883	.2128	-.570
50154.10066	.8505	-.568	50154.22742	.9621	-.262	50413.50966	.2136	-.577

K band observations of R CMa (Continued)

Hel. JD. -2400000.	Phase	Rel. mag.	Hel. JD. -2400000.	Phase	Rel. mag.	Hel. JD. -2400000.	Phase	Rel. mag.
50413.50984	.2137	-.568	50423.43968	.9552	-.384	50438.44438	.1641	-.539
50413.51490	.2182	-.568	50423.44019	.9556	-.377	50438.44600	.1655	-.559
50413.51568	.2189	-.576	50423.44427	.9592	-.346	50438.44630	.1658	-.550
50413.51659	.2197	-.575	50423.45119	.9653	-.276	50438.45134	.1702	-.574
50413.51675	.2198	-.578	50423.45165	.9657	-.262	50438.45170	.1706	-.564
50415.50422	.9694	-.242	50423.45296	.9669	-.267	50438.45495	.1734	-.567
50415.50453	.9697	-.216	50423.45328	.9671	-.264	50438.46202	.1796	-.575
50415.50598	.9710	-.231	50423.46003	.9731	-.197	50438.46344	.1809	-.576
50415.50616	.9711	-.203	50423.46056	.9736	-.208	50438.46507	.1823	-.553
50415.51774	.9813	-.191	50423.46156	.9744	-.213	50438.46541	.1826	-.550
50415.51848	.9820	-.190	50423.46187	.9747	-.212	50438.47318	.1895	-.548
50415.51935	.9827	-.195	50423.46700	.9792	-.151	50438.47355	.1898	-.552
50415.51953	.9829	-.194	50423.46730	.9795	-.179	50438.47570	.1917	-.544
50417.47489	.7042	-.565	50423.46839	.9804	-.140	50438.47604	.1920	-.551
50417.47508	.7044	-.564	50423.46874	.9807	-.146	50438.48130	.1966	-.554
50417.47589	.7051	-.587	50423.47443	.9858	-.148	50438.48210	.1973	-.563
50417.47607	.7053	-.594	50423.47475	.9860	-.149	50438.48463	.1995	-.570
50417.48136	.7099	-.588	50423.47788	.9888	-.124	50438.49092	.2051	-.571
50417.48165	.7102	-.581	50423.47835	.9892	-.123	50438.49262	.2066	-.568
50417.48252	.7110	-.589	50423.48356	.9938	-.105	50438.49294	.2069	-.568
50417.48270	.7111	-.600	50423.48436	.9945	-.096	50439.25075	.8740	-.562
50417.48726	.7151	-.593	50423.48570	.9957	-.082	50439.25198	.8751	-.554
50417.48743	.7153	-.593	50423.48607	.9960	-.075	50439.25923	.8814	-.541
50417.48830	.7160	-.594	50423.49059	.0000	-.079	50439.26033	.8824	-.525
50417.48846	.7162	-.593	50423.49121	.0005	-.108	50439.26064	.8827	-.521
50423.34653	.8732	-.553	50423.49153	.0008	-.115	50439.26780	.8890	-.529
50423.34697	.8736	-.565	50423.50643	.0139	-.143	50439.27751	.8975	-.519
50423.34804	.8745	-.567	50423.50684	.0143	-.140	50439.27785	.8978	-.510
50423.34853	.8749	-.576	50423.50720	.0146	-.149	50439.27885	.8987	-.516
50423.35469	.8803	-.577	50423.50846	.0157	-.166	50439.28375	.9030	-.523
50423.35499	.8806	-.572	50423.50902	.0162	-.176	50439.28551	.9046	-.558
50423.35724	.8826	-.549	50423.51371	.0203	-.209	50439.28679	.9057	-.550
50423.35755	.8829	-.541	50423.51402	.0206	-.212	50439.29361	.9117	-.571
50423.36348	.8881	-.547	50423.51521	.0217	-.212	50439.29508	.9130	-.546
50423.36468	.8891	-.553	50423.51581	.0222	-.213	50439.30284	.9198	-.542
50423.36614	.8904	-.535	50438.39232	.1183	-.501	50439.30314	.9201	-.529
50423.36645	.8907	-.539	50438.39269	.1186	-.513	50439.30398	.9208	-.536
50423.37422	.8975	-.548	50438.39389	.1197	-.534	50439.30439	.9212	-.540
50423.37618	.8993	-.547	50438.39418	.1199	-.528	50439.31108	.9271	-.506
50423.37652	.8996	-.541	50438.40063	.1256	-.544	50439.31139	.9274	-.504
50423.38282	.9051	-.523	50438.40163	.1265	-.545	50439.31274	.9285	-.508
50423.38345	.9057	-.538	50438.40352	.1281	-.532	50439.31317	.9289	-.505
50423.39286	.9140	-.536	50438.40482	.1293	-.541	50439.32021	.9351	-.484
50423.39318	.9142	-.529	50438.41032	.1341	-.534	50439.32126	.9360	-.481
50423.39387	.9148	-.528	50438.41120	.1349	-.532	50439.32160	.9363	-.481
50423.39544	.9162	-.529	50438.41273	.1362	-.547	50439.34267	.9549	-.327
50423.39638	.9170	-.536	50438.41305	.1365	-.540	50439.34373	.9558	-.325
50423.40335	.9232	-.524	50438.41972	.1424	-.544	50439.34404	.9561	-.335
50423.40410	.9238	-.512	50438.42072	.1433	-.546	50439.34947	.9609	-.323
50423.40584	.9254	-.518	50438.42107	.1436	-.571	50439.35046	.9618	-.315
50423.40614	.9256	-.513	50438.42682	.1487	-.565	50439.35083	.9621	-.313
50423.40693	.9263	-.536	50438.42737	.1491	-.565	50439.35544	.9661	-.295
50423.41252	.9313	-.510	50438.42880	.1504	-.543	50439.35663	.9672	-.271
50423.41282	.9315	-.515	50438.42936	.1509	-.552	50439.35711	.9676	-.240
50423.41493	.9334	-.492	50438.43550	.1563	-.557	50439.35741	.9679	-.232
50423.41542	.9338	-.494	50438.43605	.1568	-.555	50439.36293	.9727	-.209
50423.43130	.9478	-.410	50438.43741	.1580	-.547	50439.36390	.9736	-.224
50423.43159	.9480	-.407	50438.43805	.1585	-.557	50439.36500	.9746	-.235
50423.43299	.9493	-.408	50438.44336	.1632	-.538	50439.37048	.9794	-.189
50423.43331	.9496	-.411	50438.44405	.1638	-.540	50439.37146	.9802	-.161

K band observations of R CMa (Continued)

Hel. JD. -2400000.	Phase	Rel. mag.	Hel. JD. -2400000.	Phase	Rel. mag.	Hel. JD. -2400000.	Phase	Rel. mag.
50439.37175	.9805	-.153	50439.43769	.0385	-.270	50511.18722	.2011	-.556
50439.37697	.9851	-.146	50439.44603	.0459	-.357	50511.19294	.2062	-.536
50439.37790	.9859	-.149	50439.44701	.0467	-.354	50511.19431	.2074	-.555
50439.37838	.9863	-.135	50439.44742	.0471	-.358	50511.19463	.2076	-.557
50439.38429	.9915	-.100	50439.45415	.0530	-.391	50511.19576	.2086	-.558
50439.38532	.9924	-.090	50439.45521	.0540	-.402	50511.20099	.2132	-.568
50439.39049	.9970	-.091	50439.46336	.0611	-.438	50511.20135	.2136	-.563
50439.39173	.9981	-.074	50439.46371	.0614	-.473	50511.20271	.2148	-.559
50439.39209	.9984	-.067	50439.46943	.0665	-.489	50511.20304	.2151	-.584
50439.39760	.0032	-.077	50439.46975	.0668	-.483	50511.20337	.2153	-.593
50439.39866	.0042	-.102	50439.47071	.0676	-.474	50511.20442	.2163	-.586
50439.39903	.0045	-.127	50439.47600	.0723	-.495	50511.20474	.2166	-.593
50439.40433	.0092	-.124	50439.47701	.0732	-.522	50511.20894	.2202	-.601
50439.40551	.0102	-.113	50439.48318	.0786	-.548	50511.20927	.2205	-.596
50439.40614	.0108	-.129	50439.48424	.0795	-.523	50511.21063	.2217	-.591
50439.41256	.0164	-.155	50511.17310	.1887	-.562	50511.21128	.2223	-.593
50439.41357	.0173	-.136	50511.17349	.1890	-.563	50511.21650	.2269	-.585
50439.41793	.0211	-.174	50511.17445	.1899	-.580	50511.21681	.2272	-.592
50439.41892	.0220	-.166	50511.17478	.1902	-.559	50511.22432	.2338	-.575
50439.42334	.0259	-.195	50511.17879	.1937	-.536	50511.22464	.2341	-.573
50439.42434	.0268	-.226	50511.18026	.1950	-.547	50511.22568	.2350	-.571
50439.42889	.0308	-.232	50511.18059	.1953	-.533	50511.22599	.2353	-.576
50439.42985	.0316	-.257	50511.18474	.1989	-.534			
50439.43620	.0372	-.255	50511.18507	.1992	-.538			
50439.43682	.0378	-.271	50511.18628	.2003	-.557			

References

1. Allen, C. W. 1973, *Astrophysical Quantities*, 3^{rd} Ed., The Athelone Press, London
2. Al Naimiy, H. M. 1978. *Astrophys. Space Sci.*, 53, 181
3. Arévalo, M. J. & Lázaro, C. 1990, *Astron. J.*, 99, 983.
4. Argenbright, D. V., Osborn W. & Hall, D. S. 1988, *Inf. Bull. Var. Stars*, No. 3224
5. Ashok N.M., Chandrasekhar T., Sam Ragland & Bhatt H.C. 1994, *Experm. Astron.*, 4, 177
6. Batten, A. H. , Fletcher, J. M. & Mann, P. J. 1978, *Pub. Dom. Ap. Obs.*, 15, 121
7. Beichman, C. A., Neguebauer, G., Habing, H. J., Clegg. P. E. & Chester, T. J. 1988, IRAS Catalogs & Atlases, Vol. 1. Explanatory Suppliment, NASA, Washington D. C. VI - 21
8. Bell, R. A., Eriksson, K., Gustafsson, B., & Nordlund, A. 1976, *Astron. Astrophys. Sup.*, 23, 37
9. *The Bright Star Catalogue* (1982), Dorrit Hoffleit and Carlos Jaschek, Yale Univ. Observatory, New Haven, Connecticut, USA.
10. Bruke, E.W. & Roland, W. W. 1965, *Astron. J.*, 71, 38
11. Budding, E. 1977, *Astrophys. Space Sci.*, 48, 207
12. Budding, E. 1989, *Space Sci. Rev.*, 50, 205
13. Budding, E., Chen, K. Y., Hudson, G., Hudson, R., Thomas, M. & Wood, F. B. 1994, *Experimental Astronomy*, 5, 189
14. Budding, E., Wood, F. B. & Chen, K. Y. 1992, *Inf. Bull. Var. Stars*, No. 3734.
15. Budding, E. & Zeilik, M. 1987, *Astrophys. J.*, 319, 827
16. Carbon, D., & Gingerich, O. 1969, in *Theory and Observation of Stellar Atmospheres*, edited by O. Gingerich (MIT University press, Cambridge), 377
17. Chambliss, C. R. 1976, *Publ. Astron. Soc. Pac.*, 88, 22
18. Chen, K. Y. & Reuning, G. 1966, *Astron. J.*, 71, 283
19. Claret, A., & Gimenez, A. 1992, *Astron. Astrophys*, 259, 227
20. Cohen, M., Schwartz, D. E., Chokshi, A. & Walker, R. G. 1987, *Astron. J.*, 93, 1199
21. Crawford, J. A. 1955, *Astrophys. J*, 121,71
22. De Loore, C. W.H. & Doom, C. 1992, *Structure and Evolution of Single and Binary Stars*, Kluwer Academic Publishers, Dordrecht, Netherlands
23. Diaz-Cordores, J., & Gimenez, A. 1992, *Astron. Astrophys*, 259, 227

24. Drake, S. A., Simon, T & Linsky, J. L. 1986, *Astron. J.*, 91, 1229
25. Duerbeck, H. W. & Hanel, A. 1979, *Astron. Astrophys. Suppl.*, 38, 155
26. Dugan, R. S. 1924, *Contrib. Princeton Univ. Obs.*, 6, 49
27. Dugan, R. S. & Wright F. W. 1939, *Contrib. Princeton Univ. Obs.*, 19, 34
28. Edalati, M. T., Khalesse, B. & Riazi, N. 1989, *Astrophys. Space Sci.*, 151,1
29. Elias, J. H., Frogel, J. A., Matthews, K., Neugebauer G., 1982, *Astron. J.*, 87,1029
30. Etzel, P. B. 1993, in *Light Curve Modeling of Eclipsing Binary Stars*, ed. E. F. Milone (Springer, New York), P.113
31. Fringant, A. M. 1956, *Contrib. Inst. Astron. Paris*, Ser. A., 216
32. Guinan, E. F. 1977, *Astron. J.*, 82, 51
33. Guinan, E. F. 1989, *Space Sci. Rev.*, 50, 35
34. Guinan, E. F. & Ianna, P. A. 1983, *Astron. J.*, 88, 126
35. Guiricin, G., Mardirossian, F. & Mezzetti, M. 1983, *Astrophys. J. Supp. Ser*, 52, 35
36. Hall, D. S. 1989, *Space Sci. Rev.*, 50, 219
37. Hall, D. S. & Neff, S. G. 1979, *Acta. Astr.*, 29, 641
38. Heckathorn, H. M. 1966, *Publ. Godsell Ons.*, No. 15
39. Hegedus, T. 1989, *Inf. Bull. Var. Stars*, 3381
40. Hegedus, T., Szatmáry, K. & Vinkó, J. 1992, *Astrophys. Space Sci.*, 187, 57
41. Herczeg, T. & Frieboes-Conde 1974, *Astron. Astrophys.*, 30, 259
42. Hill, G. 1979, *Publ. Dom. Astrophy. Obs.*, 15,297
43. *The Hipparcos Input Catalogue* 1992, ESA SP - 1136, ESA Publications Division, C/o ESTEC, Nordwijk, The Netherlands., Vol. 2
44. Hill, J. & Osborn, W. 1997, *Inf. Bull. Var. Stars*, 4502
45. Horak, H. G. 1952, *Astrophys. J.*, 115, 61
46. Huffer, C. M. 1955, *Astrophys. J.*, 121, 677
47. Huffer, C. M. & Kopal, Z. 1951, *Astrophys. J.*, 114, 297
48. Irwin, J. B. 1952, *Astrophys. J.*, 116,211
49. Johnson, H. L. 1966, *Ann. Rev. Astron. Astrophys.*, 4, 193
50. Kholopov, P. N. (Ed.) 1985, *The General Catalogue of Variable Stars*, 5^{th} Ed. Vol. 1, Mowcow, NAUKA
51. Kitamura, M. 1967, *Pub. Astr. Soc. Japan*, 19, 615
52. Kitamura, M. & Takahashi, C. 1962, *Pub. Astr. Soc. Japan*, 14, 44
53. Klinglesmith, D. A., & Sobieski, S. 1970, *Astron. J.*, 75, 175
54. Koch, R. H. 1960, *Astron. J.*, 65, 326

55. Koch, R. H., Olson, E. C. & Yoss, K. M. 1965, *Astrophys. J.*, 141, 955
56. Koornneef, J. (1983a), *Astron. Astrophys. Suppl. Ser.*, 51, 489
57. Koornneef, J. (1983b), *Astron. & Astrophys.*, 128, 84
58. Kopal, Z. (1955), *Ann. Astrophys.*, 18, 379
59. Kopal, Z. (1959) *Close Binary Systems*, Chapman & Hall, London
60. Kopal, Z. 1965, *Adv. Astron. Astrophys.* 3, 105
61. Kopal, Z. 1979, *Language of the Stars*, D. Reidel Publishing Co., Dordrecht, Holland
62. Kurucz, R. L. 1979, *Astrophys. J. Supp. Ser.*, 40, 1
63. Kwee, K. K. & van Woerden, H. 1956, *Bull. Astr. Inst. Neth.*, 12, 327
64. Lang, K. R. 1992, *Astrophysical Data: Planets & Stars*, Springer - Verlag, New York, Inc.
65. Lazaro, C., Martinez-Pais, I. G., Arevalo, M. J. & Antonopoulou, E. 1997, *Astron. J.*, 113, 1122
66. Linnell, A. P. 1984, *Astrophys. J. Supp. Ser.*, 54, 17
67. Linnell, A. P. 1989, *Astrophys. J.*, 342, 449
68. Longmore, A. J. & Jameson, R. F. 1975, *Mon. Not. Roy. Astr. Soc.*, 173, 271
69. Lucy, L. B. 1967, *Zs. f. Astrophys.*, 65, 89
70. Lucy, L. B. 1968, *Astrophys. J.*, 153, 877
71. Maxted, P. F. L., Hill, G. & Hilditch, R. W. 1994, *Astron. Astrophys.*, 282, 821
72. Manduka, A., Bell, R. A., & Gustafsson, B. 1977, *Astron. & Astrophys.*, 61, 809
73. McCluskey, G. E. Jr. 1993, *The Algol type Interacting Binaries* in *The Realm of Interacting Binary Stars, Kluwer Academic Publishers*, Dordrecht, Netherlands., Sahade, J, McCluskey, G. E. Jr. & Kondo, Y. (eds.), p. 39
74. McCluskey, G. E. Jr. & Kondo, Y. 1984, *Publ. Astron Soc. Pac.*, 96, 817
75. Mochnacki, S. W. & Doughty, N. A. 1972, *Mon. Not. Roy. Astr. Soc.*, 156, 51
76. Morris, D. H. & Mutel, R. L. 1988, *Astron. J.*, 95, 204
77. Mutel, R. L. & Morris, D. H. 1987, *Astron. J.*, 93, 1220
78. Narusawa, S. Y., Nakamura, Y. & Yamasaki, A. 1994, *Astron. J.*, 105, 1141
79. Narusawa, S. Y., Arai, K., Nagai, K., Ohmori, S., Fujii, M. & Yasuda, T. 1997, *Inf. Bull. Var. Stars*, 4502
80. Needham, J. D., Phillips, J. P., Selby, M. J., & Margo, C. S. 1980, *Astron. Astrophys.*, 83, 370

81. Nelson, B. & Davis, W. 1972, *Astrophys. J*, 174, 617
82. Neugebauer, G. & Lighton, R. B. 1969, *Two Micron Sky Survey: A Preliminary Catalog*
83. Olson, E. C. 1982, *Astrophys. J*, 259, 702
84. Pallavicini, R., Golub, L., Rosner, R., Vaiana, G. S., Ayres, T. & Linsky, J. L. 1981, *Astrophys. J*, 248, 279
85. Peters, G. J. 1989, *Space Sci. Rev.*, 50, 9
86. Popper, D. M. & Tomkin, J. 1984, *Astrophys. J*, 285,208
87. Pringle, J. E. & Wade, R. A. 1985, *Interacting Binary Stars*, Cambridge University Press, Cambridge, U.K.
88. Radhakrishnan, K. R., Sarma, M. B. K. & Abhyankar, K. D. 1984, . *Astrophys. Space Sci.*, 99, 229
89. Radhakrishnan, K. R., Sarma, M. B. K & Abhyankar, K. D. 1985, *Bull. Astron. Soc. India*, 13, 261
90. Riazi, N., Bagheri, M. R. & Faghihi, F. 1994, . *Astrophys. Space Sci.*, 211, 293
91. Richards, M. T. 1990, *Astrophys. J*, 350, 372
92. Richards, M. T., Albright, G. E. & Larissa, M. B. 1995, *Astrophys. J*, 438, L 103
93. Richards, M. T., Mochnacki, S. W. & Bolton, C. T. 1988, *Astron. J.*, 96, 326
94. Robinson, L. J. 1965, *Inf. Bull. Variable Stars* No. 112
95. Rucinski, S. M. 1969, *Acta. Astron.*, 19, 245
96. Robinson, L. J. 1967, *Inf. Bull. Variable Stars* No. 180
97. Russell, H. N. 1948, *Astrophys. J.*, 108, 388
98. Russell, H. N. & Merrill, J. E. 1952, *Princeton Contrib.* No. 26
99. Sahade, J. 1963, *Ann. Astrophys.*, 26, 80
100. Sam Ragland 1996, Ph. D. Thesis, *Photometric Studies in Infrared Astronomy*, Gujarat University, India
101. Sarma, M. B. K., Rao, P. V. & Abhyankar, K. D. 1996, *Astrophys. J.*, 458, 371
102. Sato, K. 1971, *Publ. Astron Soc. Japan*, 23, 335
103. Savage, B. D. & Mathis, J. S. 1979, *Ann. Rev. Astron. Astrophys.*, 17, 73
104. Schaller, G., Schaerer, D., Meynet, G. & Maeder, A. 1992, *Astronom. Astrophys. Supp. Ser.*, 96, 269
105. Schmitt, J. H. M. M., Collura, A., Sciortino, S., Vaiana, G. S., Harnden, F. R. Jr. & Rosner, R. 1990, *Astrophys. J.*, 365, 704
106. Scott, J. K. 1988, *Astron. J.*, 96, 337

107. Singh, K.P., Drake, S. A. & White, N. E. 1995, *Astrophys. J.*, 445, 840
108. Smak, J. 1961, *Acta. Astr.*, 11, 171
109. Smyth, M. J., Dow, M. J. & Napier, W. M. 1975, *Mon. Not. R. Astron. Soc.*, 172, 235
110. Struve, O. & Smith, B. 1950, *Astrophys. J.*, 111, 27
111. Szafraniec, R. 1960, *Acta Astr.*, 10, 99
112. Tomkin, J. 1978, *Astrophys. J.*, 221, 608
113. Tomkin, J. 1979, *Astrophys. J.*, 231, 495
114. Tomkin, J. 1981, *Astrophys. J.*, 244, 546
115. Tomkin, J. 1985, *Astrophys. J.*, 297, 250
116. Tomkin, J. & Lambert, D. L. 1978, *Astrophys. J.*, L119
117. Umana, G., Catalano, S. & Rodono, M. 1991, *Astron.Astrophys.* 249, 217
118. Umana, G., Trigilio, C., Hjellming, R. M., Catalano, S. & Rodono, M. 1993, *Astron. & Astrophys.*, 267, 126
119. Van Hamme, W. 1993, *Astron. J.*, 106, 1096
120. Van Hamme, W. & Wilson, R. E. 1986, *Astron J.*, 92, 1168
121. Van Hamme, W. & Wilson, R. E. 1990, *Astron J.*, 100, 1981
122. Van Hamme, W. & Wilson, R. E. 1993, *Mon. Not. R. Astron. Soc.*, 262, 220
123. Von Zeipel, H. 1924, *Mon. Not. Roy. Astr. Soc*, 84, 665, 684, 702
124. Wade, R. A., & Rucinski, S. M. 1985, *Astron. Astrophys. Supp.*, 60, 471
125. White, N. E. & Marshall, F. E. 1983, *Astrophys. J.*, 268, L117
126. Wilson, R. E. 1979, *Astrophys. J.*, 234, 1054
127. Wilson, R. E. 1990, *Astrophys. J.*, 356, 613
128. Wilson, R. E. 1993, in *New Frontiers in Binary Star Research*, ASP Conf. Ser., 38, 91, Leung, J. C. & Nha, N. H. (Eds.)
129. Wilson, R. E. 1994, *Pub. Astr. Soc. Pac.*, 106, 921
130. Wilson, R. E. & Devinney, E. J. 1971, *Astrophys. J.*, 166,605
131. Wilson, R. E., De Luccia, M., Johnston, K. & Mango, S. A. 1972, *Astrophys. J.*, 177, 191
132. Wilson, R. E., Van Hamme, W. & Pettera, L. E. 1985, *Astrophys. J.*, 289, 748
133. Wood, D. B. 1971, *Publ. Astron Soc. Pac.*, 83,286
134. Wood, F. B. 1946, *Princeton. Contrib.*, 21, 31